2015

Cellulose synthesis in *Physcomitrella patens*: gene expression and mutational analysis

Mai Linh Tran
University of Rhode Island, maitran@my.uri.edu

CELLULOSE SYNTHESIS IN *PHYSCOMITRELLA PATENS*: GENE EXPRESSION AND MUTATION ANALYSIS

BY

MAI LINH TRAN

A DISSERTATION SUBMITTED IN PARTIAL FULFILLMENT OF THE

REQUIREMENTS FOR THE DEGREE OF

DOCTOR OF PHILOSOPHY

IN

CELL & MOLECULAR BIOLOGY

UNIVERSITY OF RHODE ISLAND

2015

DOCTOR OF PHILOSOPHY DISSERTATION

OF

MAI TRAN

APPROVED:

Thesis Committee:

Major Professor Alison Roberts

Joanna Norris

Gongqin Sun

Nasser H. Zawia
DEAN OF THE GRADUATE SCHOOL

UNIVERSITY OF RHODE ISLAND
2015

ABSTRACT

A detailed analysis of cellulose synthesis in nonvascular plants can contribute to a better understanding of the evolution of this important process. In this study, the nonvascular plant *Physcomitrella patens* was used as a model system to investigate the roles of the different isoforms of cellulose synthase (CESA). *PpCESA* gene expression was quantified through Reverse Transcription quantitative (RT-q) PCR and localized through construction and analysis of promoter::reporter lines to determine the roles of the *PpCESA*s throughout development. *Physcomitrella patens CESA* genes are ubiquitously expressed in the filamentous protonema stage. All of the *PpCESAs* are expressed in the gametophore as well, with *PpCESA4* and *PpCESA10* mainly expressed in the axillary hairs. This broad expression is unique to non-vascular plants, in contrast to vascular plants in which CESA expression is restricted to cells depositing either primary cell walls or secondary cell walls during development.

Upregulation under osmotic stress induced by mannitol may indicate a role for cellulose under high osmotic stress. *PpCESA6*, *PpCESA7*, and *PpCESA8* were hypothesized to be responsible for osmotic stress-induced cellulose synthesis based on mannitol-induced upregulation of expression as indicated by analysis of microarray data. The roles of CESAs in development and stress tolerance were assessed by producing knockout mutants of PpCESA6, PpCESA7, and PpCESA8. *Ppcesa8* knockout (KO) and *ppcesa6/7* KO mutants do not have dramatic developmental phenotypes. However, *ppcesa6/7KO* mutants show sensitivity towards high salinity, indicating that cellulose is important under abiotic stress.

Currently, only *ppcesa5* KO mutants show a phenotype in the gametophore and no single KO mutants have phenotypes in the protonema. Cellulose synthesis inhibitors were used to examine the role of cellulose in the protonema. Results show that protonemal tissue is relatively insensitive to cellulose inhibitors, since only high concentration of the cellulose synthesis inhibitor DCB had any effect. DCB caused rupturing of tips, indicating that cellulose is necessary in tip growth. Results also indicate that cellulose synthase-like D (CSLD) proteins may contribute to the synthesis of cellulose in moss protonema.

Since single and double KO mutants of *PpCESA6*, *PpCESA7*, and *PpCESA8* do not produce a phenotype and *PpCESA* expression is ubiquitous. PpCESAs maybe be redundant in function such that another PpCESA may compensate loss of a single PpCESA. PpCESAs are highly similar in sequence and may have not fully sub-functionalized [1] and therefore, the PpCESAs isoforms may be more interchangeable than those of seed plants. Other cell wall components, such as hemicelluloses, pectins, and arabinogalactan proteins, may also compensate for lack of cellulose. These cell wall components were also examined through immunolabeling of regenerating protoplasts. The results showed the highest abundance of crystalline cellulose and moderate levels of callose, mannan, 1,5-α-L-arabinan and arabinogalactan proteins. Very low levels of 1,4-β-D-galactan and no homogalacturonans were detected.

ACKNOWLEDGMENTS

Special thanks to my major professor, Alison Roberts, for giving me an opportunity to work in her lab and mentoring me on all of my projects. During my first year of graduate school, Alison would come with me in the lab and personally teach me simple lab techniques like PCR and moss transformations. I have always appreciated her being involved in my lab work, in addition to providing directions and insights on my projects and writing of my manuscripts. I would like to thank the members of my committee, Joanna Norris, Gongqin Sun, Steve Irvine, and David Smith for their time and feedback for my dissertation.

I would like to thank Joanna Norris and the members of the Roberts lab, Arielle Chaves, Elizabeth Berry, Tess Scavuzzo-Duggan, and Xingxing Li for giving feedback on my lab presentations and posters, and suggestions for my projects. Much of this work was also assisted by faculty and students of the Cell Molecular and Biology Department through their useful advice and feedback on my projects. I especially appreciate Bethany Jenkins and her students for helping me with the setup of my RT-qPCR experiments and Jodi Cambergs lab for the help on protein work and statistical analysis. Many other people have helped me on my projects who I have not listed here, but I would like to acknowledge their help.

Finally, I would like to thank my family and friends for supporting me throughout my time in graduate school by always keeping me positive.

PREFACE

Manuscript format is used in this thesis.

Chapter 2 is in the process of being submitted to BMC Plant Biology. Chapter 3 is a mini-manuscript in collaboration with Elizabeth Berry (University of Rhode Island) that documents the cell wall polysaccharides and proteins throughout the moss development, which is ready to be submitted into BMC Plant Biology. Chapter 4 is a manuscript that has been done in collaboration with Luis Vidali and Hao Sun for tip growth assay microscopy at Worcester Polytechnic Institute. Currently, manuscript is being prepped for submission after further characterization of cellulose inhibitors isoxaben and DCB affect on GFP-PpCESA8 trafficking has been completed. Currently, this data will be collected with our collaboration with Magdalena Bezanilla at the University of Amherst using TIRF microscopy and analyzed Thomas McCarthy and Charlie Anderson from PSU. Plans for results to be complete for the end of July 2015 and plans to submission will be in August 2015.

TABLE OF CONTENTS

LIST OF TABLES

TABLE PAGE

Manuscript 1

Manuscript 3

LIST OF FIGURES

CHAPTER 1

INTRODUCTION

Cellulose is an abundant biopolymer that has many economic uses, such as biofuels, lumber, and textiles. It is essential in plant development. Cellulose consists of approximately 18-36 β1, 4-glucan chain, bundled together forming a single microfibril unit. Microfibrils can further associate to form macrofibrils that make up the backbone of the plant's cell wall [2].

Cellulose synthase A protein family (CESAs) have been identified as key proteins in the synthesis of cellulose [3]. There are multiple CESA isoforms found in both vascular and nonvascular plants [4, 5]. These form rosette structures known as cellulose synthase complexes (CSC) [6]. The CSCs in vascular plants are hetero-oligomeric, consisting of three different CESAs, which are specific for either primary or secondary cell wall formation. Primary cell walls are flexible and found in growing tissues, while secondary cell walls are rigid due to the aromatic polymer lignin and deposited in maturing cells in vascular and support tissue [7]. The CSC composition of the vascular plant *Arabidopsis* was discovered through CESA expression analysis, including promoter-reporter constructs and RNA *in situ* hybridization, and confirmed through co-immunoprecipitation [8, 9]. *AtCESA* null mutants are characterized by either defects in vascular development or embryo lethality [8, 9]. Phylogenetic analysis and functional analysis in other seed plants indicated that hetero-oligomeric CSCs evolved early in seed plant evolution [1].

Physcomitrella patens, a nonvascular land plant, also has multiple CESA isoforms but does not have primary and secondary cell wall formation like vascular plants. The roles of the multiple CESA isoforms in *P. patens* are still unknown [4]. Understanding how the roles of the PpCESAs differ from those of the vascular plant CESAs and whether PpCESAs form hetero-oligomeric or homo-oligomeric rosettes CSCs will provide insight into the roles of the distinct CESA isoforms in the assembly and function of seed plant CSCs. An advantage of using *P. patens* is its ability to be genetically manipulated due to its high rate of homologous recombination. With this unique property, genes of interest can be investigated through knockout mutations and gene expression analysis through a gene reporter system [10].

PpCESAs maybe important developmentally and also for response to osmotic stress

Prior experiments have indicated that PpCESAs are involved in certain stages of development and may play a role in stress response. PpCESA5 has a developmental role in gametophore formation based on mutation analysis [11]. *PpCESA6* and *PpCESA7* knockout mutants do not show obvious developmental phenotype impairment [12], but the encoded proteins may play a role when under osmotic stress. When *P. patens* is subjected to osmotic stress via addition of mannitol to the culture medium, cellulose deposition is upregulated [13]. Expression of *PpCESA6*, *PpCESA7*, and *PpCESA8* is increased under these conditions based on analysis of microarray data [14]. *PpCESA6*, *PpCESA7*, and *PpCESA8* mutants have not been tested for upregulation of cellulose under osmotic stress and the effects of mannitol on expression of these genes have not been confirmed by RT-qPCR.

Physcomitrella patens upregulates cellulose under osmotic stress [13], while vascular plants downregulate cellulose [15]. These responses might be due to differences in water uptake and dehydration tolerance mechanisms. Poikilohydric mosses depend on external surface water for hydration and homeohydric vascular plants maintain a constant hydrated state through mechanisms that prevent dehydration. When *P. patens* is dehydrated, losing 95% of its water weight, it is still able to survive [16]. In *Arabidopsis, atcesa*8 mutants shows drought tolerance, which is presumed to be due to the collapsed xylem that prevents water loss [17]. *Physcomitrella patens* uses a different mechanism to combat drought because it does not contain a vascular system and does not need to maintain a constant amount of water [18].

Physcomitrella patens is also tolerant to salt stress, surviving under 350 mM NaCl [16, 19]. Analysis of microarray data suggests that *PpCESA*s are upregulated in response to salt [14]. In *Arabidopsis,* cellulose deficient mutants have shown impairment in growth under high salinity conditions [20]. Cellulose synthase like D5, *atcsld5*, mutant also has decreased osmotic stress tolerance under drought, high salinity, and mannitol [21]. On this basis, PpCESAs are also predicted to be involved in salinity stress response and impaired survival in response to salinity is expected if these genes are deleted.

Cell wall composition in *P. patens*

With the exception of *ppcesa5KO* [11], single *PpCESA* KO mutations have not produced phenotypes [12, 22]. This indicates that cell wall components other than cellulose may play leading roles in structural development in *P. patens*. In vascular

plants, some cells are still able to expand and divide when cellulose is absent or reduced due to upregulation of other cell wall polysaccharides, such as pectin and callose [23]. Non-cellulosic cell wall components, such as pectin, hemicellulose, and arabinogalactan proteins (AGPs), have been generally analyzed in *P. patens* using carbohydrate microarrays [24] and some immunofluorescent staining [25-28]. Pectin adds flexibility to the plant cell wall, hemi-cellulose cross-links cellulose, and AGPs interacts with pectin, which is found to be important in cell extension [29].

Currently, it is known that hemicelluloses xylan and xyloglucan are found in gametophores [26], while mannan was found in protonema with deposition concentrated in cell junctions [27]. Callose was found in early developing spores [28] and cellulose was found in developing gametophore buds [11]. AGPs, which crosslink pectins, were found to be essential in tip growth of protonemal cells [25]. No comprehensive study of cell wall composition has been done in all tissues and few immuno and affinity histochemical studies have been done in protoplasts.

Affect of cellulose synthesis inhibitors isoxaben and DCB

Cellulose synthesis was previously shown to be important in stabilizing tip growth. Both pollen tubes and root hairs extend through tip growth [30], similarly to *P. patens* protonemal tissue [31]. Inhibition of cellulose synthesis in both cell types that extend by tip growth is highly disruptive. Petunia and lily pollen tubes were treated with cellulose synthesis inhibitor 2,6-dichlorobenzonitrile (DCB), which caused irregular cell wall deposition and rupturing of tips, indicating that the presence of cellulose is essential in pollen tube tip growth [32]. Similarly, *Lilium* and *Solanum* pollen tubes were grown in the presence of cellulase and cellulose crystallation

inhibitor CGA (1-cyclohexyl-5-(2,3,4,5,6-pentafluorophenoxy)-1,4,2,4,6-thiatriazin-3-amine), where low concentration caused irregular pollen tube size and direction and rupturing of tips at high concentrations of either the cellulase or CGA [33].

Root hair tip growth has been studied most extensively in *Arabidopsis*, including effects of DCB and isoxaben. Isoxaben treatment resulted in clearance of YFP::AtCESA6 from the membrane seen in the YFP::AtCESA6 rescued *atcesa6* mutant. In contrast, DCB was seen to cause hyperaccumulation of YFP::CESA6 in the cell cortex and inhibited motility [34]. Interestingly, in the moss *Funaria hygrometrica*, rosette structures decreased under DCB treatments as visualized with freeze fracture electron microscopy. At high concentrations of DCB, *Funaria* protonemal tips ruptured [35].

Thesis Outline:

PpCESA expression was examined through construction and analysis of promoter-reporter constructs and RT-qPCR. *PpCESA* promoters were fused to β-glucuronidase (GUS) for localization of expression. The expression of *PpCESA*s was examined at different developmental stages and in different tissues. Reverse transcription qPCR was used to quantify *PpCESA* expression in different tissues and under different hormone conditions to help understand the role of PpCESAs developmentally. Chapter 2 results show that *PpCESAs* are ubiquitously expressed in the protonema and gametophore stage. PpCESA4 and PpCESA10 are predominately expressed in the protonema, while all other PpCESAs are predominately expressed in the gametophore.

In addition to exploring PpCESA expression patterns, cell wall components were examined through immunolabeling of regenerating *P. patens* protoplasts. Antibodies and carbohydrate binding modules were used to label protoplasts for cellulose, hemicelluloses, and pectin content. Results in Chapter 3 show cellulose, AGPs, and callose to be the most abundant in protoplasts with moderate levels of mannan, arabinan, and xyloglucan. No homogalacturonan and little 1,4-β-D-galactan was detected. Understanding the cell wall composition in protoplasts will serve as a basis for investigativing cell wall defects in mutants.

ppcesa6/7 double KO, and *ppcesa8* KO mutants were produced. *PpCESA6* and *PpCESA7* genes are very similar in sequence and occur in the genome as a tandem repeat with only 2 amino acid differences [4, 12], so double *ppcesa6/7* KO mutants were created. Mutants were assayed for developmental defects and tested for survival under salinity treatment and cellulose deposition under osmotic. Results reported in Chapter 4 have revealed that *ppcesa8KO* has relatively normal development with slightly higher colony solidity than wildtype, while *ppcesa6/7KO* mutants were more sensitive to salt treatments.

Since no *ppcesa* KO mutants produced a drastic protonemal phenotype, the importance of cellulose synthesis in tip growth of protonemal filaments was tested through cellulose synthesis inhibitors. Protonemal filaments were treated with cellulose synthesis inhibitors isoxaben and DCB and assayed for tip growth rate and morphology. Both isoxaben and DCB had no effect on tip growth rate. However, at a high concentration of DCB, rupturing of tips was observed. Rupturing of tips caused by DCB indicated the importance of cellulose synthesis in tip growth, but it also

indicated that PpCESAs may not be the only contributors to cellulose synthesis. Cellulose synthase like D proteins are also affected by DCB treatments, indicating that CSLDs may potentially produce cellulose [36].

My work demonstrates that cellulose synthesis is important in tip growth in the protonema. Lack or reduction of cellulose has caused rupturing of tips caused by cellulose synthesis inhibitor DCB. Single *ppcesa* KOs have not shown dramatic phenotypes in the protonema, indicating that the mulitple PpCESAs may be able to compensate for the loss of a single member in the protein family. This conclusion is supported by ubiquitous expression of all of the *PpCESA*s in the protonema. Moss CESAs have diverged separately from seed plant CESAs based on phylogenetic analysis [1]. Our data supports the hypothesis that moss CESAs have not subfunctionalized like those of seed plants, in which three different CESAs are required to form at CSC and the CSCs are tissue specific. Abundances of other cell wall components shown in the protoplasts demonstrate that cell walls can be dynamic and that other cell wall components can potentially compensate for decrease in cellulose.

References:

1. Somerville C: **Cellulose synthesis in higher plants**. *Annu Rev Cell and Dev Biol* 2006, **22**:53-78.
2. Delmer DP: **CELLULOSE BIOSYNTHESIS: Exciting Times for A Difficult Field of Study**. *Annu Rev Plant Physiol Plant Mol Biol* 1999, **50**:245-276.
3. Roberts AW, Bushoven JT: **The cellulose synthase (CESA) gene superfamily of the moss *Physcomitrella patens***. *Plant Mol Biol* 2007, **63**:207-219.
4. Richmond TA, Somerville CR: **The cellulose synthase superfamily**. *Plant Physiol* 2000, **124**:495-498.

5. Kimura S, Laosinchai W, Itoh T, Cui X, Linder R, Brown RM: **Immunogold Labeling of Rosette Terminal Cellulose-Synthesizing Complexes in the Vascular Plant *Vigna angularis***. *Plant Cell* 1999, **11**:2075-2086.
6. Lerouxel O, Cavalier D, Liepman A, Keegstra K: **Biosynthesis of plant cell wall polysaccharides - a complex process**. *Curr Opin Plant Biol* 2006, **9**:621 - 630.
7. Taylor NG, Howells RM, Huttly AK, Vickers K, Turner SR: **Interactions among three distinct CesA proteins essential for cellulose synthesis**. *Proc Natl Acad Sci* 2003, **100**:1450-1455.
8. Persson S, Paredez A, Carroll A, Palsdottir H, Doblin M, Poindexter P, Khitrov N, Auer M, Somerville CR: **Genetic evidence for three unique components in primary cell-wall cellulose synthase complexes in *Arabidopsis***. *Proc Natl Acad Sci* 2007, **104**:15566-15571.
9. Roberts AW, Roberts EM, Haigler CH: **Moss cell walls: structure and biosynthesis**. *Front Plant Sci* 2012, **3**:166.
10. Schaefer DG: **A new moss genetics: targeted mutagenesis in Physcomitrella patens**. *Annual review of plant biology* 2002, **53**:477-501.
11. Goss CA, Brockmann DJ, Bushoven JT, Roberts AW: **A CELLULOSE SYNTHASE (CESA) gene essential for gametophore morphogenesis in the moss *Physcomitrella patens***. *Planta* 2012, **235**:1355-1367.
12. Wise HZ, Saxena IM, Brown RM: **Isolation and characterization of the cellulose synthase genes PpCesA6 and PpCesA7 in *Physcomitrella patens***. *Cellulose* 2011, **18**:371-384.
13. Dimos CS: **Functional Analysis of the Cellulose Synthase-Like D (CSLD) Gene Family in *Physcomitrella patens***. University of Rhode Island; 2010.
14. Cuming AC, Cho SH, Kamisugi Y, Graham H, Quatrano RS: **Microarray analysis of transcriptional responses to abscisic acid and osmotic, salt, and drought stress in the moss, *Physcomitrella patens***. *New Phytol* 2007, **176**:275-287.
15. Zhong R, Morrison WH, 3rd, Freshour GD, Hahn MG, Ye ZH: **Expression of a mutant form of cellulose synthase AtCesA7 causes dominant negative effect on cellulose biosynthesis**. *Plant Physiol* 2003, **132**:786-795.
16. Frank W, Ratnadewi D, Reski R: **Physcomitrella patens is highly tolerant against drought, salt and osmotic stress**. *Planta* 2005, **220**:384-394.
17. Chen Z, Hong X, Zhang H, Wang Y, Li X, Zhu JK, Gong Z: **Disruption of the cellulose synthase gene, AtCesA8/IRX1, enhances drought and osmotic stress tolerance in Arabidopsis**. *Plant J* 2005, **43**:273-283.
18. Mishler BD, Oliver MJ: **Putting *Physcomitrella patens* on the tree of life: the evolution an ecology of mosses**. In: *The Moss Physcomitrella patens.* Edited by Knight C, Perroud PF, Cove D, vol. 36: John Wiley & Sons; 2009: 1-15.
19. Wang XQ, Yang PF, Liu Z, Liu WZ, Hu Y, Chen H, Kuang TY, Pei ZM, Shen SH, He YK: **Exploring the Mechanism of Physcomitrella patens Desiccation Tolerance through a Proteomic Strategy**. *Plant Physiol* 2009, **149**:1739-1750.
20. Kang JS, Frank J, Kang CH, Kajiura H, Vikram M, Ueda A, Kim S, Bahk JD, Triplett B, Fujiyama K *et al*: **Salt tolerance of Arabidopsis thaliana requires**

maturation of N-glycosylated proteins in the Golgi apparatus. *Proceedings of the National Academy of Sciences of the United States of America* 2008, **105**:5933-5938.
21. Zhu J, Lee BH, Dellinger M, Cui X, Zhang C, Wu S, Nothnagel EA, Zhu JK: **A cellulose synthase-like protein is required for osmotic stress tolerance in Arabidopsis**. *Plant J* 2010, **63**:128-140.
22. Roberts AW. In.; 2015.
23. Hao H, Chen T, Fan L, Li R, Wang X: **2, 6-Dichlorobenzonitrile causes multiple effects on pollen tube growth beyond altering cellulose synthesis in Pinus bungeana Zucc**. *PLoS One* 2013, **8**:e76660.
24. Moller I, Sorensen I, Bernal AJ, Blaukopf C, Lee K, Obro J, Pettolino F, Roberts A, Mikkelsen JD, Knox JP *et al*: **High-throughput mapping of cell-wall polymers within and between plants using novel microarrays**. *Plant J* 2007, **50**:1118-1128.
25. Lee KJ, Sakata Y, Mau SL, Pettolino F, Bacic A, Quatrano RS, Knight CD, Knox JP: **Arabinogalactan proteins are required for apical cell extension in the moss *Physcomitrella patens***. *Plant Cell* 2005, **17**:3051-3065.
26. Kulkarni AR, Pena MJ, Avci U, Mazumder K, Urbanowicz BR, Pattathil S, Yin Y, O'Neill MA, Roberts AW, Hahn MG *et al*: **The ability of land plants to synthesize glucuronoxylans predates the evolution of tracheophytes**. *Glycobiology* 2012, **22**:439-451.
27. Liepman AH, Nairn CJ, Willats WG, Sorensen I, Roberts AW, Keegstra K: **Functional genomic analysis supports conservation of function among cellulose synthase-like a gene family members and suggests diverse roles of mannans in plants**. *Plant Physiol* 2007, **143**:1881-1893.
28. Schuette S, Wood AJ, Geisler M, Geisler-Lee J, Ligrone R, Renzaglia KS: **Novel localization of callose in the spores of Physcomitrella patens and phylogenomics of the callose synthase gene family**. *Ann Bot* 2009, **103**:749-756.
29. Cosgrove D: **Growth of the plant cell wall**. *Nature Rev Mol Cell Biol* 2005, **6**:850 - 861.
30. Hepler PK, Vidali L, Cheung AY: **Polarized cell growth in higher plants**. *Annu Rev Cell Dev Biol* 2001, **17**:159-187.
31. Doonan JH, Cove DJ, Lloyd CW: **Microtubules and microfilaments in tip growth: evidence that microtubules impose polarity on protonemal growth in *Physcomitrella patens***. *Journal of cell science* 1988, **89**:533-540.
32. Anderson JR, Barnes WS, Bedinger P: **2,6-Dichlorobenzonitrile, a cellulose biosynthesis inhibitor, affects morphology and structural integrity of petunia and lily pollen tubes**. *J Plant Physiol* 2002, **159**:61-67.
33. Aouar L, Chebli Y, Geitmann A: **Morphogenesis of complex plant cell shapes: the mechanical role of crystalline cellulose in growing pollen tubes**. *Sex Plant Reprod* 2010, **23**:15-27.
34. DeBolt S, Gutierrez R, Ehrhardt DW, Somerville C: **Nonmotile cellulose synthase subunits repeatedly accumulate within localized regions at the plasma membrane in Arabidopsis hypocotyl cells following 2,6-dichlorobenzonitrile treatment**. *Plant Physiol* 2007, **145**:334-338.

35. Rudolph U, Gross H, Schepf E: **Investigations of the turnover of the putative cellulose-synthesizing particle "rosettes" within the plasma membrane of Funaria hygrometrica protonema cells**. *Protoplasma* 1989, **148**:57-69.
36. Park S, Szumlanski AL, Gu F, Guo F, Nielsen E: **A role for CSLD3 during cell-wall synthesis in apical plasma membranes of tip-growing root-hair cells**. *Nat Cell Biol* 2011, **13**:973-980.

Manuscript 1

Submitted to *BMC Plant Biology*, June 2015

Cellulose synthase (CESA) gene expression profiling of *Physcomitrella patens*

Authors:

Mai L. Tran, University of Rhode Island, maitran@my.uri.edu

Alison W. Roberts, University of Rhode Island, ARoberts@ds.uri.edu

120 Flagg Road, Kingston, Rhode Island 02881

Abstract:

Background: The *Cellulose Synthase (CESA*) gene family of seed plants comprises six clades that encode isoforms with conserved expression patterns and functions in protein complex formation and primary and secondary cell wall synthesis. The *CESA* gene family of mosses, which lack lignified secondary cell walls, diversified independently of the seed plant *CESA* family. There are seven CESA isoforms encoded in the genome of the moss *Physcomitrella patens* and freeze fracture electron microscopy has revealed rosette cellulose synthesis complexes (CSCs) in the tips of growing protonema. However, only *PpCESA5* has been characterized functionally and there is little information available on the expression of the other members of this gene family. We have profiled *PpCESA* expression through quantitative RT-PCR, analysis of promoter::reporter lines, and cluster analysis of public microarray data in an effort to identify co-expression patterns that could help reveal the functions of PpCESA isoforms in protein complex formation and development of specific tissues.

Results: All *PpCESA*s are expressed at some level in nearly every tissue. Based on histochemical analysis of promoter-reporter lines and quantitative RT-PCR, *PpCESA4* and *PpCESA10* are down-regulated in gametophores, whereas *PpCESA3*, *PpCESA5*, *PpCESA6*, *PpCESA7,* and *PpCESA8* are up-regulated. Only *PpCES10* is significantly up-regulated in protonema. *PpCESA6*, *PpCESA7* and *PpCESA8* expression is associated with rhizoid development. No strong co-expression patterns were observed.

Conclusions: Broad overlapping expression of the *PpCESA*s is consistent with a high degree of PpCESA interchangeability and indicates a different pattern of functional specialization in the evolution of the seed plant and moss *CESA* families.

Keywords:

Cellulose synthases, *Physcomitrella patens*, gene expression

Background:

Cellulose is an abundant biopolymer with many commercial applications, yet the mechanism of its biosynthesis is still being understood. Cellulose synthases (CESAs) have been identified as key proteins in the synthesis of cellulose in plants [3]. There are multiple CESA isoforms found in both vascular and nonvascular plants [2, 4] and in both cases the CESAs form rosette structures known as cellulose synthase complexes (CSC) [6, 37].

In vascular plants, CSCs are specific for either primary or secondary cell wall formation and are hetero-oligomeric, consisting of three different CESAs [8, 9, 38]. Along with phenotype analysis of CESA mutants and protein-protein interaction studies, analysis of CESA coexpression patterns provided critical information for understanding the composition of the hetero-oligomeric Arabidopsis CSCs. Initially *AtCESA4*, *ACESA7*, and *AtCESA8* mutants in Arabidopsis were discovered to have the same phenotype with reduction of cellulose and irregular xylem. Coexpression of these genes was demonstrated by northern blot [39] and microarray analysis [40]. Later, coimmunopreciptation experiments confirmed that the encoded proteins interact, forming the CSCs that synthesize cellulose in the secondary cell wall [38]. Similarly, AtCESA1 and AtCESA3 are essential in primary cell wall formation, along with AtCESA6-like proteins [9]. These AtCESAs are coexpressed based on promoter-reporter analysis. Co-immunoprecipitation and bimolecular complementation experiments showed that AtCESA1, AtCESA3, and AtCESA6 interact to form the

CSC in the primary cell wall [9, 40, 41]. No studies on CESA composition of the CSCs of nonvascular plants like *P. patens* have been done.

Physcomitrella patens, a nonvascular land plant, also has multiple CESA isoforms and rosette CSCs, but it does not have lignified secondary cell walls like vascular plants so the divergence of primary and secondary type CESA may not be expected [1]. Seven *CESA* genes have been identified in *P. patens* and phylogenetic analysis indicates that they diversified independently from the seed plant *CESA*s [4]. However, their individual functions are still unknown [1]. Understanding how the functions of the PpCESAs differ from those of vascular plant CESAs will provide insight into the roles of the distinct CESA isoforms in CSC assembly and function in moss.

Since the *P. patens* genome has been fully sequenced and can be easily genetically manipulated, it is possible to investigate gene function through knockout mutations and gene expression through promoter-reporter analysis [42]. Prior experiments in *P. patens* have indicated that PpCESAs might be involved in different stages of development. PpCESA5 has a developmental role in gametophore formation [11]. Although *PpCESA6* and *PpCESA7* single knockout mutants do not show obvious developmental phenotypes, double knockouts of *PpCESA6* and *PpCESA7* have shorter gametophores [12]. With the exception of an analysis of EST abundances in various *P. patens* cDNA libraries [4, 43] and a few focused studies [3, 15] *PpCESA* expression patterns have not been characterized.

In this study, we examined *PpCESA* expression through relative quantitative RT-PCR, analysis of lines transformed with *promoter::β-glucuronidase* (*GUS*) reporters, and hierarchical cluster analysis of public microarray data to test for tissue and

developmental stage specific *CESA* expression. We also aimed to determine whether specific *P. patens CESA*s are coexpressed as in vascular plants such as Arabidopsis and determine whether there are any unique patterns suggesting potential *PpCESA* functions and interactions.

Materials and Methods:

Vector construction

Genomic DNA was extracted from *P. patens* protonemal tissue grown on solid BCDAT medium as described previously [44]. *PpCESA* genomic sequences were downloaded from http://www.cosmoss.org/ (Table 1). Primers (Table 1) were designed to amplify approximately 2 kb of nucleotides upstream of the start of each *PpCESA* coding sequence and were flanked with attB1 and attB5r sites for Gateway Multisite cloning (Invitrogen, Grand Island, NY, USA). *PpCESA* promoters were amplified from 4 μL of genomic DNA in 50 μL reactions using Phusion High-Fidelity PCR Master Mix (New England Biolabs, Ipswich, MA, USA) with a 30 s denaturation at 98°C; 35 cycles of 7 s at 98°C, 7 s at 58-68°C (Table 1), and 1 min at 72°C; and a final 5 min extension at 72°C. Using the same PCR conditions, the *GUS* gene was amplified from pRITA (Genbank FB507484.1) and the *CESA5* coding sequence was amplified from pdp24095 (RIKEN BRC,Ibaraki, Japan) with primers flanked by attB5 and attB2 sites (Table 1). CESA promoter PCR products were cloned into pDONR P1-P5r and *GUS* and *PpCESA5* coding sequence PCR products were cloned into pDONR P5-P2 using BP Clonase II (Invitrogen).

The si3pTH plasmid containing a hygromycin^{R} expression cassette flanked by 5' and 3' segments of the 108 targeting locus (gift of Pierre-Francois Perrroud) was modified

into a destination vector by inserting a Gateway cassette. si3pTH was digested with Sal1, targeting a site between the hygromyocin^{R} gene and the 3' 108 locus. The Gateway cassette (Invitrogen) was amplified with primers flanked with XhoI restriction sites (Table 1) using Platinum Taq (Invitrogen) with a 2 min denaturation at 95°C; 35 cycles of 30 s at 95°C, 30 s at 64°C, and 1 min at 72°C; and a final 5 min extension at 72°C, cloned into PCR TOPO 2.1 (Invitrogen) and sequence verified. The XhoI fragment containing the Gateway cassette was ligated into the SalI site of si3 pTH and the Gateway enabled vector (si3-pTH-GW) was propagated in ccdb cells (Invitrogen).

To construct the *PpCESApro*::*GUS* vectors, entry clones containing the *PpCESA* promoters and *GUS* gene were inserted into the si3-pTH-GW destination vector using LR Clonase II Plus. Similarly, entry clones containing the *PpCESA5* promoter and *PpCESA5* coding sequence were inserted in si3-pTH-GW for the rescue vector (Invitrogen). *PpCESA5pro::PpCESA5* and all *PpCESApro::GUS,* except for *PpCESA8pro::GUS* were linearized with SwaI, while *PpCESA8pro::GUS* vector was linearized with PvuII.

Culture and Transformation

Wild type *P. patens* strain Gransden 2011 [45] was homogenized using a hand-held homogenizer and hard tissue probe tips (Omni International Inc. , Kennesaw, GA, USA) in 4 to 6 mL of water and subcultured on solid BCDAT medium overlain with 5 - 7 d, 25˚C. Transformations were performed as described previously [44]. Three to seven stably transformed lines from each *proCESA::GUS* transformation were grown and analyzed for gene expression. Homogenized tissue was subcultured on solid

BCDAT medium for 6 d and for analysis of gametophore development, tissue clumps were cultured on solid BCD medium for 2 to 3 weeks [44].

GUS histochemical staining

Transgenic *CESApro::GUS* lines were incubated in 200 µL of 1 mM 5-bromo-4-chloro-3-indoyl-β-glucuronide in 100 mM sodium phosphate, pH 7.0 at 37°C for 6 h for protonemal filaments and 16 h for gametophore tissue. Tissue was fixed in 5% (v/v) formaldehyde for 10 min and 5% (v/v) acetic acid for 10 min. Chlorophyll was removed with a series of 50%, 70%, and 95% (v/v) ethanol washes [46]. Filaments and single gametophores were dissected from fixed colonies with fine forceps. Images were captured through a Leica M165FC stereo microscope with a Leica DFC310FX camera (Leica Microsystems Inc., Buffalo Grove, IL, USA).

Primer design for qPCR

CESA coding sequences were aligned using Clustal with Geneious software (Biomatters Limited, Auckland, New Zealand). Unique 18-23 bp regions with melting points of 60°C that amplified 50-400 bp regions were selected as potential qPCR primers and were further tested using the NCBI/Primer-Blast tool [47] to detect potential nonspecific amplication, primer dimer, and hairpin formations.

All primers were tested for specificity by PCR against plasmids containing cDNA clones of each of the seven *PpCESAs* using Taq polymerase (New England Biolabs) in 25 µL reactions with 1 µM primers and 1 ng of template with a 2 min denaturation at 95°C; 32 cycles of 30 s at 95˚C, 30s at 60˚C, and 30 s at 72˚C; and a final 5 min extension at 72˚C and analyzed by gel electrophoresis. Primer concentrations were optimized and tested for efficiency. Nonspecific and/or inefficient primers outside the

90-110% range were redesigned. Primers that amplify Actin (ACT) and v-Type h(+) translocating pyrophosphatase (vH+PP) were used as references for all samples [48].

RNA extraction and transcription

RNA was extracted from approximately 100 mg of squeeze dried protonema tissue using a Plant Rneasy Mini kit or less than 100 mg of gametophores using a Micro kit (QIAGEN Inc., Venlo, Limburg, Netherlands). Tissue was frozen in liquid nitrogen with 700 μL of RLT buffer and 100 mg garnet beads (BioSpec Products, Bartlesville, OK, USA) and disrupted with a Tissue Lyzer (QIAGEN Inc.) with a frequency of 30 Hz for 10 min. Contaminating DNA was removed on column using RNase-Free DNase (QIAGEN Inc). For hormone treatments, RNA was extracted from triplicate cultures grown from protoplasts on PRMB for 3 days [44] and transferred to BCD, BCDAT, BCD + 3 uM benzylaminopurine or BCD + 1 uM naphthaleneacetic acid (Sigma-Aldrich, St. Louis, MO, USA) for 7 d. Gametophores were collected with micro dissecting scissors (Electron Microscopy Sciences, Hatfield, PA, USA) after 3 weeks on BCD and protonemal tissue was collected after 6 d on BCDAT for RNA extraction. All samples were collected in biological replicates of 3.

All RNA quality was tested using a Bioanalyzer with the Plant RNA 6000 Nano chip, except for gametophore RNA, where the concentration of RNA collected from gametophores were too low (Aglient Technologies, Santa Clara, CA, USA). RNA with RIN quality scores of 7 or above was reverse transcribed using Mulv transcriptase (New England Biolabs) according to manufacturer's instructions and diluted 1:1 with nuclease-free water.

Quantitative PCR

All cDNA samples were tested in duplicate with no template control in every run and a no reverse transcriptase control for each sample. The 20 µL qPCR reactions were analyzed on a Roche Lightcycler480 Multiwell Plate 96 with SYBR Green I Master Mix (Hoffmann-La Roche AG, Basel, Switzerland), 25 ng of reverse transcribed DNA, and primers at optimized concentrations (Table 2). Reactions were denatured 10 min at 95˚C and subjected to 32 cycles of 10 s at 95˚C, 20 s at 60˚C, and 20 s at 72˚C for quantification, followed by 5 s denaturation at 95˚C, 1 min annealing at 65˚C, and ramping at 2.2˚C/s to 97˚C for melting curve analysis. Target/average reference cross point ratios were calculated for each sample and standard errors were calculated between the three biological replicates. For overall statistical analysis of qPCR results, all treatments with 3 biological replicates were log transformed to meet normal distribute and homogeneity and subjected to one-way Anova. For Anova P value < 0.05, data was analyzed pair-wise with Tukey-Kramer T test.

Microarray analysis

PpCESA expression data from public microarray experiments [49] were analyzed using the hierarchical clustering tool for anatomy, development, and perturbations [50]. The *PpCESA*s are represented on the arrays as Phypa_105213 (*PpCESA5*), Phypa_233978 (*PpCESA8*), Phypa_202222 (*PpCESA3*), Phypa_213586 (*PpCESA4*), Phypa_192909/ Phypa_192906 (*PpCESA6/7*), and Phypa_169568 (*PpCESA10*).

Results:

Promoter::GUS localization

To localize *CESA* expression, *promoter::GUS* reporter vectors for all 7 *CESAs* were transformed into wild type *P. patens*. After initial examination of minimum of 7

transgenic lines for consistency, two independent lines were used for detailed analysis of each promoter. To observe *PpCESA* expression in protonema, homogenized tissue was grown on BCDAT and sampled for staining daily from day 4 to day 7 after plating. No differences in *PpCESA* expression patterns were seen during this 4-d time course. However, 6 d-old cultures provided the most complete representation of primary and branching filaments and few senescing filaments. GUS activity shows that all seven *PpCESA* promoters were active throughout the protonema (Figure 1). In contrast to the protonema, *CESA* expression in the gametophores had a more varied pattern (Figures 2-4). All transgenic lines were grown in duplicate on BCD medium and sampled for staining over a time course of 3 weeks. Different stages of gametophore development were examined including early buds, buds with leaves, young gametophores with 6-10 leaves, and mature gametophores that had stopped producing new leaves. In the young gametophore buds, all CESA promoters were active except for *proCESA4* and *proCESA10* (Figure 2). As the buds matured and produced leaves, all *CESA* promoters except *proCESA4* and *proCESA10* were active in the apical meristem as shown for *proCESA3* (Figure 2I). In contrast, *proCESA4* and *proCESA10* showed activity mainly in the axillary hairs of gametophores with 2 to 3 leaves as shown for *proCESA4* (Figure 2J). In two-week-old gametophores with 6 to 10 leaves, all promoters were active in the axillary hairs (Figure 3). Promoters for *CESA3*, *CESA5*, *CESA6*, *CESA7* and *CESA8* were active in gametophore stems and in rhizoids (Figure 3). *CESA6* was strongly expressed at the base of the stem and throughout the older rhizoids (Figure 3D). Lines transformed with *proCESA4::GUS* and *proCESA10::GUS* had either no staining or very faint staining showing little or no

activity of these promoters in the gametophore stems and rhizoids (Figures 3B, G). Mature gametophores were examined, but there was no *PpCESA* expression when gametophores were fully grown (data not shown).

PpCESA expression in leaves was examined by growing the gametophores until they had approximately 6 to 10 leaves. Young leaves to fully expanded leaves with prominent midribs were examined under the compound microscope. *PpCESA3*, *PpCESA5*, and *PpCESA6* promoters were active in young leaves (Figure 3A,C,D) and throughout the center of older leaves developing a midvein, with activity concentrated at the base of the leaf (Figure 4A,C,D). In lines transformed with *proCESA7::GUS*, faint staining was seen at the base and in the center of both young and old leaves (Figure 3E and Figure 4E). No staining was seen in the gametophore leaves in the *proCESA4::GUS* lines. *ProCESA8* was very active in young gametophore leaves (Fig. 3E) and found concentrated in the midvein in older gametophore leaves (Figure 4E). *ProCESA10* was active in the margins of young leaves (Fig. 3G) and predominately at the base in older leaves (Figure 4G). No *CESA* promoters were active in the midribs of fully developed leaves.

The functionality of the cloned *PpCESA5* promoter was tested by rescuing the *cesa5KO* mutant phenotype [11] with a *proCESA5::PpCESA* construct. The mutant phenotype of *cesa5KO*, consisting of no production of gametophores or stunted gametophores, was rescued with the *proCESA5::PpCESA5* vector (Figure 5). The other promoters could not be tested because other single CESA knockouts produced no obvious morphological phenotype.

<u>*CESA* expression levels measured by RT-qPCR</u>

Because some of the *PpCESA* sequences are very similar, all primers were tested for specificity by PCR using plasmids containing full-length PpCESA cDNA clones as templates and analysis by gel electrophoresis. All primer pairs amplified fragments of the expected size when paired with their corresponding cDNA template and no amplification was seen when primers were paired with other CESA cDNA templates or in no template control reactions (Additional File 1). All primer pairs had efficiencies of 90% to 110% (Table 1). Despite repeated attempts, we were unable to design efficient primers that specifically amplified *PpCESA6*, which is nearly identical to *PpCESA7* throughout the CDS and UTR sequences [12].

RT-qPCR was performed on cultured protonemal tissue and on leafy gametophores isolated by dissection to measure the expression levels in these tissues. The results show that *PpCESA10* ($P<0.0001$) is more highly expressed in the protonemal tissue and *PpCESA3*, *PpCESA5*, and *PpCESA7* are more highly expressed in the gametophores ($P<0.005$) (Figure 6).

To test whether differences in *PpCESA* expression extrapolated from analysis of EST abundances [4, 43, 51] are valid, *CESA* expression was measured by RT-qPCR in tissues that had been induced to differentiate on media containing different nitrogen sources and hormone supplements (Figure 7). Homogenized protonema was grown for 7 d on medium containing ammonium and nitrate as nitrogen sources (BCDAT), which stimulates protonemal growth, and medium containing only nitrate as a nitrogen source (BCD), which promotes gametophore development. *Physcomitrella patens* was also grown for 7 d on BCD with added cytokinin, which promotes over-production gametophores, and auxin, which promotes over-production of rhizoids [43, 52].

RT-qPCR revealed that *PpCESA8* is upregulated in tissue cultured on BCD vs. BCDAT medium, whereas all other *PpCESA*s are expressed at equal levels on both media (Figure 7). This extends the analysis of EST abundance in which only *PpCESA3* and *PpCESA8* were represented in cDNA libraries from tissue grown on BCDAT medium [4]. The auxin treatment resulted in significant upregulation of *PpCESA3, PpCESA4, PpCESA7* and *PpCESA8* compared to the untreated BCDAT control, whereas only *PpCESA7* and *PpCESA8* were upregulated compared to the untreated BCD control. The expression of *PpCESA5* and *PpCESA10* was not significantly different in cultures with and without auxin (Figure 7). These data are consistent with overrepresentation of *PpCESA7* and *PpCESA8* in cDNA libraries from auxin-treated tissues compared to libraries from untreated tissues. However, they also demonstrate expression of *PpCESA3* and *PpCESA4* in auxin-treated tissues [4]. The cytokinin treatment resulted in significant upregulation of all *PpCESA*s, except *PpCESA10*, compared to both BCDAT and BCD controls. This is consistent with overrepresentation of *PpCESA4, PpCESA5* and *PpCESA7* in cDNA libraries from cytokinin-treated cultures [4], and also indicates that *PpCESA3* and *PpCESA8* are expressed in cytokinin-treated cultures.

Microarray analysis of PpCESA expression

Microarray expression profiles of the 7 *PpCESA*s (including profiles of *PpCESA6* and *PpCESA7* combined) analyzed relative to anatomy and development showed high expression of *PpCESA10* and *PpCESA5* in protonema and in association with protonemal development, including germination of protoplasts and spores (Additional File 2). In contrast, all *PpCESA*s except *PpCESA10* were expressed at moderate to

high levels in gametophores and in association with gametophore growth and development. Although phyllids (i.e. leaves) are part of the gametophore, the phyllid experiments included in the array experiment involved dedifferentiation of excised phyllids and initiation of protonemal growth [49]. Thus, expression of *PpCESA10* and *PpCESA5* in these samples is not necessarily indicative of expression in gametophores. Many of the experimental perturbations tested had little effect on *PpCESA* expression (Additional File 2). However, upregulation of *PpCESA10* and *PpCESA8* was detected at most time points in the phyllid dedifferentiation experiment, whereas *PpCESA5* was highly upregulated in the first two hours after leaf excision and downregulated at later time points. *PpCESA8* and *PpCESA4* were downregulated by high light and dehydration/rehydration treatments. *PpCESA3, PpCESA5* and *PpCESA8* were downregulated in the dark.

Discussion:

Rosette CSC structures are visible with freeze fracture electron microscopy in protonemal tips of *P. patens* and the related species *Funaria hygrometrica* [1, 37], indicating that cellulose is synthesized in protonemal filaments. High expression of *PpCESA10* in the protonema detected by RT-qPCR indicates that PpCESA10 is important for protonemal cellulose synthesis. This is consistent with microarray data [49] analyzed through Genevestigator (Nebion AG), which show high *PpCESA10* expression in the protonema (Additional File 2). However, promoter-GUS analysis indicates that all PpCESAs participate in deposition of the protonemal cell wall. Most PpCESAs appear to participate in cell wall synthesis in gametophores, with expression varying in select locations. All *PpCESAs*, except for *PpCESA10* were

moderately to highly expressed in gametophore development through microarray data [49]. Measured by RT-qPCR, *PpCESA3, PpCESA5,* and *PpCESA7* had significantly higher expression in gametophores compared to protonema. Previously, analysis of ESTs suggested that *PpCESA4, PpCESA5*, *PpCESA6* and *PpCESA7* are overrepresented in libraries when treated with cytokinin, which promotes gametophore development [4, 43]. RT-qPCR confirmed upregulation of these genes, and also *PpCESA3* and *PpCESA8*, under treatment with cytokinin. Mutational analysis has confirmed the role of PpCESA5 in gametophore development [11]. High expression of *PpCESA4* under cytokinin treatment is also seen in our RT-qPCR and an overrepresentation of *PpCESA4* and *PpCESA10* ESTs under cytokinin treatment [4, 43] suggests that *PpCESA4* and *PpCESA10* are also expressed in the gametophore, but very little expression is seen in our promoter::GUS analysis.

The cellulose of the bud and stem of gametophores appears to be predominately synthesized by PpCESA3, PpCESA5, PpCESA6, PpCESA7, and PpCESA8. Within the gametophore leaves, PpCESA3, PpCESA5, PpCESA6 and PpCESA8 appear to be synthesizing cellulose at the leaf base and developing midrib, while *PpCESA10* is expressed at the margins of the leaves. Microarray data has shown increase of PpCESA8 and PpCESA10 under leaf development with PpCESA5 initially strong expression after leaf excision, which is consistent with both our *CESApro::GUS* staining and RT-qPCR. *PpCESA3* co-expression with NAC transcription factor *PpVN7* [53] is also consistent with a role in midrib cellulose synthesis. Expression of all *PpCESA*s in the axillary hairs of young gametophores is indicated by histochemical staining (Figure 2).

PpCESA6, PpCESA7 and PpCESA8 appear to be the main contributors to cellulose synthesis in the rhizoids. This is supported by upregulation of *PpCESA7* and *PpCESA8* by auxin compared to BCD based on RT-qPCR, and over representation of *PpCESA6* and *PpCESA8* ESTs in libraries from auxin-treated tissue [4]. Strong histochemical staining of *proCESA6::GUS* lines in rhizoid tissue and PpCESA6-GFP localization in rhizoids [12], also suggest that PpCESA6 is involved in cellulose synthesis in rhizoids. However, *ppcesa6KO, ppcesa7KO,* [12] and our analysis of *ppcesa8KO* and have shown no defect in rhizoid development indicating that PpCESA6, PpCESA7, and PpCESA8 may function redundantly in cellulose synthesis in the rhizoids [12].

Beyond localizing and quantifying gene expression throughout *P. patens* development, expression analysis may help elucidate interactions between the PpCESAs within hetero-oligomeric CSCs, as in *Arapidopsis* [9, 40]. *Physcomitrella patens CESA*s have overlapping expression with all the CESAs being expressed in the protonema and almost all CESAs are expressed in gametophore based on GUS histochemical staining. However, possible interactions are indicated by expression levels in the gametophore and protonema from RT-qPCR results. For example, high coexpression of *PpCESA3*, *PpCESA5*, *PpCESA7,* and *PpCESA8* under cytokinin and auxin treatment makes them most likely to interact in a hetero-oligmeric CSC. Similar expression of PpCESA4 and PpCESA10 makes them likely to interact in the protonema as a hetero-oligomeric CSC. The overlapping expression and lack of phenotype of single *Pp*CESAKOs, other than *ppcesa5KO,* indicate that the PpCESAs are interchangeable [12]. Phylogenetic tree of CESAs indicate that PpCESAs are not orthologous in specialized functionality

to seed plant CESAs, where they form hetero-oligomeric complexes. Since CESAs are originally homo-oligomeric, it is possible that PpCESAs still form homo-oligomeric, making PpCESAs more functional redundant [1].

Conclusion:

Complex expression of *PpCESAs* at different times and in different tissues within the gametophore is consistent with functional development of multiple cell types and the need for structural support [1]. Overlapping expression and lack of phenotypes in single *PpCESA* knockout lines, except for *ppcesa5 KO* [11], indicates that some of the PpCESAs may function redundantly. Some of the PpCESAs are coexpressed, indicating that PpCESA interactions within hetero-oligomeric CSC is possible. This expression analysis can serve as a gateway to further explore whether the *P. patens* CSCs are homo-oligomeric or hetero-oligomeric.

Avalibility of supporting data:

Additional File 1. Primer Specificity test

Additional File 2. Array Expression Analysis

List of abbreviations used:

GUS: β-glucuronidase

CESA: cellulose sythase A

Pro : promoter

CSC: cellulose synthase complex

Irx: irregular xylem

RT-qPCR: reverse transcriptase quantitative polymer chain reaction

Pp vH+PP: v-Type h(+) translocating pyrophosphatase

PpACT: actin

Competing interests

We have no conflicts of interest or competing interests to declare.

Acknowledgements

This material is based in part upon work supported as part of The Center for LignoCellulose Structure and Formation, an Energy Frontier Research Center funded by the U.S. Department of Energy, Office of Science, Office of Basic Energy Sciences under Award Number DE-SC0001090 and in part upon research supported by National Science Foundation Award IOS-1257047 and in part upon work conducted using the Rhode Island Genomics and Sequencing Center which is supported in part by the National Science Foundation under EPSCoR Grants Nos. 0554548 & EPS-1004057. Pierre-Francois Perroud donated the Si3pTH plasmid for our GUS expression experiments.

References:

1. Roberts AW, Roberts EM, Haigler CH: **Moss cell walls: structure and biosynthesis**. *Front Plant Sci* 2012, **3**:166.
2. Somerville C: **Cellulose synthesis in higher plants**. *Annu Rev Cell and Dev Biol* 2006, **22**:53-78.
3. Delmer DP: **CELLULOSE BIOSYNTHESIS: Exciting Times for A Difficult Field of Study**. *Annu Rev Plant Physiol Plant Mol Biol* 1999, **50**:245-276.
4. Roberts AW, Bushoven JT: **The cellulose synthase (CESA) gene superfamily of the moss *Physcomitrella patens***. *Plant Mol Biol* 2007, **63**:207-219.
5. Richmond TA, Somerville CR: **The cellulose synthase superfamily**. *Plant Physiol* 2000, **124**:495-498.

6. Kimura S, Laosinchai W, Itoh T, Cui X, Linder R, Brown RM: **Immunogold Labeling of Rosette Terminal Cellulose-Synthesizing Complexes in the Vascular Plant *Vigna angularis***. *Plant Cell* 1999, **11**:2075-2086.
7. Lerouxel O, Cavalier D, Liepman A, Keegstra K: **Biosynthesis of plant cell wall polysaccharides - a complex process**. *Curr Opin Plant Biol* 2006, **9**:621 - 630.
8. Taylor NG, Howells RM, Huttly AK, Vickers K, Turner SR: **Interactions among three distinct CesA proteins essential for cellulose synthesis**. *Proc Natl Acad Sci* 2003, **100**:1450-1455.
9. Persson S, Paredez A, Carroll A, Palsdottir H, Doblin M, Poindexter P, Khitrov N, Auer M, Somerville CR: **Genetic evidence for three unique components in primary cell-wall cellulose synthase complexes in *Arabidopsis***. *Proc Natl Acad Sci* 2007, **104**:15566-15571.
10. Schaefer DG: **A new moss genetics: targeted mutagenesis in Physcomitrella patens**. *Annual review of plant biology* 2002, **53**:477-501.
11. Goss CA, Brockmann DJ, Bushoven JT, Roberts AW: **A CELLULOSE SYNTHASE (CESA) gene essential for gametophore morphogenesis in the moss *Physcomitrella patens***. *Planta* 2012, **235**:1355-1367.
12. Wise HZ, Saxena IM, Brown RM: **Isolation and characterization of the cellulose synthase genes PpCesA6 and PpCesA7 in *Physcomitrella patens***. *Cellulose* 2011, **18**:371-384.
13. Dimos CS: **Functional Analysis of the Cellulose Synthase-Like D (CSLD) Gene Family in *Physcomitrella patens***. University of Rhode Island; 2010.
14. Cuming AC, Cho SH, Kamisugi Y, Graham H, Quatrano RS: **Microarray analysis of transcriptional responses to abscisic acid and osmotic, salt, and drought stress in the moss, *Physcomitrella patens***. *New Phytol* 2007, **176**:275-287.
15. Zhong R, Morrison WH, 3rd, Freshour GD, Hahn MG, Ye ZH: **Expression of a mutant form of cellulose synthase AtCesA7 causes dominant negative effect on cellulose biosynthesis**. *Plant Physiol* 2003, **132**:786-795.
16. Frank W, Ratnadewi D, Reski R: **Physcomitrella patens is highly tolerant against drought, salt and osmotic stress**. *Planta* 2005, **220**:384-394.
17. Chen Z, Hong X, Zhang H, Wang Y, Li X, Zhu JK, Gong Z: **Disruption of the cellulose synthase gene, AtCesA8/IRX1, enhances drought and osmotic stress tolerance in Arabidopsis**. *Plant J* 2005, **43**:273-283.
18. Mishler BD, Oliver MJ: **Putting *Physcomitrella patens* on the tree of life: the evolution an ecology of mosses**. In: *The Moss Physcomitrella patens.* Edited by Knight C, Perroud PF, Cove D, vol. 36: John Wiley & Sons; 2009: 1-15.
19. Wang XQ, Yang PF, Liu Z, Liu WZ, Hu Y, Chen H, Kuang TY, Pei ZM, Shen SH, He YK: **Exploring the Mechanism of Physcomitrella patens Desiccation Tolerance through a Proteomic Strategy**. *Plant Physiol* 2009, **149**:1739-1750.
20. Kang JS, Frank J, Kang CH, Kajiura H, Vikram M, Ueda A, Kim S, Bahk JD, Triplett B, Fujiyama K *et al*: **Salt tolerance of Arabidopsis thaliana requires maturation of N-glycosylated proteins in the Golgi apparatus**. *Proceedings*

of the National Academy of Sciences of the United States of America 2008, **105**:5933-5938.
21. Zhu J, Lee BH, Dellinger M, Cui X, Zhang C, Wu S, Nothnagel EA, Zhu JK: **A cellulose synthase-like protein is required for osmotic stress tolerance in Arabidopsis**. *Plant J* 2010, **63**:128-140.
22. Roberts AW. In.; 2015.
23. Hao H, Chen T, Fan L, Li R, Wang X: **2, 6-Dichlorobenzonitrile causes multiple effects on pollen tube growth beyond altering cellulose synthesis in Pinus bungeana Zucc**. *PLoS One* 2013, **8**:e76660.
24. Moller I, Sorensen I, Bernal AJ, Blaukopf C, Lee K, Obro J, Pettolino F, Roberts A, Mikkelsen JD, Knox JP *et al*: **High-throughput mapping of cell-wall polymers within and between plants using novel microarrays**. *Plant J* 2007, **50**:1118-1128.
25. Lee KJ, Sakata Y, Mau SL, Pettolino F, Bacic A, Quatrano RS, Knight CD, Knox JP: **Arabinogalactan proteins are required for apical cell extension in the moss *Physcomitrella patens***. *Plant Cell* 2005, **17**:3051-3065.
26. Kulkarni AR, Pena MJ, Avci U, Mazumder K, Urbanowicz BR, Pattathil S, Yin Y, O'Neill MA, Roberts AW, Hahn MG *et al*: **The ability of land plants to synthesize glucuronoxylans predates the evolution of tracheophytes**. *Glycobiology* 2012, **22**:439-451.
27. Liepman AH, Nairn CJ, Willats WG, Sorensen I, Roberts AW, Keegstra K: **Functional genomic analysis supports conservation of function among cellulose synthase-like a gene family members and suggests diverse roles of mannans in plants**. *Plant Physiol* 2007, **143**:1881-1893.
28. Schuette S, Wood AJ, Geisler M, Geisler-Lee J, Ligrone R, Renzaglia KS: **Novel localization of callose in the spores of Physcomitrella patens and phylogenomics of the callose synthase gene family**. *Ann Bot* 2009, **103**:749-756.
29. Cosgrove D: **Growth of the plant cell wall**. *Nature Rev Mol Cell Biol* 2005, **6**:850 - 861.
30. Hepler PK, Vidali L, Cheung AY: **Polarized cell growth in higher plants**. *Annu Rev Cell Dev Biol* 2001, **17**:159-187.
31. Doonan JH, Cove DJ, Lloyd CW: **Microtubules and microfilaments in tip growth: evidence that microtubules impose polarity on protonemal growth in *Physcomitrella patens***. *Journal of cell science* 1988, **89**:533-540.
32. Anderson JR, Barnes WS, Bedinger P: **2,6-Dichlorobenzonitrile, a cellulose biosynthesis inhibitor, affects morphology and structural integrity of petunia and lily pollen tubes**. *J Plant Physiol* 2002, **159**:61-67.
33. Aouar L, Chebli Y, Geitmann A: **Morphogenesis of complex plant cell shapes: the mechanical role of crystalline cellulose in growing pollen tubes**. *Sex Plant Reprod* 2010, **23**:15-27.
34. DeBolt S, Gutierrez R, Ehrhardt DW, Somerville C: **Nonmotile cellulose synthase subunits repeatedly accumulate within localized regions at the plasma membrane in Arabidopsis hypocotyl cells following 2,6-dichlorobenzonitrile treatment**. *Plant Physiol* 2007, **145**:334-338.

35. Rudolph U, Gross H, Schepf E: **Investigations of the turnover of the putative cellulose-synthesizing particle "rosettes" within the plasma membrane of Funaria hygrometrica protonema cells**. *Protoplasma* 1989, **148**:57-69.
36. Park S, Szumlanski AL, Gu F, Guo F, Nielsen E: **A role for CSLD3 during cell-wall synthesis in apical plasma membranes of tip-growing root-hair cells**. *Nat Cell Biol* 2011, **13**:973-980.
37. Reiss HD, Schnept E, Herth W: **The plasma membrane of the *Funaria* caulonema tip cell: morphology and distribution of particle rosettes, and the kinetics of cellulose synthase**. *Planta* 1984, **160**:428-435.
38. Taylor NG: **Identification of cellulose synthase AtCesA7 (IRX3) in vivo phosphorylation sites--a potential role in regulating protein degradation**. *Plant Mol Biol* 2007, **64**:161-171.
39. Taylor NG, Laurie S, Turner SR: **Multiple Cellulose Synthase Catalytic Subunits Are Required for Cellulose Synthesis in *Arabidopsis***. *Plant Cell* 2000, **12**:2529–2539,.
40. Brown DM, Zeef LA, Ellis J, Goodacre R, Turner SR: **Identification of novel genes in *Arabidopsis* involved in secondary cell wall formation using expression profiling and reverse genetics**. *Plant Cell* 2005, **17**:2281-2295.
41. Desprez T, Juraniec M, Crowell EF, Jouy H, Pochylova Z, Parcy F, Hofte H, Gonneau M, Vernhettes S: **Organization of cellulose synthase complexes involved in primary cell wall synthesis in *Arabidopsis thaliana***. *Proc Natl Acad Sci* 2007, **104**:15572-15577.
42. Schaefer DG: **A new moss genetics: targeted mutagenesis in *Physcomitrella patens***. *Annu Rev Plant Biol* 2002, **53**:477-501.
43. Nishiyama T, Fujita T, Shin IT, Seki M, Nishide H, Uchiyama I, Kamiya A, Carninci P, Hayashizaki Y, Shinozaki K *et al*: **Comparative genomics of *Physcomitrella patens* gametophytic transcriptome and *Arabidopsis thaliana*: implication for land plant evolution**. *Proc Natl Acad Sci* 2003, **100**:8007-8012.
44. Roberts AW, Dimos CS, Budziszek MJ, Jr., Goss CA, Lai V: **Knocking out the wall: protocols for gene targeting in *Physcomitrella patens***. *Methods Mol Biol* 2011, **715**:273-290.
45. Rensing SA, Lang D, Zimmer AD, Terry A, Salamov A, Shapiro H, Nishiyama T, Perroud PF, Lindquist EA, Kamisugi Y *et al*: **The *Physcomitrella* genome reveals evolutionary insights into the conquest of land by plants**. *Science* 2008, **319**:64-69.
46. Wang Y, Secco D, Poirier Y: **Characterization of the PHO1 gene family and the responses to phosphate deficiency of *Physcomitrella patens***. *Plant Physiol* 2008, **146**:646-656.
47. Ye J, Coulouris G, Zaretskaya I, Cutcutache I, Rozen S, Madden TL: **Primer-BLAST: a tool to design target-specific primers for polymerase chain reaction**. *BMC Bioinforma* 2012, **13**:134.
48. Le Bail A, Scholz S, Kost B: **Evaluation of reference genes for RT qPCR analyses of structure-specific and hormone regulated gene expression in *Physcomitrella patens* gametophytes**. *PLoS One* 2013, **8**:e70998.

49. Hiss M, Laule O, Meskauskiene RM, Arif MA, Decker EL, Erxleben A, Frank W, Hanke ST, Lang D, Martin A *et al*: **Large-scale gene expression profiling data for the model moss *Physcomitrella patens* aid understanding of developmental progression, culture and stress conditions**. *Plant J* 2014, **79**:530-539.
50. Zimmermann P, Hirsch-Hoffmann M, Hennig L, Gruissem W: **GENEVESTIGATOR. *Arabidopsis* microarray database and analysis toolbox**. *Plant Physiol* 2004, **136**:2621-2632.
51. Sakakibara K, Nishiyama T, Sumikawa N, Kofuji R, Murata T, Hasebe M: **Involvement of auxin and a homeodomain-leucine zipper I gene in rhizoid development of the moss *Physcomitrella patens***. *Development* 2003, **130**:4835-4846.
52. Cove D, Quatrano RS: **The Use of Mosses for the Study of Cell Polarity**. In: *New Frontiers in Bryology*. Springer Netherlands; 2004: 189-203.
53. Xu B, Ohtani M, Yamaguchi M, Toyooka K, Wakazaki M, Sato M, Kubo M, Nakano Y, Sano R, Hiwatashi Y *et al*: **Contribution of NAC transcription factors to plant adaptation to land**. *Science* 2014, **343**:1505-1508.

Table 1: Primers used for *CESApromoter::GUS* vector construction

Primer Name	Sequence ID	Sequence	Annealing Temp.
CesA3PROattB1	Pp1s8_137V6	GGGGACAAGTTTGTACAAAAAAGCAGGCTAATACACACACAGCGTCCCAAT	58˚C
CesA3PROattB5r		GGGGACAACTTTTGTATACAAAGTTGTGCTGCAACGCCACTCCGCT	
CesA4PROattB1	Pp1s90_244V6	GGGGACAAGTTTGTACAAAAAAGCAGGCTTGATTCATGTTGTGCGTGAT	59˚C
CesA4PROattB5r		GGGGACAACTTTTGTATACAAAGTTGGATGCAAGAATTTCTTTTTCC	
CesA5PROattB1	Pp1s30_48V6	GGGGACAAGTTTGTACAAAAAAGCAGGCTTGCGTTGTCTTATCGACTGC	64˚C
CesA5PROattB5r		GGGGACAACTTTTGTATACAAAGTTGCGCTCACCGGCGCTGCAACA	
CesA6PROattB1	Pp1s189_96V6	GGGGACAAGTTTGTACAAAAAAGCAGGCTTTGAGGGATCCATTCCAGTT	64˚C
CesA6PROattB5r		GGGGACAACTTTTGTATACAAAGTTGGCTTCCCTAACTCCACCACT	
CesA7PROattB1	Pp1s189_92V6	GGGGACAAGTTTGTACAAAAAAGCAGGCTTTTCGTGTACAATATCGCATCAT	64˚C
CesA7PROattB5r		GGGGACAACTTTTGTATACAAAGTTGGCCGCCAAACCACCTTC	
CesA8PROattB1	Pp1s112_75V6	GGGGACAAGTTTGTACAAAAAAGCAGGCTTTTGAGCTTTGAGCAATGTTGG	62˚C
CesA8PROattB5r		GGGGACAACTTTTGTATACAAAGTTGTGCAATACGACGCCGCTAGC	
CesA10PROattB1	Pp1s213_4V6	GGGGACAAGTTTGTACAAAAAAGCAGGCTTGTTCACCTCGCTGTCTGTC	64˚C
CesA10PROattB5r		GGGGACAACTTTTGTATACAAAGTTGGCTGCCGAAATCCCTCCCTC	
GUSattB5	Genbank FB507484.1	TATCATCTCGAGATTACTGCAGGTCGAGCCCACTGG	62˚C
GUSattB2		ATCACAAGTTTGTACAAAAAAGCTGAACGCTCGAGTGAGCTG	
CesA5attB5	Pp1s30_48V6	GGGGACAACTTTGTATACAAAAGTTGCGATGGAGGCTAATGCAGGCCTTAT	68˚C
CesaA5attB2		GGGGACCACTTTGTACAAGAAAGCTGGGTACTAACAGCTAAGCCCGCACTCGAC	

Table 2: Primers used for RT-qPCR.

Description:		Sequence	Amplicon size	µL per 20µL	Tm
CESA3	cesa3f2	TCTAATTGAGCCGAGGGCACC	172	1	86˚C
	cesa3r	ATCCTCCGGCACCTTCATTG			
CESA4	cesa4f2	CGGTCAATTTGGACAACCATG	102	0.8	80˚C
	cesa4r2	GCGTTGCAGATAGCATCACT			
CESA5	cesa5df	TGCAGGCTCACACAATCGTA	129	1.5	85˚C
	cesa5cR	GTCAACCGTGACTCCCACAT			
CESA7	cesa7aF	GCGAATGCAGGGCTGCTG	92	1	86˚C
	cesa7bR	ACATTACTCAACGGCCTCGG			
CESA8	cesa8F5	AATTCACGGGCCACGGCCTGA	135	1.2	83˚C
	cesa8R4	GCAAGTGCGACAAACTGGAAAGG			
CESA10	cesa10f2	GGAGATTGACTCATGCCACCT	194	1.7	85˚C
	cesa10r2	AACCTCCCTCTCCACTTGCT			

Figure Legend:

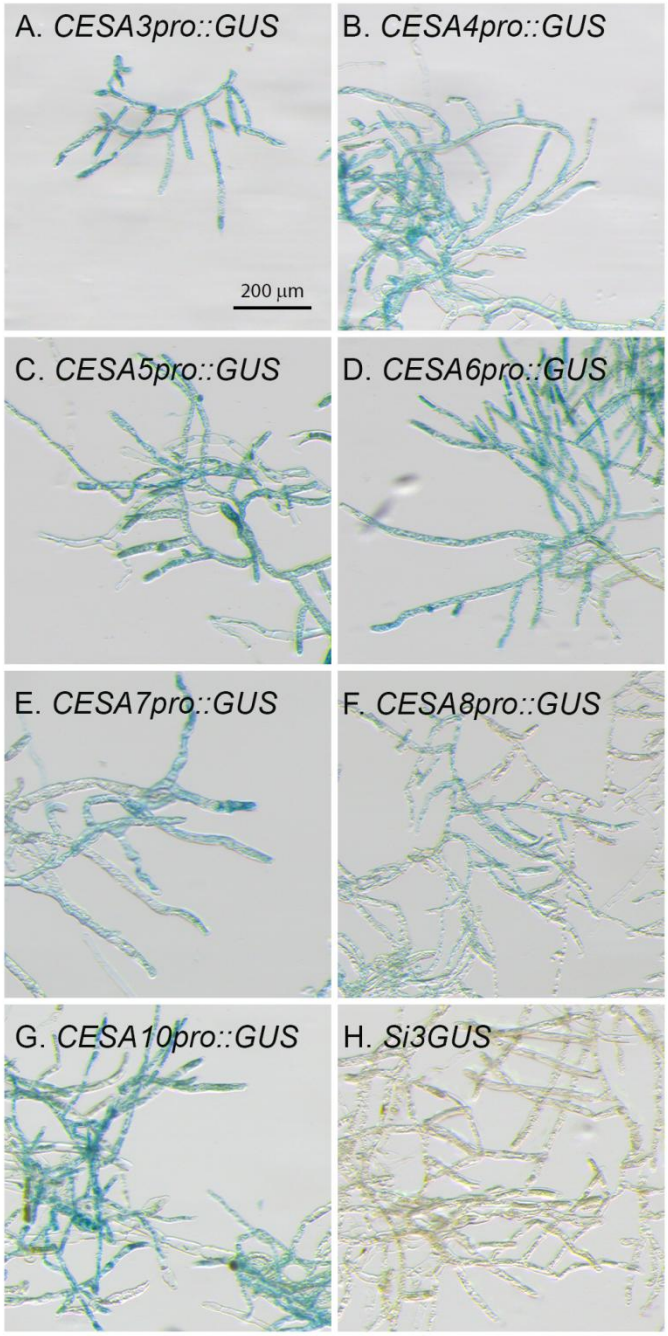

Figure 1. ***PpCESA* expression in protonema analyzed by histological staining** *CESApro::GUS* lines grown on BCDAT medium for 6 d were stained 6h. Protonema shows expression in (**A**) *CESA3pro::GUS*, (**B**) *CESA4pro::GUS*, (**C**) *CESA5pro::GUS*, (**D**) *CESA6pro::GUS*, (**E**) *CESA7pro::GUS*, (**F**) *CESA8pro::GUS*, and (**G**) *CESA10pro::GUS.* There is no staining the protonemal tissue of the negative control line (**H)**, GUS only with no promoter).

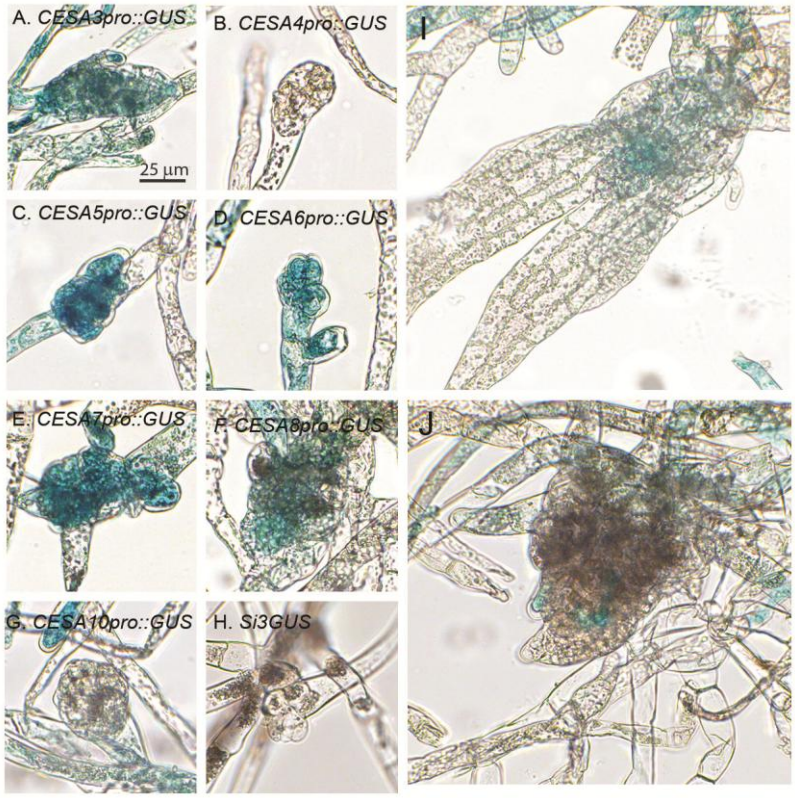

Figure 2. ***PpCESA*** **expression in young and older buds analyzed by histological staining**

CESApro::GUS lines grown on BCD for 1 week and stained for 6 h. Expression throughout young buds in **(A)** *CESA3pro::GUS*, (**C**) *CESA5pro::GUS*, (**D**) *CESA6pro::GUS*, (**E**) *CESA7pro::GUS*, and (**F**) *CESA8pro::GUS*. No staining was seen within the buds in (**B**) *CESA4pro::GUS*, (**F**) *CESA10pro::GUS*, and (**G**) negative control *GUS* line. Expression in (**H**) the apical meristem of older buds with leaves in *CESA3pro::GUS*, and (**J**) expression in axillary hairs in *CESA4pro::GUS*.

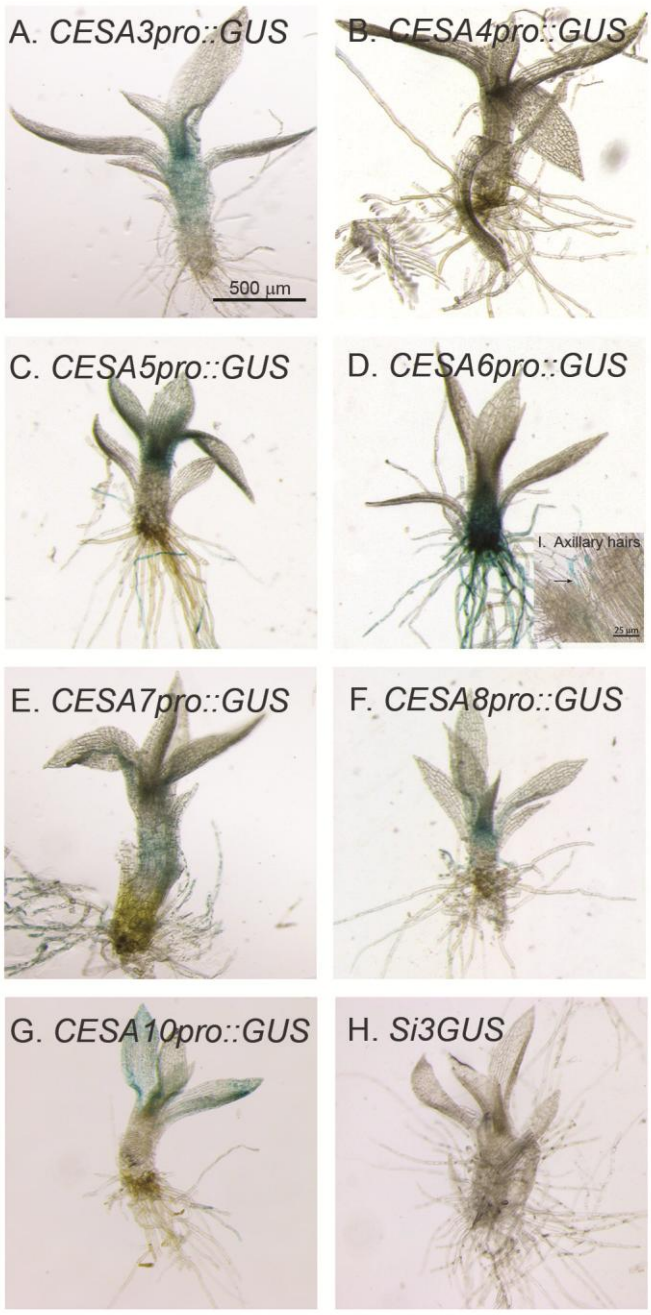

Figure 3. **Majority of *PpCESA*s are expressed in gametophores based on histological staining**
CESApro::GUS lines grown on BCD for 2 weeks and stained for 16 h. Expression in gametophore bases, leaves, and young rhizoids in **(A)** *CESA3pro::GUS*, (**C**) *CESA5pro::GUS*, (**E**) *CESA7pro::GUS*, and (**F**) *CESA8pro::GUS*. (**D**) Strong expression throughout gametophore stems and older rhizoids, and also in leaves in *CESA6pro::GUS.* Expression only within leaves in (**G**) *CESA10pro::GUS*. No expression in (**B**) *CESA4pro::GUS* and (**H**) negative control *GUS* line.

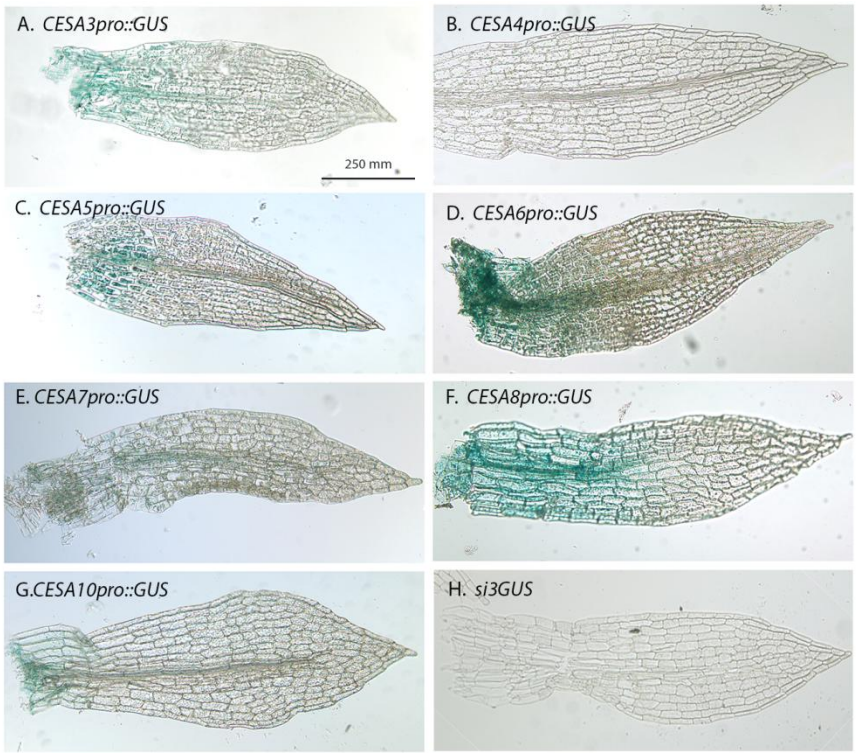

Figure 4. **Differential expression in leaves with a developed or developing midvein analyzed by histological staining**
Leaves from gametophores with 6-10 leaves from *CESApro::GUS* lines were stained for 16 h. Strong staining in the leaf bases in (**A**) *CESA3pro::GUS*, (**C**) *CESA5pro::GUS*, (**D**) *CESA6pro::GUS*, and (**F**) *CESA8pro::GUS* lines. Faint staining in the leaf bases of (**E**) *CESA7pro::GUS and* (**G**) *CESA10pro::GUS*. Weak staining in developing veins in **(A)** *CESA3pro::GUS*, (**D**) *CESA6pro::GUS*, (**E**) *CESA7pro::GUS* and (**F**) *CESA8pro::GUS*.

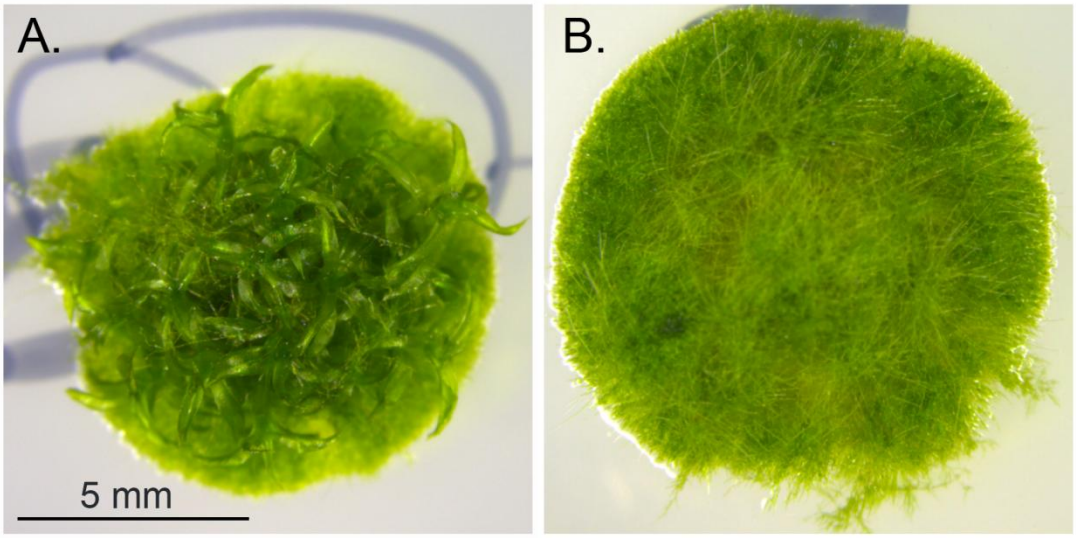

Figure 5. R**escue of *cesa5KO* with *CESA5pro::CESA5cDNA***
(**A**) cesa5KO rescue with *CESA5pro::CESA5cDNA* and (**B**) *cesa5KO*.

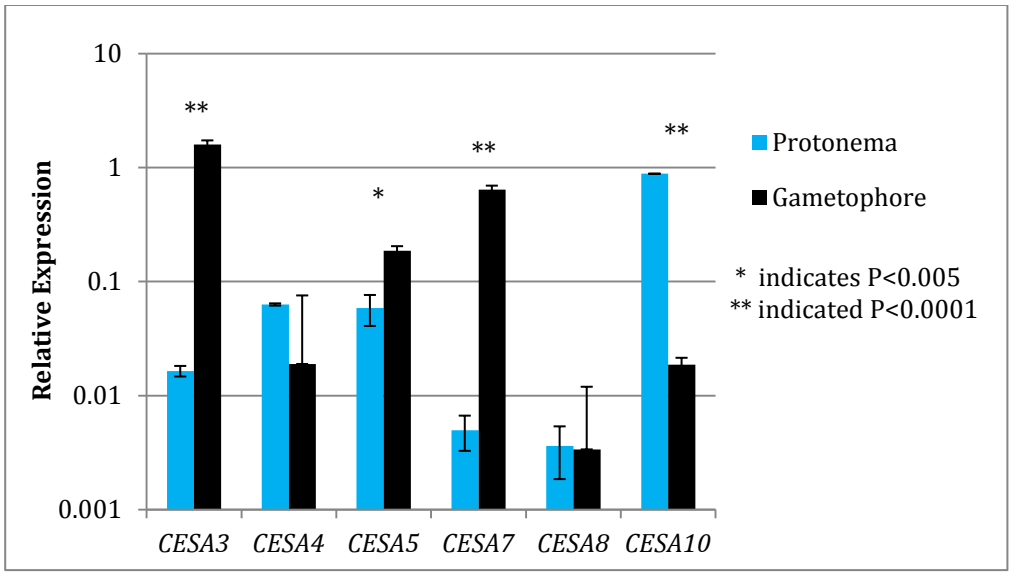

Figure 6. **Relative expression of *CESAs* of in 6-day-old protonemal and 3-week-old gametophore tissue of *P. patens*.**
Expression levels were measured using qPCR and normalized to PpVhpp and PpACT. Three independent samples were assayed in duplicate for the gametophore and protonema qPCR. Stars indicate significant difference, where * P<0.005 and ** is P<0.0001. *CESA10* is most highly expressed in protonemal tissue (blue bars). *CESA3*, *CESA5*, and *CESA7* are more highly expressed in gametophores (black bars). *CESA8* has similar expression in both the gametophores and protonema.

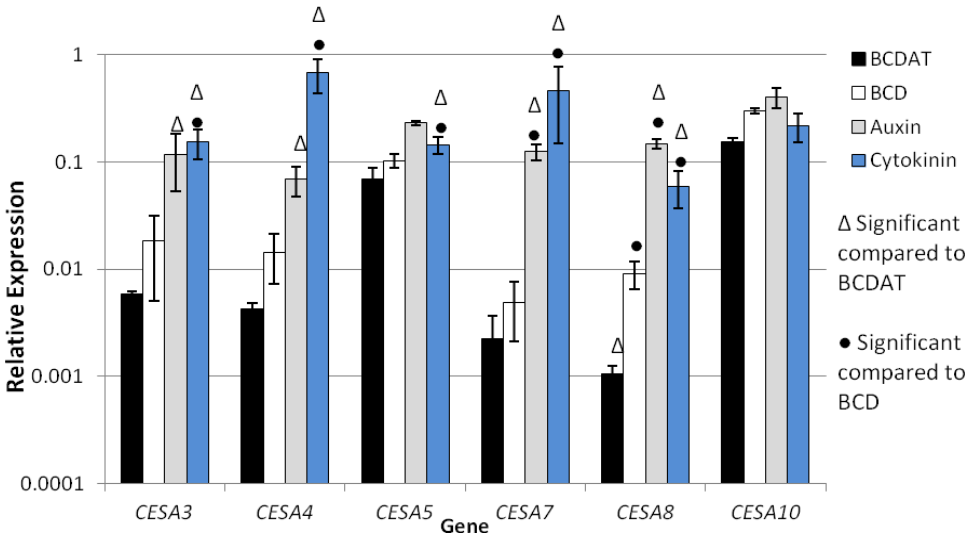

Figure 7. **Relative expression patterns of *PpCESAs* grown on BCDAT, BCD, BCD+auxin, and BCD+cytokinin for 7 days.**
Expression levels were measured using qPCR and were normalized to PpVhpp and PpACT. Three independent samples were assayed in duplicate. *CESA8* has higher expression on BCD media, which induces gametophore development, while all other *CESAs* have equivalent expression in both BCDAT and BCD, where BCDAT induced protonemal tissue. Higher expression levels of *CESA3*, *CESA4*, *CESA7*, and *CESA8* were found for auxin–treated tissues that over-produce rhizoids and higher expression levels for *CESA3*, *CESA4*, *CESA5*, *CESA7*, and *CESA8* in cytokinin-treated tissues that overproduce gametophores. *CESA10* expression level remains constant on all media (BCDAT, BCD, BCD+auxin, and BCD+cytokinin).

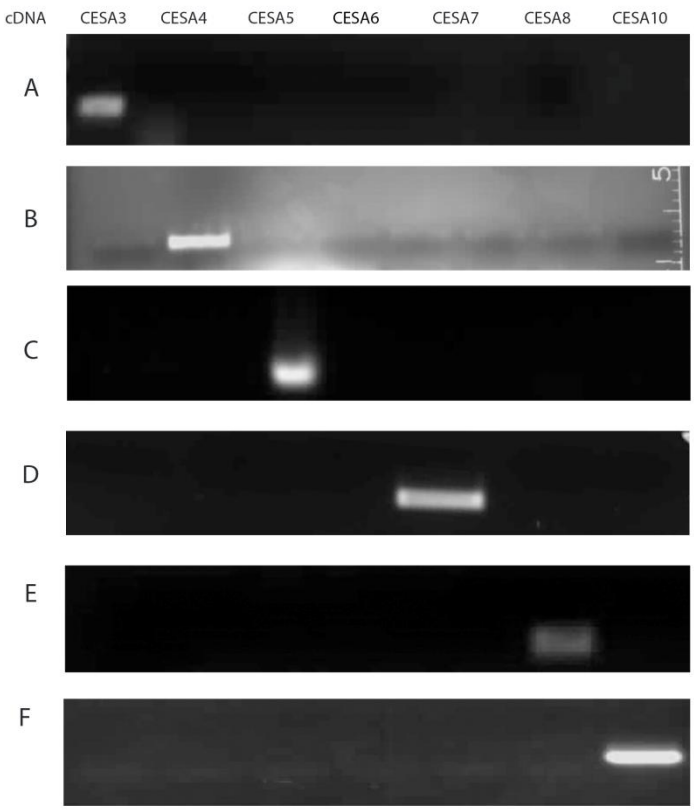

Additional File 1: **Primer Specificity**
2% agarose gel that PCR reactions used to test primer specificity tested for primers (**A**) CESA3, (**B**) CESA4, (**C**) CESA5, (**D**) CESA7, (**E**) CESA8, and (**F**) CESA10 against the following cDNA plasmids listed above. All primers listed are specific with correct band sizes.

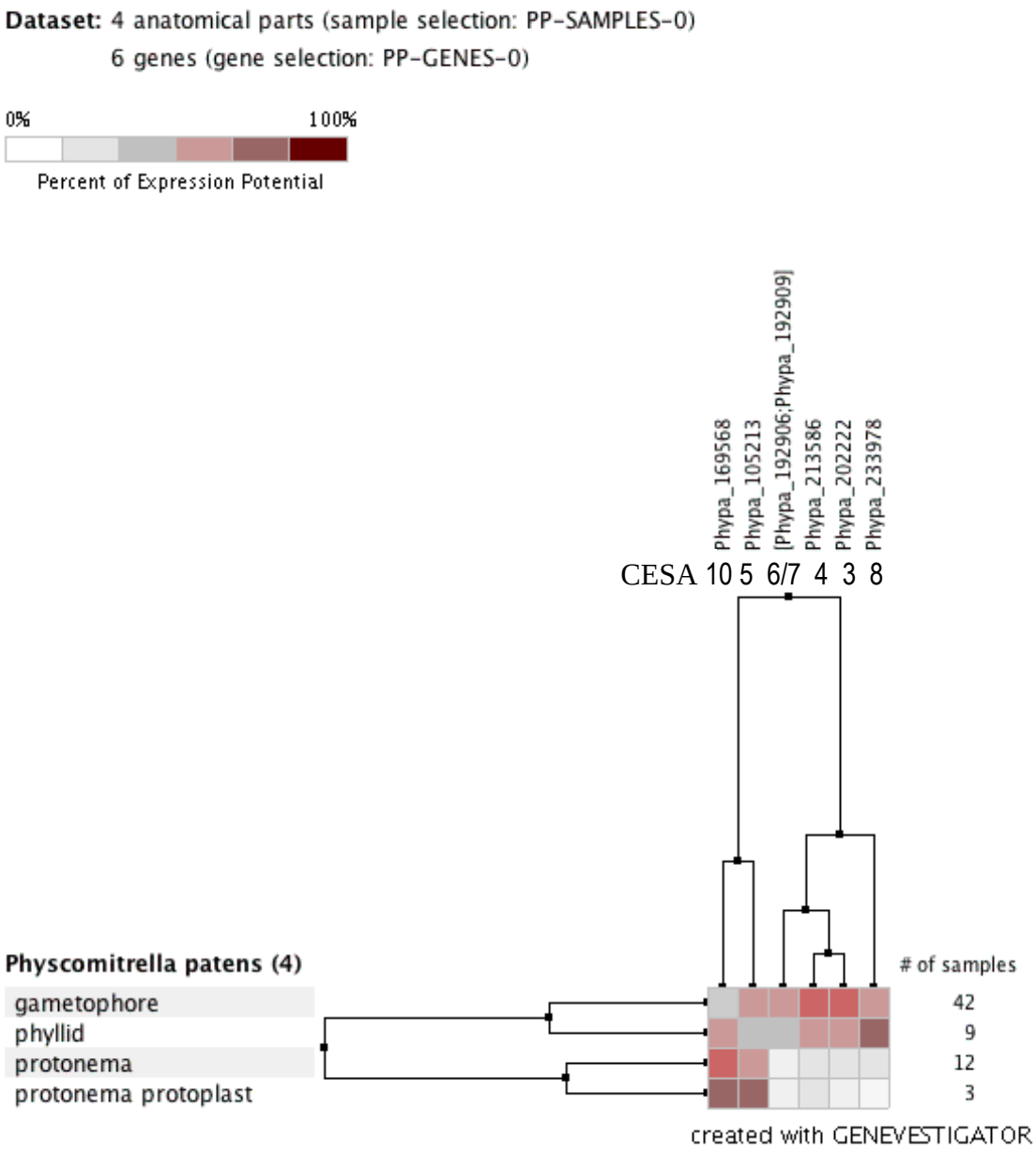
Dataset: 4 anatomical parts (sample selection: PP-SAMPLES-0)
6 genes (gene selection: PP-GENES-0)
0%
100%
Percent of Expression Potential
Phypa_169568
Phypa_105213
[Phypa_192906;Phypa_192909]
Phypa_213586
Phypa_202222
Phypa_233978
CESA 10 5 6/7 4 3 8
Physcomitrella patens (4)
gametophore
phyllid
protonema
protonema protoplast
# of samples
42
9
12
3
created with GENEVESTIGATOR

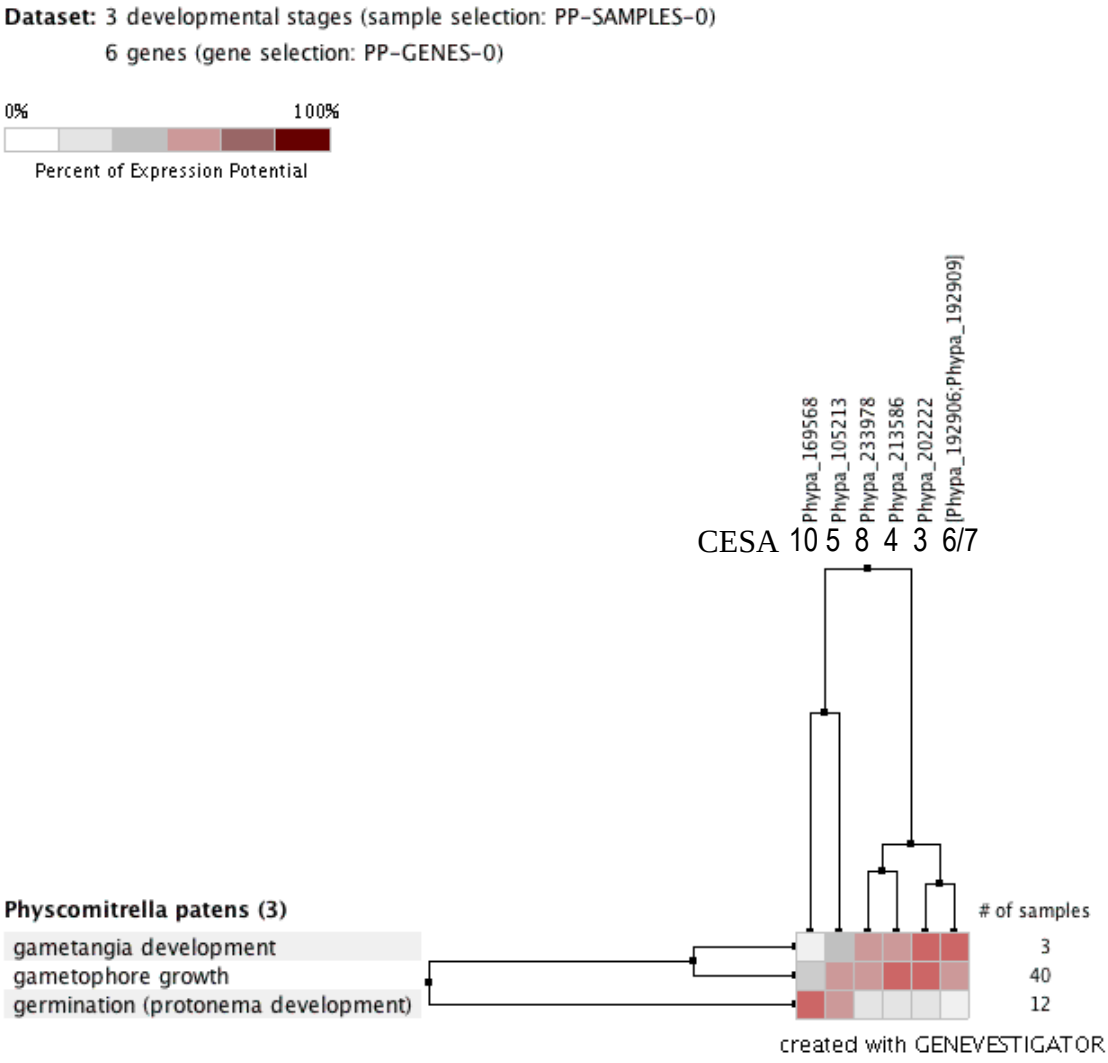
Dataset: 3 developmental stages (sample selection: PP-SAMPLES-0)
6 genes (gene selection: PP-GENES-0)
0%
100%
Percent of Expression Potential
Phypa_169568
Phypa_105213
Phypa_233978
Phypa_213586
Phypa_202222
[Phypa_192906;Phypa_192909]
CESA 10 5 8 4 3 6/7
Physcomitrella patens (3)
gametangia development
gametophore growth
germination (protonema development)
# of samples
3
40
12
created with GENEVESTIGATOR

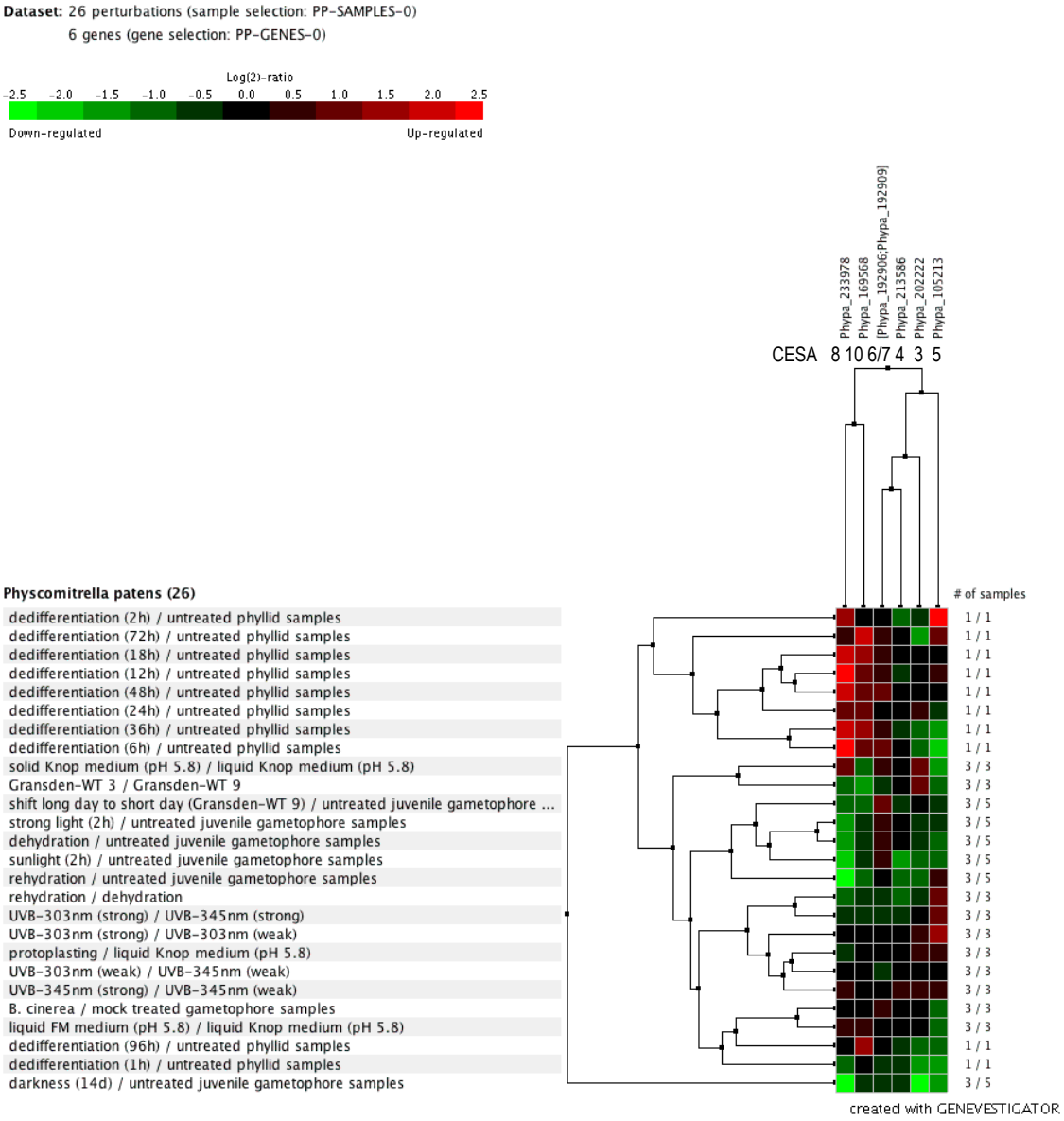

Additional File 2: **Hierarchical clustering of *PpCESA* expression**
Hierarchical clustering of Phypa_105213 (*PpCESA5*), Phypa_233978 (*PpCESA8*), Phypa_202222 (*PpCESA3*), Phypa_213586 (*PpCESA4*), Phypa_192909/ Phypa_192906 (*PpCESA6/7*), and Phypa_169568 (*PpCESA10*) of anatomy, developmental stages, and perturbations from microarray data. For anatomy and developmental stages, white indicates 0% expression and dark purple indicates 100% expression. For perutbations, green shadings indicate down-regulation, while red shadings indicate up-regulation.

Manuscript 2

Cell wall composition after 24 h regeneration of protoplasts

Formatted for the publication in *BMC Plant Biology*

Mai Tran, Elizabeth Berry, and Alison Roberts

Authors:

Mai L. Tran, University of Rhode Island, maitran@my.uri.edu

Elizabeth Berry, University of Rhode Island, elizabeth_berry@my.uri.edu

Alison W. Roberts, University of Rhode Island, ARoberts@ds.uri.edu

120 Flagg Road, Kingston, Rhode Island 02881

Abstract:

Although the study of the vascular plant cell wall has been extensive, there has been no comprehensive study of the cell wall of non-vascular plant *Physcomitrella patens*, particularly protoplast cell walls. Protonemal filaments from the moss *P. patens* can be digested into protoplasts, which are single plant cells devoid of a cell wall. These protoplasts can regenerate cell walls within 24 h. With immuno and affinity histochemical staining, we examined the distribution of polysaccharides and proteins in the regenerated cell wall through microscopy and measured the intensity of staining using flow cytometry. Cellulose, arabinogalactan proteins (AGPs), and callose were found to be most abundant in protoplasts. No homogalacturonan and very little 1,4-β-D-galactan were detected. Moderate to low levels of mannan, arabinan, and xyloglucan were present in protoplasts.

Introduction:

The plant cell wall is very dynamic and has many components, such as pectin, hemicelluloses, arabinogalactan proteins (AGPs), and cellulose. In previous studies, examining the different cell wall polysaccharides has led to the understanding how plant cells grow, divide, and interact with neighboring cells [54]. Cellulose acts as a structural scaffold to the cell wall, while hemicelluloses associate with cellulose to help cell plants growth [29]. Cellulose has been shown to be essential in plant growth from mutational analysis [2]. Hemicellulose links cellulose microfibrils and matrix together through hydrogen bonding and has also shown a role in storage of carbohydrates as mannan [27, 55]. Pectin synthesis and modification is highly regulated and been associated with cell wall flexibility [29]. AGPs have been shown to

covalently bond to pectin and are necessary for apical cell extension in *P. patens* [25, 54].

Immuno and affinity histochemical techniques using carbohydrate-binding modules (CBMs) and monoclonal antibodies are beneficial in studying these cell wall components in different plant organs and developmental stages [54]. Limited characterization of *P. patens* cell wall components through immuno-histochemical staining was done in caulonema, chloronema, rhizoids, and gametophores. AGPs and 1, 5-α arabinin are found throughout filamentous tissue and slightly concentrated at tips [25]. Protoplasts were also seen to have 1,5-α arabinan. Low amounts of xylan were seen in throughout gametophores, but more concentrated in axillary hairs. Xyloglucan was also abundant throughout gametophores [26]. Mannan was found in protonema with deposition concentrated in cell junctions [27]. Callose was found in early developing spores [28] and cellulose was found in developing gametophore buds [11]. No comprehensive study of cell wall composition has been done in all the tissues and few immuno and affinity histochemical studies have been done in protoplasts.

In addition to histochemical staining, high throughput microarrays have been used by others to profile the abundance of cell wall components in different tissues of *P. patens* [24]. In protonema high levels of mannan, arabinan, and crystalline cellulose and moderate to low amounts of galactan, nonfucosylated xyloglucan, xylan, and AGPs were detected. The highest amounts of cellulose, arabinan, and AGPs were seen in gametophores and sporophytes [24].

Protoplasts of *P. patens* represent the simplest form of a plant with only one cell type, consisting of only a single cell with no cell wall. Using this uniform cell type allowed

us to quantify labeling intensity efficiently through flow cytometry without needing to sort cell types for data analysis. We allowed the protoplasts to regenerate its cell wall for 24 h. At this point, the protoplasts had deposited their cell walls and some had begun to divide and form a filament. This allowed us to examine the first cell wall components that were deposited during regeneration and the initiation of cell division. With flow cytometry, we also determined relative abundance of each cell wall components by capturing the mean fluorescent intensity per cell in high volumes. These results were compared with carbohydrate microarrays [24]

Materials and Methods:

Moss protonemal tissue was digested into protoplasts and protoplasts were grown on PRMB media for 24 h, according to [44]. After 24 h, protoplasts were collected by washing the plates with 3 mL of de-ionized water and centrifuging the resulting suspension with a clinical centrifuge at speed 4 with no braking for 3 min. Protoplast density was measured with a hemocytometer [44]. Protoplasts were resuspended in 1 mL of fixation solution (7% formaldehyde, 50 mM PIPES, pH 6.8, 2.5 mM magnesium sulphate, 5 mM EGTA) for either 20 min at room temperature or overnight at 4°C. Fixed protoplasts were washed three times with 3 mL of Phosphate-buffered saline (PBS) and collected each time by centrifuging for 3 min at speed 4 with a clinical centrifuge. Aliquots of 100,000 protoplasts were transferred into 1.5 mL tubes. Protoplasts were blocked with 200 μL blocking solution (5% non-fat milk 1XPBS solution) for 20 min and were centrifuged at 1000 x g for 5 min in a microcentrifuge. Protoplasts were then labelled using LM2, LM5, LM6, LM10, LM15, LM18, LM19, LM20, and JIM13 (Plant Probes, **University of Leeds,** United

Kingdom), diluted 1:5 in blocking solution, or incubated in blocking solution with no primary antibody as a negative control for 1.5 h and then labelled with anti-Rat IgG AlexaFluor488 (Invitrogen, Grand Island, NY, USA) diluted 1:50 in blocking solution for 1 h. After each labeling step, all protoplasts were washed thrice with 1XPBS by pelleting protoplasts at 1000 x g for 5 min, aspirating the previous solution, and adding 200 μL of 1XPBS with occasional agitation. Alternatively, fixed and washed protoplasts were stained with CBM3a and CBM28 at concentrations 1:200 in blocking solution for 1 h, then mouse anti-polyhistidine at 1:100 in blocking solution for 1.5 h (Sigma, St. Louis, MO, USA), and anti-mouse IgG AlexaFluor488 (Invitrogen) secondary antibody at 1:50 in blocking solution for 1 h. Again, after each labeling step, protoplasts were carefully washed thrice with 1XPBS (Roberts et al. 2011). Also, fixed a washed protoplasts were stained with 400-2 and 400-4 (Biosupplies Australia, Bundoora, Victoria, Australia) dilulted 1:200 in blocking solution for 1 h and anti-mouse IgG AlexaFluor488 (Invitrogen) secondary antibody at 1:50 in blocking solution for 1 h. After each labeling step, protoplasts were carefully washed thrice with 1XPBS [44].

Stained protoplasts were resuspended in 500 uL of 1xPBS. 10 μL of suspension was mounted on a glass slide with Prolong Gold antifade mounting reagent (Invitrogen) for imaging and the rest was analyzed using a BD Influx flow cytometer with 100 μM flow tip, FACS sheath fluid, and FACS Software V1.0 with (BD Bioscience, San Jose, CA, USA). Flow rates were set to approximately 200 cells sec^{-1}. Voltages were set to gate negative control (protoplasts with no primary antibody staining) and protoplasts with the highest AlexFluor488 fluorescence (stained with CBM3a) within

the 530/40 plotting range. Approximately 30,000 events were collected per sample. Population 1 was selected based on FSC and SSC for round protoplasts (Figure 1A) [56]. Population 1 was examined for chlorophyll autofluorescence with 692/40 filter, which revealed two populations of protoplasts with high and low intensities for chlorophyll autofluorescence (Figure1B). Population 2 with high chlorophyll autofluorescence and population 3 with low chlorophyll autofluorescence were gated separately and measured for fluorescent intensity of AlexaFluor488 with 530/40(488) filter (Figure1C). All experiments were repeated in duplicates with 3 pooled biological replicates. T-test was used to test for statistical significances between high and low chlorophyll mean fluorescence intensity between the stains and mean fluorescence intensity between positive and negative staining.

Protoplasts were examined with an Olympus BH2-RFCA compound microscope (Olympus America Inc, Center Valley, PA, USA) at 12.5x magnification and images were acquired with Leica DFC310FX camera (Leica Microsystems Inc., Buffalo Grove, IL, USA).

Results:

Flow cytometry data.

Populations of round protoplasts were selected based on FSC and SSC and cellular debris was omitted which has very low FSC at 10^2 and SSC at 10^1. As expected, negative controls had no or very low fluorescence with mean fluorescence intensity of less than 20 and served as a baseline for the measurement of fluorescent intensity. Round protoplasts had a very wide range of chlorophyll autofIuorescence, and the two

populations delineated on the scatter plot of FSC and 692/40 were designated as either high levels or low levels of chlorophyll autofluorescence.

Mean fluorescent intensities of 24 h regenerated protoplasts were examined in populations with low and high levels of chlorophyll autofluorescence. High chlorophyll content indicates mature protoplast regeneration since they have a thicker cell wall compared to low chlorophyll content protoplasts with a fully rounded shape (Figure 3B). Low chlorophyll content protoplasts are irregular shape and have very thin cell wall (Figure 3A).

Very high levels of crystalline cellulose labeling with CBM3a were detected in regenerating protoplasts. Significantly higher CBM3a labeling was detected in high chlorophyll autofluorescent protoplasts ($P<0.0001$). Very low amounts of amorphous cellulose labeling (CBM28) was observed in both low and high chlorophyll content in the protoplasts. Moderate levels of anti-callose labeling (400-2) were detected and there was no difference in high and low chlorophyll autofluorescent protoplast populations.

Moderately low levels of anti-mannan labeling with 400-4 were detected in both high and low chlorophyll autofluorescence protoplast populations. Low levels of anti-nonfucosylated xyloglucan labeling (LM15) were detected in protoplasts with higher levels of anti-xyloglucan labeling seen in high chlorophyll autofluorescence protoplast. Fucosylated xyloglucan was not tested, since almost no fucosylated xyloglucan was previous detected in carbohydrate microarrays [24]. No xylan was detected in protoplasts and fluorescence was not statistically different from the negative control.

No labeling of esterified and nonesterified homogalacturonans was detected by flow cytometry using LM19 and LM20 antibodies when compared to no primary antibody control ($P>0.05$). This is consistent with microscopic analysis where no labeling was detected. Very low levels of anti-1,4-β-D-galactan (LM5) were detected by flow cytometry similar to the microscopic analysis. Moderate levels anti-1,5-α-L-arabinan (LM6) were detected with higher levels in high chlorophyll autofluorescence protoplasts ($P<0.0001$). 1,5-α-L-arabinan appears to be the most abundant pectin epitope in protoplasts with higher amounts in mature protoplasts ($P<0.0001$).

High levels of anti-AGPs labeling with LM2 and JIM13 antibodies were also detected in regenerated protoplasts. Interestingly, JIM13 labelled anti-AGPs appear more abundant in high chlorophyll than low chlorophyll autofluorescence protoplasts, while LM2 labeling is greater in low chlorophyll protoplasts versus high chlorophyll ($P<0.0001$).

Microscopy.

Immuno-labelled protoplasts were examined with a compound microscope. Protoplasts were sorted as immature, mature round, and dividing protoplasts as well as developing filament.

Crystalline cellulose (CBM3a) is strongly labelled throughout immature, mature round, and dividing protoplasts as well as developing filament (Figure 3E-H). Faint amorphous cellulose (CBM28) is labelled in immature protoplasts, but no amorphous cellulose is detected in other protoplasts stages (Figure 3I-L). Callose (400-2) has strong punctate staining throughout all stages of protoplast development (Figure 3M-P).

Mannan (400-4) had moderate labeling in young protoplasts and less in the mature and dividing protoplasts (Figure 3 Q-T). No staining was seen in the extended filament. Low levels of anti-nonfucosylated xyloglucan (LM15) are in the mature protoplasts, with no staining in other protoplasts stages (Figure 3U-X).

No labeling of esterified homogalacturonans (LM19) staining was seen in protoplasts (Figure 3Y-AA). Nonesterified homogalacturonans (LM20) had light punctate staining in young protoplasts (Figure3 BB). Slightly more nonesterified homogalacturonan is seen in mature protoplasts and dividing protoplasts. No staining of nonesterified homogalacturonan was seen in the filaments.

Very low levels of anti-1,4-β-D-galactan (LM5) punctate staining was seen in immature protoplast with lighter staining in mature, dividing, and growing filament (Figure 3 CC-FF). Moderate punctate staining was seen with anti-1,5-α-L-arabinan (LM6) (Figure 3 GG-JJ). 1,5-α-L-arabinan appeared to be the most abundant pectin in protoplasts with higher amounts in mature protoplasts.

Anti-AGPs (LM2) had slightly stronger staining in young protoplasts and medium staining in mature and dividing protoplasts. No staining was seen in growing filament (Figure KK-NN).

Discussion:

The most abundant polysaccharide in regenerated protoplasts is crystalline cellulose, which is deposited as the cell matures. Crystalline cellulose content appeared greater in protoplasts than protonema and gametophore tissue from microarray analysis [24]. One of the reasons why crystalline cellulose may appear to be more abundant is that protoplasts, devoid of a cell wall, are grown under high osmotic conditions to prevent

rupturing of the cell. The high osmotic media may cause the upregulation of cellulose [13]. Another polysaccharide that is abundant in protoplasts is callose. Callose has been shown to be important in abiotic stress and plant development [57] and was found to be the second most abundant polysaccharide in protoplast in our study. Protoplasts undergo high levels of abiotic stress from the removal of the cell wall using Drislease enzymes and washing in osmotic media; therefore, high levels of callose are expected.

Among hemicelluloses, mannan is the most abundant in protoplasts. Moderate levels of mannan have been previously seen in both chloronema and caulonema tissue with a stronger deposition between cell junctions [24, 27]. Currently, the exact function of mannan is unknown, but there are indications of its role in cell differentiation [54]. Low levels of nonfucosylated xyloglucan were detected in protoplasts with LM15. Low levels were also seen in protonemal tissue when microarrays were probed with LM15 [24]. However, the shoot axis of the gametophore labelled strongly using CCRC-M88 [26]. CCRC-M88 (National Center for Biomedical Glycomics, Athens, GA, USA) has a higher cross reactivity with XXGG xyloglucan [58] compared to LM15, which has a higher cross reactivity with XXXG xyloglucan[59]. *Physcomitrella patens* xyloglucan was found to be the XXGG type [60]. Both branched and unbranched xylan was found at low levels in chloronemal tissue [24] but no xylan was found in protoplasts. Only axillary hairs show strong xylan labeling [24, 26].

α 1, 5-arabinan (LM6) and galactan (LM5) were the only pectin epitopes detected in protoplasts. No homogalacturonan was detected with FACS. Previously, microarray

analysis showed low detection of esterified homogalacturonan (JIM5 and JIM7) and moderate levels of nonesterified homogalacturonan (mAb2F4) in protonemal tissue [24]. Based on our results and microarray data, early stages of *P. patens* do not contain high levels of homogalacturonan. High levels of α 1, 5-arabinan (LM6) are deposited in mature and dividing protoplasts, which can occur as side chains of either pectin or AGP. There are only low amounts of galactan in young protoplasts. Less galactan is seen in older protoplasts. Because anti-arabinan (LM6) is also believed to associate with AGPs, our data matches very well with high levels of AGPs detected by JIM13 and moderate levels of AGPs through LM2 [25]. Based on microscopy, LM2 labels more strongly than JIM13. Since LM2 and JIM13 recognize different epitopes, different types of AGPs are recognized by the different antibodies and are expected to reveal slightly different profiles of AGPs [61, 62].

Conclusion:

P. patens is becoming an ideal model plant for studying the cell wall due to its fully sequenced genome, quick regeneration time, and ability to be genetically manipulated [42]. However, currently there has not been a comprehensive study in the cell wall composition in protoplasts. Here, flow cytometry and immuno and affinity histochemical labeling help us understand the localization of different cell wall components. Knowing the cell wall composition and abundance can allow us to understand how the cells develop early in growth. With a comprehensive study, we can analyze mutant phenotypes more effectively for defects within cell wall composition.

Figure Legend:

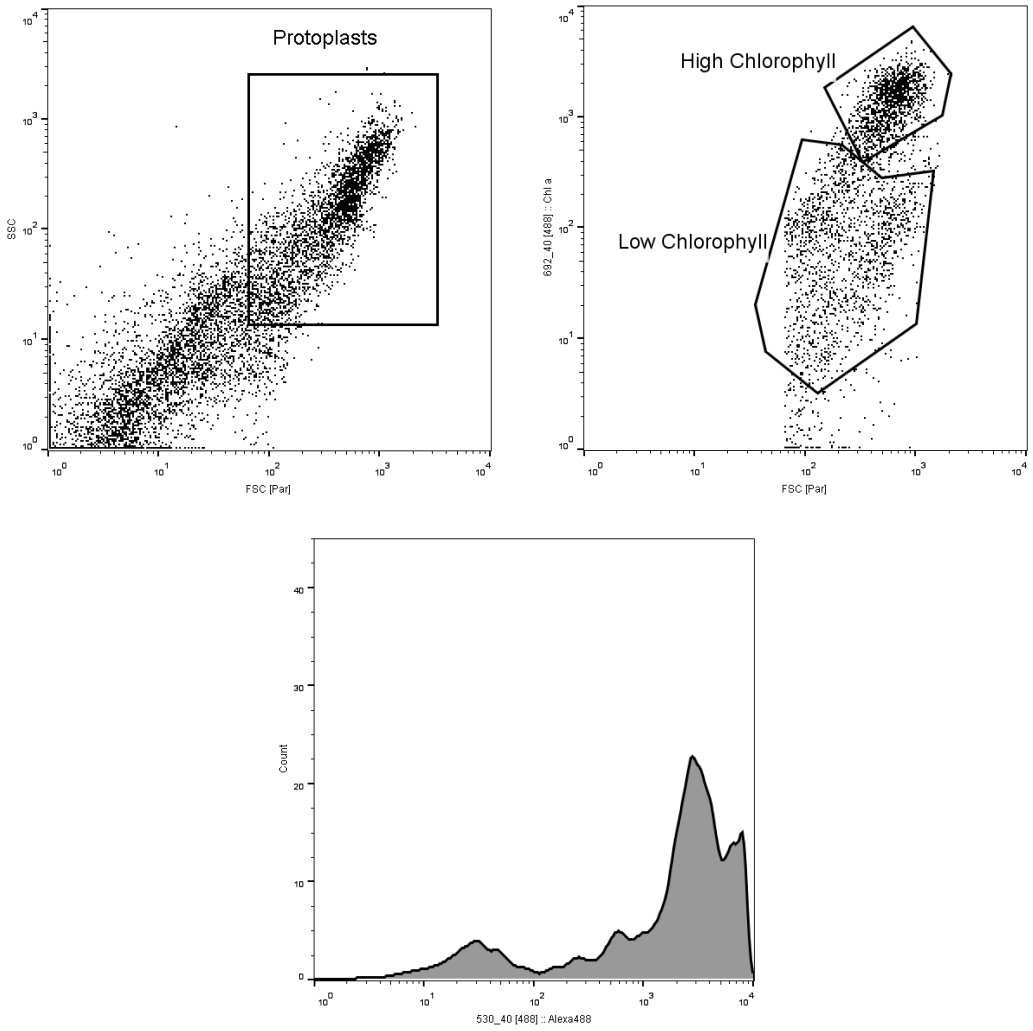

Figure 1. Gating of flow cytometry data
(**A**) Population 1 created from gating of round protoplasts based on FSC and SSC scattered plots. (B) Gating of high and low chlorophyll autofluorescence based on population 1. (**C**) Histogram of fluorescence intensities on the high/low chlorophyll autofluorescences from (**B**).

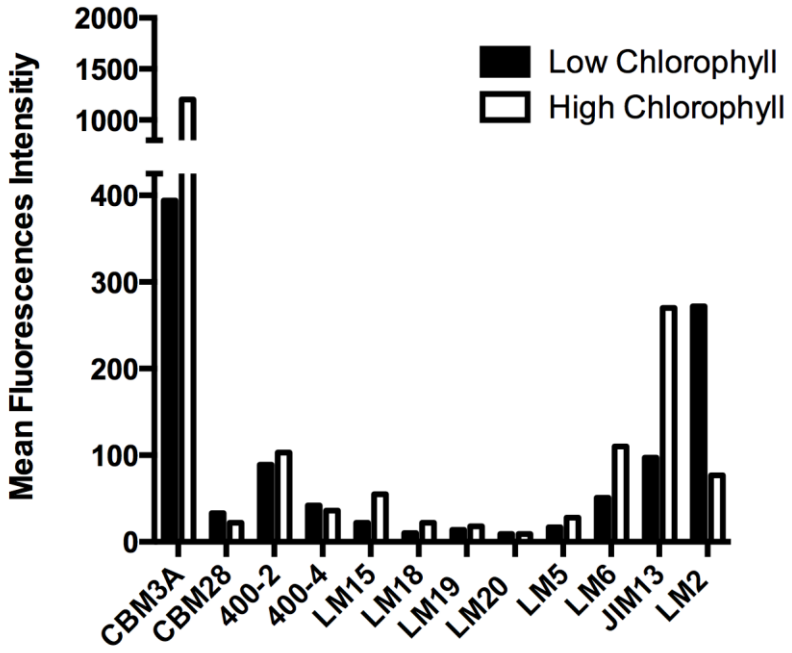

Figure 2. Mean fluorescent intensities of 24 h regenerated protoplasts
Protoplasts were grown on PRMB media to allow 24 h of cell wall regeneration. Regenerated protoplasts were fixed and stained with the following probes: LM2, LM5, LM6, LM10, LM15, LM18, LM19, LM20, 400-2, 400-4, CBM3a, CBM28, and JIM13 (www.plantprobes.net). 30,000 stained regenerated protoplasts were analyzed with flow cytometry. Results were gated for round protoplasts based on forward scatter (FSC) and side scatter (SSC). Round protoplast population was then gated for high and low chlorophyll autofluorescences and mean fluorescent is graphed.

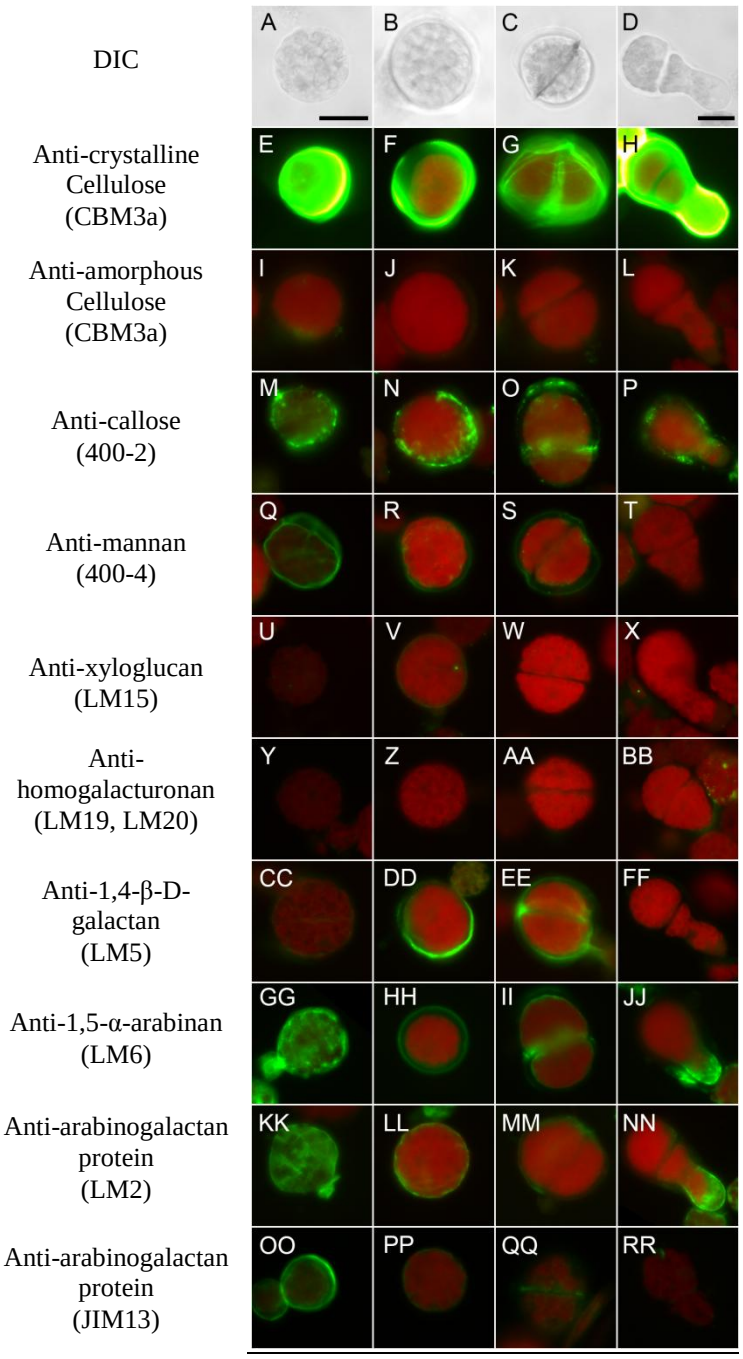

Figure 3. Micrographs of 24 h regenerated protoplasts
24 h regenerated protoplasts were fixed and stained with the following probes: LM2, LM5, LM6, LM10, LM15, LM18, LM19, LM20, 400-2, 400-4, CBM3a, CBM28, and JIM13 (Plant Probes). Protoplasts were mounted onto a glass slide with Prolong Gold anti-fade reagent and imaged at 10X magnification. Differential interference contrast images displays four stages of regeneration A) thin-walled stage, B) thick-walled stage, C) divided, and D) filament extension. Head columns of images of cells are at the same stage and labelled with different probes. Protoplasts were labelled with E-H) CBM3a for crystalline cellulose, I-L) CBM28 for non-crystalline cellulose, M-P) anti-

callose (BS-400-2), Q-T) anti-mannan (BS-400-4), U-X) anti-xyloglucan (LM15), Y-BB) anti-homogalacturonan (LM19 in Y-AA, LM20 in BB), CC-FF) anti-1,4-β-D-galactan (LM5), GG-JJ) anti-1,5-α-L-arabinan (LM6), KK-NN) anti-arabinogalactan protein (LM2), and OO-RR) anti-arabinogalactan protein (JIM13). Scale bar shown is at 20 µm.

References:

1. Knox JP: **Revealing the structural and functional diversity of plant cell walls**. *Curr Opin Plant Biol* 2008, **11**:308-313.
2. Cosgrove D: **Growth of the plant cell wall**. *Nature Rev Mol Cell Biol* 2005, **6**:850 - 861.
3. Somerville C: **Cellulose synthesis in higher plants**. *Annu Rev Cell and Dev Biol* 2006, **22**:53-78.
4. Cosgrove DJ: **Growth of the plant cell wall**. *Nat Rev Mol Cell Biol* 2005, **6**:850-861.
5. Liepman AH, Nairn CJ, Willats WG, Sorensen I, Roberts AW, Keegstra K: **Functional genomic analysis supports conservation of function among cellulose synthase-like a gene family members and suggests diverse roles of mannans in plants**. *Plant Physiol* 2007, **143**:1881-1893.
6. Lee KJ, Sakata Y, Mau SL, Pettolino F, Bacic A, Quatrano RS, Knight CD, Knox JP: **Arabinogalactan proteins are required for apical cell extension in the moss *Physcomitrella patens***. *Plant Cell* 2005, **17**:3051-3065.
7. Kulkarni AR, Pena MJ, Avci U, Mazumder K, Urbanowicz BR, Pattathil S, Yin Y, O'Neill MA, Roberts AW, Hahn MG *et al*: **The ability of land plants to synthesize glucuronoxylans predates the evolution of tracheophytes**. *Glycobiology* 2012, **22**:439-451.
8. Schuette S, Wood AJ, Geisler M, Geisler-Lee J, Ligrone R, Renzaglia KS: **Novel localization of callose in the spores of Physcomitrella patens and phylogenomics of the callose synthase gene family**. *Ann Bot* 2009, **103**:749-756.
9. Goss CA, Brockmann DJ, Bushoven JT, Roberts AW: **A CELLULOSE SYNTHASE (CESA) gene essential for gametophore morphogenesis in the moss *Physcomitrella patens***. *Planta* 2012, **235**:1355-1367.
10. Moller I, Sorensen I, Bernal AJ, Blaukopf C, Lee K, Obro J, Pettolino F, Roberts A, Mikkelsen JD, Knox JP *et al*: **High-throughput mapping of cell-wall polymers within and between plants using novel microarrays**. *Plant J* 2007, **50**:1118-1128.
11. Roberts AW, Dimos CS, Budziszek MJ, Jr., Goss CA, Lai V: **Knocking out the wall: protocols for gene targeting in *Physcomitrella patens***. *Methods Mol Biol* 2011, **715**:273-290.
12. Bergounioux C, Perennes C, Miege C, Gadal P: **The effect of male sterility on protoplast division inPetunia hybrida. Cell cycle comparison by flow cytometry**. *Protoplasma* 1986, **130**:138-144.
13. Dimos CS: **Functional Analysis of the Cellulose Synthase-Like D (CSLD) Gene Family in *Physcomitrella patens***. University of Rhode Island; 2010.
14. Chen XY, Kim JY: **Callose synthesis in higher plants**. *Plant Signal Behav* 2009, **4**:489-492.
15. Pattathil S, Avci U, Baldwin D, Swennes AG, McGill JA, Popper Z, Bootten T, Albert A, Davis RH, Chennareddy C *et al*: **A comprehensive toolkit of plant cell wall glycan-directed monoclonal antibodies**. *Plant Physiol* 2010, **153**:514-525.

16. Marcus S, Verhertbruggen Y, Herve C, Ordaz-Ortiz J, Farkas V, Pedersen H, Willats W, Knox JP: **Pectic homogalacturonan masks abundant sets of xyloglucan epitopes in plant cell walls**. *BMC Plant Biol* 2008, **8**:60.
17. Pena MJ, Darvill AG, Eberhard S, York WS, O'Neill MA: **Moss and liverwort xyloglucans contain galacturonic acid and are structurally distinct from the xyloglucans synthesized by hornworts and vascular plants**. *Glycobiology* 2008, **18**:891-904.
18. Knox JP, Linstead PJ, Cooper JPC, Roberts K: **Developmentally regulated epitopes of cell surface arabinogalactan proteins and their relation to root tissue pattern formation**. *The Plant Journal* 1991, **1**:317-326.
19. Yates EA, Valdor JF, Haslam SM, Morris HR, Dell A, Mackie W, Knox JP: **Characterization of carbohydrate structural features recognized by anti-arabinogalactan-protein monoclonal antibodies**. *Glycobiology* 1996, **6**:131-139.
20. Schaefer DG: **A new moss genetics: targeted mutagenesis in *Physcomitrella patens***. *Annu Rev Plant Biol* 2002, **53**:477-501.

Manuscript 3

Roles of PpCESA6, PpCESA7 and PpCESA8 in *Physcomitrella patens* development and stress tolerance

Manuscript formatted for the publication in journal to be decided.

Authors:

Mai L. Tran[1], University of Rhode Island, maitran@my.uri.edu

Hao Sun[2], Worcester Polytechnic Institute, hsun3@wpi.edu

Luis Vidali[2], Worcester Polytechnic Institute, lvidali@wpi.edu

Alison W. Roberts[1], University of Rhode Island, ARoberts@ds.uri.edu

[1]120 Flagg Road, Kingston, Rhode Island 02881

[2]60 Prescott Street, Worcester, Massachusetts 01605

Abstract:

Protonemal tissue is the filamentous tissue of moss that extends through tip growth. Cellulose deposition has been hypothesized to be important in the development of protonema, since cellulose is important in other tip growing cells, such as root hairs and pollen tubes. Furthermore, cellulose deposition in protonema of the moss *Physcomitrella patens* is increased dramatically under osmotic stress induced by supplementing the culture medium with mannitol. This enhanced cellulose deposition may play a role in *P. patens* drought tolerance. Based on analysis of public microarray data [1], *PpCESA*6, *PpCESA*7, and *PpCESA*8 are hypothesized to be responsible for the upregulation of cellulose deposition in response to osmotic stress.

Knockout (KO) mutants of *PpCESA*6, *PpCESA*7, and/or *PpCESA*8 were constructed to test the prediction that they are required for enhanced cellulose deposition under osmotic stress. No significant differences were found in *ppcesa8*KO and *ppcesa6/7KO* compared to wildtype protonemal tissues when analyzed for cellulose deposition under mannitol induced osmotic stress using CBM3a affinity cytochemistry. No drastic defects were seen in tip growth in the *ppcesa* mutants growing under normal culture conditions. Osmotic stress tolerance was tested through mannitol and high salinity treatments. *Ppcesa8KO* and *ppcesa6/7KO* mutant lines were not sensitive to mannitol induced treatments. *Ppcesa6/7KO* lines, but not *ppcesa8ko* had reduced salinity tolerance compared to wildtype *P. patens*.

The importance of cellulose synthesis in protonemal tip growth was investigated through cellulose synthesis inhibitors, isoxaben and DCB, since *ppcesa8*KO and *ppcesa6/7KO*, as well as other PpCESA single and double KO

mutations, have no drastic effect on protonemal growth. Results showed no significant difference in tip growth rate with and without cellulose synthesis inhibitors. However, addition of 20 μM DCB resulted in rupturing of tips. It is known that DCB, but not isoxaben, inhibits CSLDs. This may indicate that these proteins contribute to cellulose synthesis in the protonema. This would also be consistent with the observation that *PpCESA* single and double KO mutants have no drastic effect on protonemal development despite the importance of cellulose in tip growth.

Introduction:

Cellulose is one of the major components of the plant cell wall. Cellulose is made up of β-1, 4-glucan chains bundled together to form microfibrils. Cellulose synthases (CESAs) are the enzymes that synthesize glucan chain and have been characterized to be the primary contributors to cellulose synthesis. Mutations in CESAs in *Arabidopsis*, a vascular plant, have been shown to produce mild dwarf phenotypes to lethal mutants, indicating the importance of cellulose in vascular plant development [2]. Much of our understanding of cellulose synthesis is based on studies done in vascular plants. However, currently, very few studies of cellulose synthesis have been done in nonvascular plants, such as *Physcomitrella patens.*

Physcomitrella patens is a nonvascular plant whose genome has been fully sequenced [3, 4]. It is considered to be a good model organism because of its ability to be genetically manipulated due to its unusually high rate of homologous recombination [5, 6]. *Physcomitrella patens* is a simple moss plant with two haploid stages, a filamentous protonemal stage and gametophore stage, where it produces small leafy stalks [7].

Seven CESAs isoforms have been identified in *P. patens* [8]. As of now, PpCESA5 [9], PpCESA6, and PpCESA7 [10] have been investigated for their roles in development through knockout mutations. Currently, *ppcesa5KO* is the only *PpCESA* KO mutant that is known to have a phenotype; it is defective in the formation of the gametophore (Goss, Brockmann, Bushoven, & Roberts, 2012). *PpCESA6* and *PpCESA7* single KO mutants have no obvious developmental phenotype impairment, with shorter gametophores seen in the double knockout [10]. The roles of the other PpCESA isoforms are currently unknown; however, none of the single *PpCESA* knockouts appears to impair the development of the protonemal [11].

The protonemal tissue is a filamentous stage of the moss. Previously, carbohydrate microarrays showed moderate amounts of cellulose in the *P. patens* cell wall [12]. Cellulose is concentrated at the protonemal filament tips observed through microscopy using cellulose binding module 3 (CBM3a) affinity cytochemistry [13]. Cellulose is also implicated to be important in protonemal growth based on the abundance of rosette cellulose synthase complexes (CSCs) in protonemal tips of *Funaria hygrometrica* [14] and *P. patens* [15].

The protonemal filament extends by tip growth similarly to pollen tubes and root hairs of many other species [16, 17]. The effect of the cellulose synthesis inhibitor, 2, 6-dichlorobenzonitrile (DCB) on various pollen tubes, such as lily, petunia [18], and *Pinus bungeana* [19], includes distortion of cell walls and changes in cell wall components, such as an increase in pectin [18, 19]. It also causes rupturing of the tips at very high concentrations [18]. Treatment with the cellulose synthesis inhibitor isoxaben caused shorter tips, as well as tip swelling in conifer pollen tubes

[20]. These results indicate that although pollen tubes have very little cellulose content, cellulose is necessary in tip growth and development. *Arabidopsis* root hairs treated with DCB have also caused rupturing of tips and with isoxaben treatments, it caused retarded growth (Park et al., 2011).

Both isoxaben and DCB have been well characterized to inhibit cellulose synthesis, but the mechanism of inhibition is very different. DCB treatment immobilizes AtCESA6-YFP in the plasma membrane, while isoxaben causes accumulation of AtCESA6-YFP in the Golgi vesicles below the membrane [21]. DCB treatment of the protonemal filaments of the moss *Funaria hygrometrica* caused no changes in tip growth rate and rupturing of tips at high concentrations. Rosette CSCs visualized by freeze fracture electron microscopy also showed irregular distribution after 10 min of treatment in *F. hygrometrica* [22]. In contrast to results from live cell imaging in Arabidopsis, freeze fracture electron microscopy in *F. hygrometrica* indicated that rosette CSCs decrease in the plasma membrane with DCB treatment.

Prior experiments have indicated that PpCESAs may be involved in stress responses. *Physcomitrella patens* upregulates cellulose deposition when subjected to osmotic stress through the addition of mannitol to the culture medium [13]. The thickening of the cell wall has also been observed under drought conditions [23]. Microarray data showed *PpCESA6*, *PpCESA7*, and *PpCESA8* were expressed at higher levels under mannitol stress [1]. Interestingly, vascular plants downregulate cellulose under osmotic stress [24], and *Arabidopsis cesa*8 mutants are drought tolerant [25]. This downregulation of cellulose may be beneficial to vascular plants under drought stress.

These opposite responses of osmotic stress-induced cellulose upregulation in *P. patens* and downregulation in *Arabidopsis* might be due to differences in water uptake and dehydration tolerance mechanisms. Mosses are poikilohydric, while vascular plants are homeohydric [26]. Poikilohydric mosses, including *P. patens*, depend on external water to provide hydration. *Physcomitrella patens* is able to survive becoming dehydrated under water stress [27]. Homeohydric vascular plants, on the other hand, are adapted to maintain a constantly hydrated state through mechanisms that prevent water loss. *Physcomitrella patens* does not have a vascular system and does not need to maintain a constant water level, so it uses a different mechanism to combat drought [15].

Ppcesa6/7KO and *ppcesa8KO* mutants were produced and used to investigate the roles of the mutated genes in protonemal development and stress response. Since cellulose upregulation is seen under osmotic stress, the influence of mannitol induced osmotic stress and sensitivity to high salinity treatments in the mutants was analyzed. Mutant lines were also assayed for developmental phenotypes. None of the mutants had a dramatic phenotype in the protonema. Wildtype protonemal tissues were treated with cellulose synthesis inhibitors, isoxaben and DCB, to examine the role of cellulose in tip growth, since no dramatic phenotype was observed in the protonema of any of the *ppcesaKO* single knockouts. Protonemal tissue was assessed for tip growth rate, swelling, and rupturing of tips as seen previously in pollen tubes.

Materials and Methods:

Vector construction

Double KO mutations of *PpCESA6* and *PpCESA7* were made instead of single KO mutations because these genes only differ by only 2 amino acids [8, 10]. To construct a vector to knockout both *PpCESA6* and *PpCESA7*, sequences upstream of *PpCESA6* and downstream of *PpCESA7* were amplified from *P. patens* genomic DNA extracted from wildtype protonemal tissue as previously described [28]. The 5' UTR region of *CESA6* was amplified with 0.5 μM primers flanked with attB1 and attB4 sites (Table 1) using 4 μL of extracted genomic DNA as a template. Phusion polymerase (New England Bioscience, Ipswich, MA, USA) was used in a 50 μL PCR reaction under cycling conditions of 98°C for 1 min; 32 cycles of (98°C for 7 s, 60°C for 7 s, and 72°C for 45 s) with a final extension at 72°C for 5 min. Similarly, the 3' UTR region of *PpCESA7* was amplified with primers flanked with attB3 and attB2 sites (Table 1) as described for amplification of the 5'UTR region of *PpCESA6*. To construct entry clones, PCR amplicons were inserted into the appropriate pDONR vectors with BP Clonase II according to the manufacturer's instructions (Invitrogen, Grand Island, NY, USA) and were sequence verified. Entry clones of 5'UTR *PpCESA6* and 3'UTR *PpCESA7* were inserted into the BSNRG destination vector [28] using LR Clonase II Plus according to the manufacturer's instructions (Invitrogen), creating the *PpCESA6/7KO* vector. The final vector was linearized with BsrGI (New England Bioscience) and prepared for transformation into *P. patens* as described previously [28].

For the *cesa8KO* vector construction, a hygromycin selection cassette was inserted into a *PpCESA8* cDNA clone (Goss & Roberts, 2009). Again, final vector was

digested with EcoRI and NsiI (New England Bioscience) and precipitated for transformation [29].

Transformation and genotyping of *ppcesa8KO* and *ppcesa6/7KO*.

ppcesa8KO and *ppcesa6/7KO* vectors were transformed into wild-type Grandsen 2011 moss as previously described [28]. Genomic DNA was extracted from stably transformed colonies that survived two rounds of hygromycin selection as described previously [28].

PCR was used to test for proper integration of *PpCESA6/7KO* vector. Genomic DNA extracted from *ppcesa6/7KO* lines (4 μL) was subjected to 25 μL PCR reactions using Paq5000 polymerase, and cycle conditions of 95°C for 3 min; 32 cycles of (95°C for 45 s, 57°C for 45 s, 72°C for 2 min) with a final extension at 72°C for 5 min. Primers CESA6KOF2 and BHRRR (0.5 μM) were used to check for 5' integration and 10 μM CESA7FlankR2 and BHRRF primers (Table 1) were used to check for 3' integration. Primers CESA6KOF2 and BHRRR will amplify from the integration sites from the genomic sequence upstream of the 5' homologous recombination site of *CESA6/7KO* vector to the hygromycin resistant cassette, while primers BHRRF and CESA7FlankR2 will amplify from the hygromycin resistant cassette to downstream of the vector 3' homologous recombination site (Figure 1). This confirms the proper integration of the *PpCESA6/7KO* vector, which is expected to disrupt the CESA6 and CESA7 genes. Lines with proper 5' and 3' integration were tested for deletion of target genes with a 25 μL PCR using Paq5000 polymerase. *PpCESA6* deletion was checked using 0.5 μM of CESA6-5F and 0.5 μM CESA6-5R primers and PpCESA7 deletion was checked using 0.5 μM CESA7F and 0.5 μM CESA7R primers, with the

following cycling conditions: 95°C for 2 min denaturing step, 32 cycles of (95°C for 30 s, 60°C for 30 s, 72°C for 1 min) and a final extension at 72°C for 0.5 μM. Wildtype genomic DNA was used as a positive control.

ppcesa8KO lines were genotyped with 0.5 μM CESA8KOF and 0.5 μM BHRRR primers to check for 5' integration and 0.5 μM CESA8KOR and 0.5 μM BHRRF primers to check for 3' integration of the vector (Table 1). Genomic DNA (4 μL) from more than 15 lines of *ppcesa8KO* transformants was subjected to 25 μL PCR reactions using Paq5000 polymerase (Agilent, Santa Clara, CA, 95051) under cycle conditions of 95°C for 2 min denaturing step, 32 cycles of (95°C for 45 s, 57°C for 45 s, 72°C for 2 min) and a final extension at 72°C for 5 min. The *ppcesa8KO* lines with proper 5' and 3' integration were tested for deletion of the target gene in a 25 μL PCR reaction using Paq5000 polymerase with 0.5 μM p193 and 0.5 μM CESA8delF2 primers (Table 1) under cycle conditions of 95°C for 2 min; 32 cycles of (95°C for 30 s, 60°C for 30 s, 72°C for 1 min) with a final extension at 72°C for 5 min. Wildtype genomic DNA was used as a positive control.

Transformed lines were considered to be successfully knocked out if 1) the target gene(s) were not detected and 2) they had proper 5' and 3' integration. Verified knockout lines were then used for phenotyping.

Phenotyping assay

Phenotyping assays were performed to test the ability of KOs to produce caulonema, gametophores, rhizoids, and regenerate from protoplasts. Three lines of each KO along with 3 biological replicates of wildtype moss were used in all phenotyping assays. To maintain protonemal tissue stocks, moss was subcultured weekly by

homogenizing tissue in 4 mL water using an Omni International homogenizer with hard tissue tip probes (USA Scientific, Ocala, FL, USA) and plating on BCDAT plates with cellophane overlay. For the rhizoid assay, a small clump of tissue approximately 0.5 cm in diameter for each line or biological replicate was placed on 1 μM auxin BCD plates and grown for 2 weeks in continuous light [30]. For the gametophore assay, a clump of moss tissue 0.5 cm in diameter for each line or biological replicate was placed on BCD medium for 2 weeks [30].

For the colony morphology assay, tissue was digested into protoplasts with driselase (Sigma-Aldrich, St. Louis, MO, USA) according to Roberts et al., 2014. Protoplasts were plated on PRMB overlain with cellophane with a final concentration of 5000 protoplasts were plate. Three plates were made for each line. The plates were grown under continuous light for 4 d and cellophane membranes were then transferred to BCDAT plates for an additional 2 d. Approximately 50 chlorophyll autofluorescence images of regenerated protoplasts were captured at 63X magnification using a Leica M165FC stereo microscope with GFP filter Leica 10447407 and DFC310FX camera (Leica Microsystems Inc., Buffalo Grove, IL, USA). Images were analyzed for area, perimeter and solidity with ImageJ (National Institutes of Health, USA) using a macro developed by [31].

Cellulose deposition under osmotic stress

cesa8KO lines, *cesa6/7KO* lines, and wildtype tissue were digested into protoplasts with driselase as previously described [28]. Protoplasts were plated in 1 mL PRML at a density of approximately 15,000 protoplasts per plate on PRMB overlain with cellophane. After incubation for 2 d under continuous light at 25°C, cellophanes were

transferred to BCDAT for 2 d under the same conditions. Regenerated protoplasts were washed with distilled water, collected into a 15 mL conical tube, and centrifuged for 7 min at speed 3 in a clinical centrifuge with no brake. Regenerated protoplasts were fixed and stained with primary antibody CBM3a (Plant Probes, University of Leeds, United Kingdom) and secondary antibody Anti-mouse Alexa488 (Invitrogen) as previously described [28]. Staining was observed with an Olympus BH2 fluorescence microscope (Olympus Corporation, Lake Successs, NY, USA) at 10X magnification and images were captured with a Leica DFC310FX camera (Leica Microsystems Inc.). Cellulose staining intensities were quantified with ImageJ. Fluorescence intensity was measured for areas of the filaments grown without mannitol, which were characterized by normal cell length, and areas of the filaments grown with mannitol, which were characterized by short cell length and thick cell diameter. The ratios of fluorescent intensities were calculated.

Salt Sensitivity assay

To test if the KO lines are sensitive to high salinity, 0.5 cm in diameter clumps of 7-d tissue from 3 biological replicates of wildtype and 3 lines of KO lines were grown 500 mM NaCl for one week. Images were taken using a Leica M165FC stereo microscope with a Leica DFC310FX camera (Leica Microsystems Inc.) after salinity treatment. All experiments were repeated in either duplicate or triplicate.

Cellulose synthesis inhibitor assay

For cellulose synthesis inhibitor assays, tissue was cultured from a small piece of moss filament on PNO3 solid medium [32] in glass bottom petri dish P35G-0.17-14-C (Mat Tek, Ashland, MA) for 7 d under continuous light [33]. Ethanol was used as a solvent

for DCB and isoxaben with a stock concentration of 40 mM and added to medium at a final concentration of 20 μM (0.05% ethanol). The protonema were saturated with 100 μL of 20 μM DCB or 20 μM isoxaben in PNO3 liquid medium. For negative controls, protonema was treated with 100 μL of PNO3 liquid media with or without 0.05% ethanol. The filament tips were examined for tip growth analysis from 20 to 25 min immediately after treatment using a Zeiss Axiovert 200M DICII contrast microscopy (Zeiss, Carl-Zeiss-Strasse 22, 73447 Oberkochen) with dimensions set at 516X516 with AxioCam software. Time series of images were taken every 30 s for 20 min. Image stacks were assembled into kymographs using Image J (National Institutes of Health, USA) and distance of tip growth was measured at the base of the slope. The distance of tip growth was divided by time for tip growth rate [33]. All experiments were performed in triplicate with three different biological replicates.

Statistical analysis

ANOVA was used for overall comparison between the lines, and Tukey Kramer's unpaired t-test was used for pairwise comparison if the ANOVA p-value was significant.

RT-qPCR of *PpCSLDs* and *PpCESAs*

Four-d-old protonemal tissue plates were split into 3 parts, where 1) has no treatment control, 2) is transferred to BCDAT, and 3) is transferred to PRMB (BCDAT+mannitol). RNA was extracted from all treatments, converted to cDNA, and analyzed using RT-qPCR, as described in Chapter 2.

To test *CSLD* expression in the protonema, 100 mg of 4-d-old protonema tissue was collected for RNA extraction and converted to cDNA according to Chapter 2. PpCSLD expression was analyzed using RT-qPCR according to [13].

Results:

Genotyping

The *ppcesa8KO* lines 4C, 7C, and 10C were found to have proper 5' and 3' integration (Figure 1). No *CESA8* target gene was detected using PCR from all three *ppcesa8KO* lines (Figure 2). Similarly, *ppcesa6/7KO* lines 6A, 7B, and 1D had proper 5' and 3' integration from PCR and no *PpCESA6* nor *PpCESA7* gene was detected with PCR (Figure 2).

ppcesa8KO protonema have high solidity

Three lines of *ppcesa6/7KO* mutants, 3 lines of *ppcesa8KO* mutants, and 3 biological replicates of wildtype tissue were assayed for defects in caulonema, gametophore, and rhizoid development. Both *ppcesa6/7KO* and *ppcesa8KO* mutants produced straight caulonema filaments with no difference in length compared to wildtype ($P>0.05$, Figure 3, Table 2, and Table 3). Gametophores were observed to grow similarly to wildtype in all 3 *ppcesa8KO* lines (Figure 5). *ppcesa6/7KO* mutants all develop gametophores. However, *ppcesa6/7KO* 7B appears to have shorter and fewer gametophores than wildtype. Since only 1 out of 3 lines has this phenotype, the dwarf gametophore phenotype is not likely due to the KO of *PpCESA6* and *PpCESA7* (Figure 6). Rhizoids produced by *ppcesa6/7KO* and *ppcesa8KO* mutants were similar to wildtype (Figure 7 and Figure 8).

Three lines of *ppcesa6/7KO*, 3 lines of *cesa8KO*, and 3 biological replicates of wildtype tissue were grown from protoplasts to 6-d-old filaments and measured for area, solidity, and perimeter as previously described [32]. Solidity was scored from 0 to 1. The lowest solidity with the highest branching of the filaments was scored 0 and the highest solidity possible with less branching of filaments was scored 1 [32]. *ppcesa6/7KO* mutants and wildtype lines had no difference in area, solidity, or perimeter growth (Figure 9). However, *ppcesa8KO* (4C, 7C, and 10C) protonema lines have significantly higher solidity than those of wildtype ($P<0.05$, Anova and $P<0.05$, t test for individual lines compared to wildtype), with no difference in area growth and perimeter (Figure 10).

ppcesa8KO and *ppcesa6/7KO* mutants show no defect in cellulose upregulation under osmotic stress

Three replicates of *ppcesa8KO*, *ppcesa6/7KO*, and wildtype lines were grown on BCDAT medium and PRMB, which is BCDAT medium supplemented with mannitol. Fluorescence intensity was measured for cells grown on mannitol to cells grown on no mannitol, which were distinguished based on cell diameter where mannitol treated cells were much shorter, and ratios were calculated. Fluorescent intensity ratios showed no differences between *ppcesa8KO* or *ppcesa6/7KO* mutants to wildtype moss using ANOVA (Figure 11).

PpCESA expression does not change under mannitol treatment

Three replicates of protonema tissue treated with mannitol showed no difference in *PpCESA* expression compared to no transfer control and no mannitol control (Figure 12.).

ppcesa6/7KO mutants are sensitive to salt based on chlorophyll degradation

Three tissue clumps from 3 lines each of *ppcesa8KO* mutants, *ppcesa6/7KO* mutants, and replicate clumps of wildtype tissue were grown on BCD supplemented with NaCl and growth was monitored over the course of 7 d. Images were taken at day 7 and examined for salt sensitivity where sensitive mutants have chlorophyll degradation. After 7 d of treatment both *cesa8KO* mutants and wildtype lines similar chlorophyll content, indicating that *ppcesa8KO* mutants have similar salt sensitivity as wildtype moss (Figure 13). However, after 7 d of treatment of NaCl, *ppcesa6/7KO* showed greater sensitivity to salt compared to wildtype tissue, where chlorophyll content in *ppcesa6/7KO* decreased dramatically compared to wildtype moss (Figure 14).

Protonemal growth rate is not inhibited by DCB or isoxaben

Protonemal tissues were treated with isoxaben and DCB for 5 d. No differences were seen in overall colony growth, as seen in *Arabidopsis* (Figure 15). Tip growth rate was measured before rupturing of tips through kymographs from 20 μM isoxaben and 20 μM DCB treatments. There is no effect on tip growth rate in treated protonemal tissue ($P>0.05$) when compared to negative controls of PNO3 with and without diluents (Figure 16 and Figure 15). However, treatment with 20 μM DCB resulted in rupturing of the protonema tips after less than 20 min of treatment (Figure 17). No rupturing of tips was seen with treatments of isoxaben (Figure 17).

Discussion:

Both *ppcesa8KO* and *ppcesa6/7KO* mutant lines are all able to produce protonema and gametophore tissues. *Ppcesa8KO* and *ppcesa6/7KO* mutant lines have no dramatic phenotype aside from *ppcesa8KO* have higher colony solidity than wildtype. High

solidity in *ppcesa8KO* mutant is caused by less branching of the filaments. This shows that cellulose is needed for normal morphology in the protonema.

The *ppcesa6/7KO* mutant lines appear to be more salt sensitive than wildtype, suggesting that cellulose is important for tolerance under high salinity environments. The single *ppcesa8KO* mutants were not as sensitive to high salinity as the double *ppcesa6/7KO* mutants, which may suggest that knock out of multiple *PpCESA*s is needed to see an affect of osmotic stress due to compensation from other PpCESAs present. Analyzing the *ppcesaKOs* for upregulation of other *PpCESA* isoforms with RT-qPCR would test whether *PpCESA*s are compensating for each other. These results are further supported by lack of cellulose downregulation in the *ppcesa8KO* and *ppcesa6/7KO* mutants under osmotic treatments through CBM3a labeling. This indicates that cellulose is still being made in the protonema despite the absence of *PpCESA6*, *PpCESA7*, and *PpCESA8*.

To see if cellulose plays a key role in protonemal development, cellulose synthesis was inhibited with isoxaben and DCB. Protonemal tips were ruptured at high concentrations of DCB. Neither isoxaben nor DCB affected the tip growth rate. This may be due to other cell wall polysaccharide compensating for the lack of cellulose, such as pectin or callose [34, 35]. Isoxaben did not cause rupturing of tips even at very high concentrations. These differences maybe be due to the different mechanism of inhibiting cellulose where DCB inhibits motility in the plasma membrane causing an accumulation of AtCESA6-YFP particles [21]. Interestingly, DCB has similar affect on protonemal filaments in *Funaria* in causing rupturing of tips. However, rosette structures that are believed to be the CSCs were decreased in the membrane based on

freeze fractured experiments after 10 min of treatment [22]. Although the effects of DCB are the same in *Arabidopsis* and the moss *Funaria*, the mechanism in its affect on CSCs may be different. We are currently planning future experiments using *ppcesa8KO* rescued with GFP-PpCESA8 lines to monitor PpCESA trafficking under treatments of DCB and isoxaben. These experiments will inform us if the mechanism of cellulose inhibition of DCB and isoxaben is the same in *Arabidopsis*.

Another explanation for the rupturing of tips with DCB, but not isoxaben, may be that DCB affects cellulose synthase like D proteins (CSLDs) whereas isoxaben has no affect on CSLDs. Recent studies have shown CSLD's potential in producing cellulose [36]. *Atcsld3KO* mutants have shown rupturing of tips in root hairs [36], while *atcsld1* and *atcsld4* mutants shown rupturing in pollen tubes [37], similar to the DCB treatments. Some *atcsld* mutations have also resulted in decreased cellulose content based on S4B staining [36, 37]. Furthermore, the catalytic subunit of CSLDs have been shown to be interchangable with AtCESA6, suggesting that CSLDs are able to synthesize cellulose[36].

PpCSLDs are highly expressed in the protonema as seen by RT-qPCR, particularly PpCSLD1 (Figure 18). CSLDs might be responsible for cellulose synthesis in tip growth based on high expression of CSLDs and rupturing of tips after treatments with DCB, which inhibits CSLDs as well as CESAs. These results indicate the importance of cellulose in protonemal tip growth and that CSLDs may possibly have a role in cellulose synthesis.

Conclusions:

These data suggest that *P. patens* is very resilient to the absence of cellulose in protonemal development, since PpCESA knockout mutants have yet to cause lethality in protonema tissue. In contrast, *Arabidopsis* single knockout mutants *atcesa1* and *atcesa3* have caused gametophytic lethals [38] and *atcesa4, atcesa7,* and *atcesa8* cause collasped xylem [39, 40]. The cellulose synthesis inhibitor isoxaben also causes no defects to protonemal tip growth. Only treatment with a high concentration of DCB had an effect, where the protonemal tips ruptured. This suggests the PpCESAs and/or PpCSLDs can compensate for each other. PpCSLDs needs to be further investigated for its role in synthesizing cellulose in the protonema. PpCESA single KO mutants should also be investigated for upregulation of other PpCESA isoforms and multiple *PpCESA* KO mutations may be necessary to produce a phenotype in the protonemal tissue.

Table 1. Primers designed for vector construction and genotyping

Name	Sequence	Description	Amplicon Size (bp)
CESA6KOattB1	GGGGACAAGTTTGTACAAAAAAGCAGGCTGACATTTCACCCAGTGAGCA	CESA6 5' UTR region	1060
CESA6KOattB4	GGGGACAACTTTGTATAGAAAAGTTGGGTCTTTCTTCCTCGCACCTCAC		
CESA7KOattB3	GGGGACAAGTTTGTACAAAAAAGCAGGCTTACTCTTAACCGCAGCCTTG	CESA7 3' UTR region	599
CESA7KOattB2	GGGGACAACTTTGTATAATAAAGTTGGTGATGGAGGAATCGAGGAA		
CESA8KOF	CTGGACAGACTTTCTCTCCGTTAT	5' integration of vector	1121
BHRRR	TCTATTTCTTTGCCCTCGGA		
CESA8KOR	CGTAAGAATATCCTCCGTCACC	3' integration of vector	747
BHRRF	TGACAGATAGCTGGGCAATG		
CESA6KOF2	GCTTCAATGCTGTACCACAAACCAC	5' integration of vector	1647
BHRRR	TCTATTTCTTTGCCCTCGGA		
CESA7FlankR	AAGCCCTAACTTCCAGCACC	3' integration of vector	833
BHRRF	TGACAGATAGCTGGGCAATG		
CESA8delF2	GTCTTCTTCGATGTACTGACAC	CESA8 gene deletion	339
P193	TACTTCCACGGCTTCTTGCT		
CESA6targF	GTGAGGTGCGAGGAAGAAAG	CESA6 gene deletion	141
CESA6targR	TTCCCTAACTCCACCACTGC		
CESA7targF	GCGAATGCAGGGCTGCTG	CESA7 gene deletion	1178
CESA7targR	ACATTACTCAACGGCCTCGG		

Table 2. Caulonema length of *cesa8KO* mutants

	Wildtype	*cesa8KO 4C*	*cesa8KO 7C*	*cesa8KO 10C*	P value
Average length (cm)	0.47	0.57	0.60	0.63	0.49
Standard Error	0.27	0.33	0.35	0.37	

Table 3. Caulonema Length of *cesa6/7KO* mutants

	Wildtype	*cesa6/7KO 6A*	*cesa6/7KO 7B*	*cesa6/7KO 1D*	P value
Average length (cm)	1.11	1.06	0.98	1.00	0.77
Standard Error	0.048	0.076	0.075	0.14	

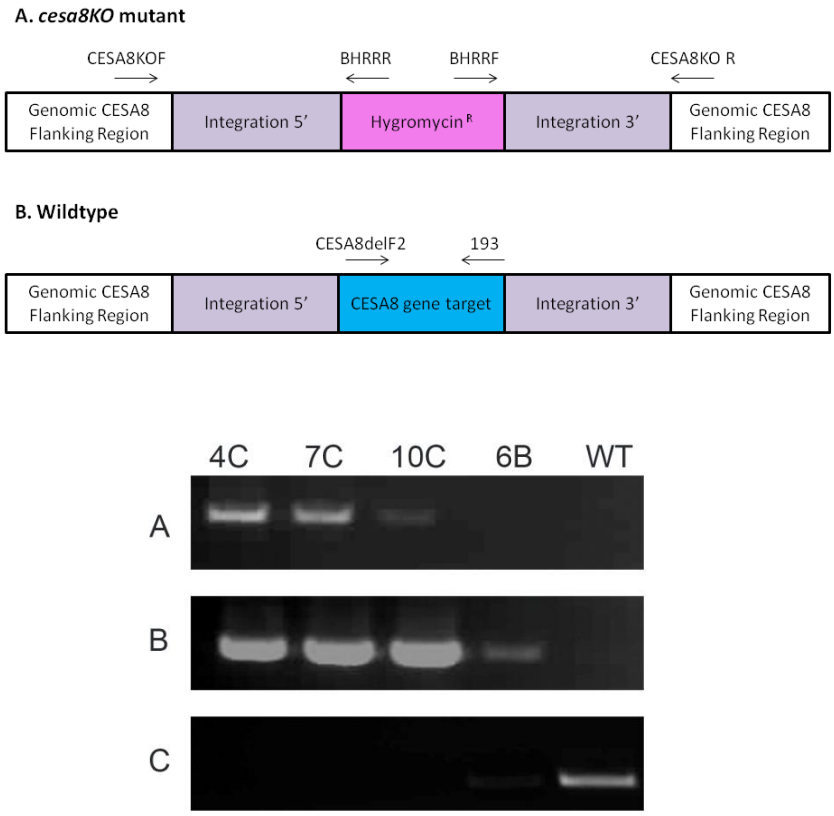

Figure 1. Genotyping *ppcesa8KO* transformants
(**A**) Diagram of *ppcesa8ko* vector integrated in *P. patens* chromosomal DNA by homologous recombination. Arrows pointing to the right represent forward primers, while arrows to the left represent reverse primers. (**B**) Wildtype DNA with intact *PpCESA8* genes. *PpCESA8* deletion primers were used to test gene deletion. 1% Agarose gel shows (**B**) a PCR product of 1121 bp spanning the *PpCESA8* 5' integration site for *ppcesa8KO* mutant lines 4C, 7C, and 10C and no band in wildtype negative control, (**D**) a PCR product of 747 bp spanning the Pp*CESA8* 3' integration site for *ppcesa8KO* mutant lines 4C, 7C, and 10C and no band in wildtype negative control, and (**E**) no amplification of *PpCESA8* gene in *ppcesa8KO* lines 4C, 7C, and 10C and a PCR product of 339 bp in wildtype positive control.

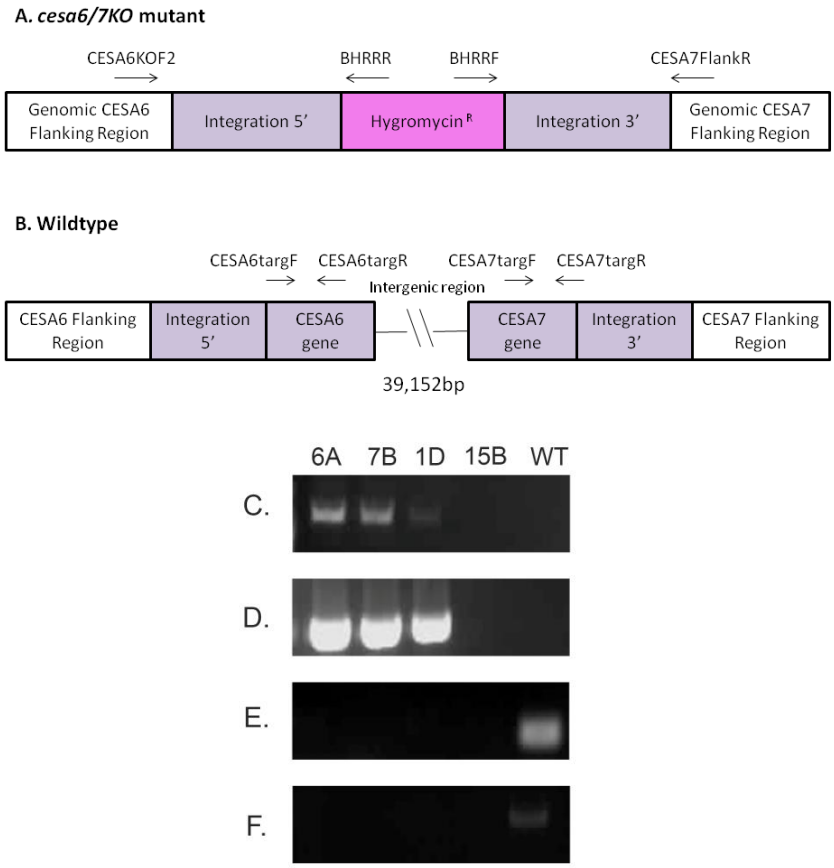

Figure 2. Genotyping *ppcesa6/7KO* transformants

(**A**) Diagram of *ppcesa6/7KO* vector integrated in *P. patens* chromosomal DNA by homologous recombination. Arrows pointing to the right represent forward primers, while arrows to the left represent reverse primers. (**B**) Wildtype DNA with intact *PpCESA6* and *PpCESA7* genes. *PpCESA6* and *PpCESA7* deletion primers were used to test gene deletions. 1% Agarose gel shows (**C**) a PCR product of 1647bp spanning the *PpCESA6* 5' integration for *cesa6/7KO* mutant lines 6A, 7B, and 10C and no band in wildtype negative control, (**D**) a PCR product of 833bp spanning the *PpCESA7* 3' integration site of *cesa6/7KO* mutant lines 6A, 7B, and 10C and no band in the wildtype negative control, and (**E**) no amplification of *CESA6* in *cesa6/7KO* lines 6A, 7B, and 1D and a PCR product of 141bp in the positive wildtype control and (**F**) no amplification of *CESA7* genes from PCR in *ppcesa6/7KO* lines 6A, 7B, and 1D and a PCR product of 1178bp in the positive wildtype control.

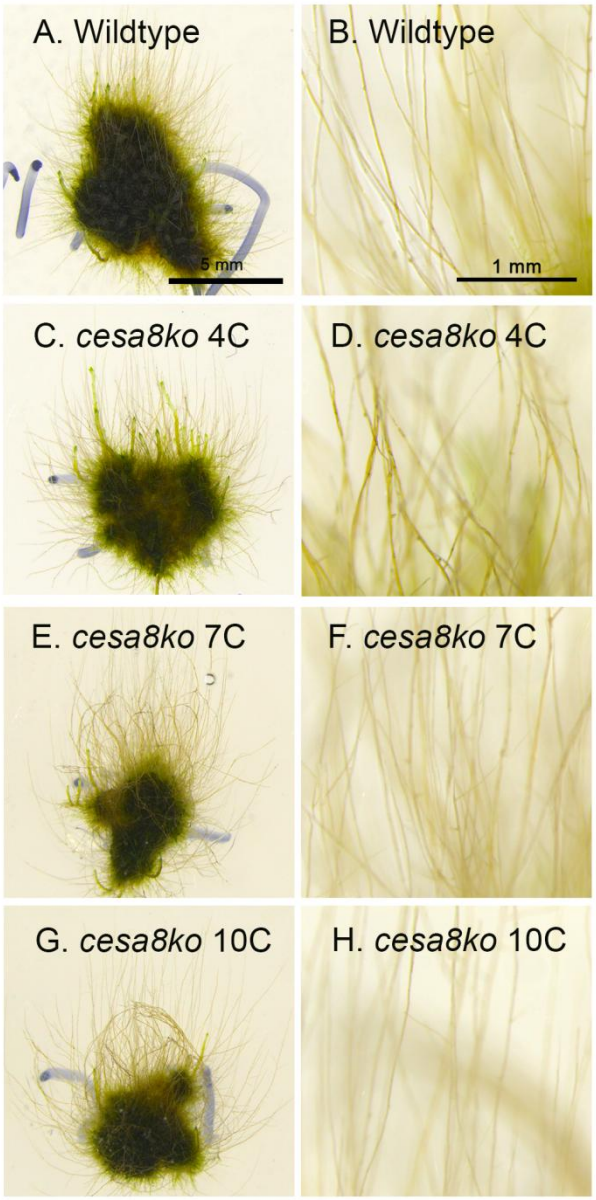

Figure 3. Caulonema assay of *ppcesa8KO*

Wildtype and *ppcesa8KO* mutant lines were grown on 35 mM Sucrose+BCDAT for 7 days under continuous light at 25˚C, and upright in dark incubator, 25˚C for 2 weeks. Representative colonies of (**A**) wildtype, (**C**) *ppcesa8KO* 4C, (**E**) *ppcesa8KO* 7C, and (**G**) *ppcesa8KO* 10C and caulonemal filaments of (**B**) wildtype, (**D**) *ppcesa8KO* 4C, (**F**) *ppcesa8KO* 7C, and (**H**) *ppcesa8KO* 10C showing upright growth.

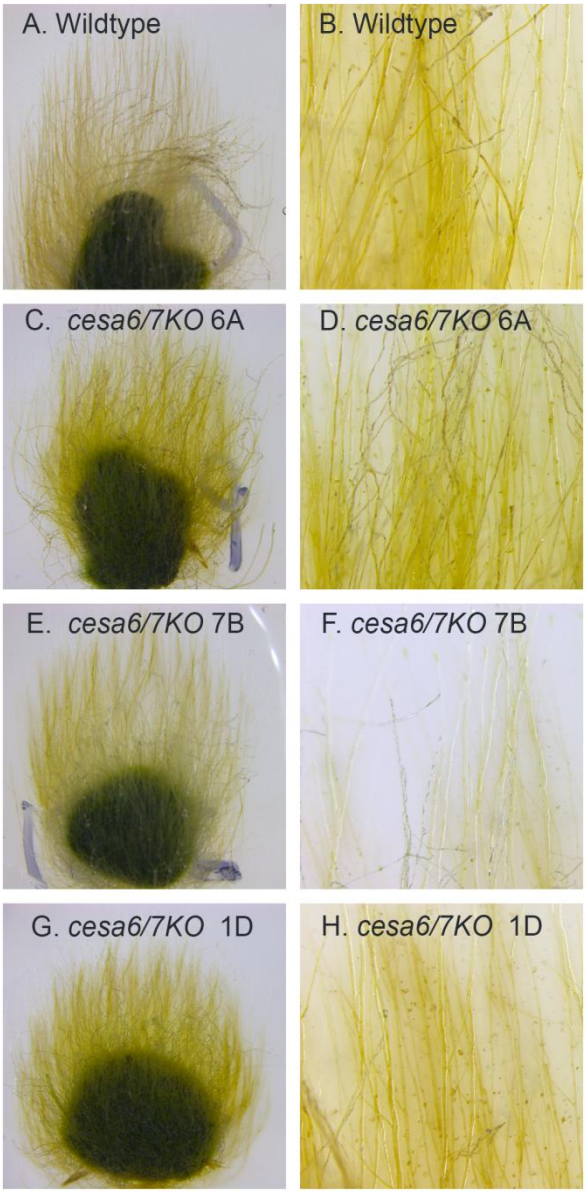

Figure 4. Caulonema assay of *ppcesa6/7KO*

Wildtype and *ppcesa6/7KO* mutant lines were grown on 35mM Sucrose+BCDAT for 7 days under continuous light at 25˚C, and upright in dark incubator, 25˚C for 2 weeks. Representative caulonemal colonies of (**A**) wildtype and (**C**) *ppcesa6/7KO* 6A, (**E**) *ppcesa6/7KO* 7B, and (**G**) *ppcesa6/7KO* 1D and caulonemal filaments of (**B**) wildtype and (**D**) *ppcesa6/7KO* 6A, (**F**) *ppcesa6/7KO* 7B, and (**H**) *ppcesa6/7KO* 1D showing upright growth.

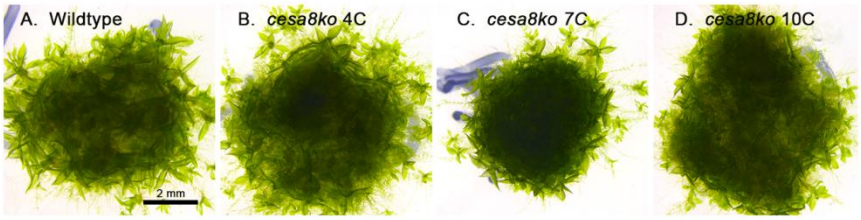

Figure 5. Gametophore assay of *ppcesa8KO*

(**A**) Wildtype, (**B**) *ppcesa8KO* 4C, (**C**) *ppcesa8KO* 7C, and (**D**) *ppcesa8KO* 10C grown on BCD at 25˚C for 2 weeks. All gametophore tissue grew similarly to wildtype (N=3 for each experiment, repeated in duplicate).

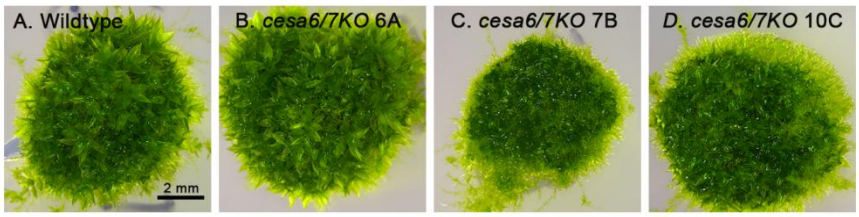

Figure 6. Gametophore assay of *cesa6/7KO*

(**A**) Wwildtype, (**B**) *ppcesa6/7KO* 6A, (**C**) *ppcesa6/7KO* 7B, and (**D**) *ppcesa6/7KO* 1D were grown on BCD at 25˚C for 2 weeks. All gametophore tissue grew similarly to wildtype, except for (**C**) *ppcesa6/7KO* 7B, where number of gametophores produced is lower (N=3 for each experiment, repeated in duplicate).

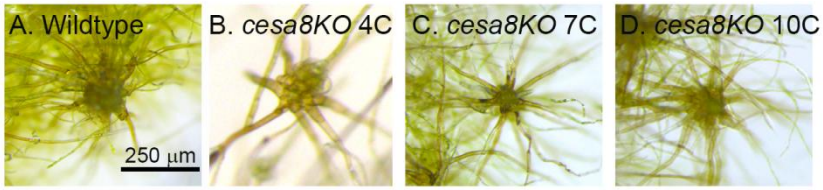

Figure 7. Rhizoids of *ppcesa8KO* and wildtype moss

7-day-old **A**) Wildtype, (**B**) *ppcesa8KO* 4C, (**C**) *ppcesa8KO* 7C, and (**D**) *ppcesa8KO* 10C were grown on BCD+auxin. All lines produced rhizoids. (N=3 for each experiment, repeated in duplicate).

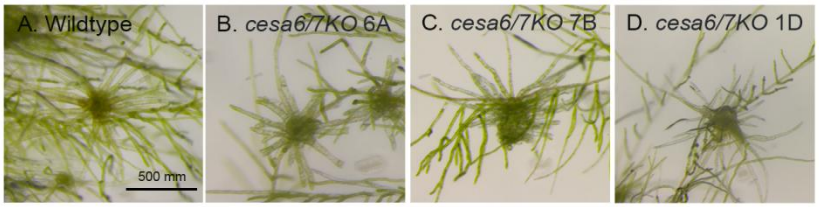

Figure 8. Rhizoids assay of *ppcesa6/7KO* and wildtype moss
7-day-old (**A**) wildtype, (**B**) *ppcesa6/7KO* 6A, (**C**) *ppcesa6/7KO* 7B, and (**D**) *ppcesa6/7KO* 1D lines were grown on BCD+auxin for 2 weeks. All lines produced rhizoids. (N=3 for each experiment, repeated in duplicate).

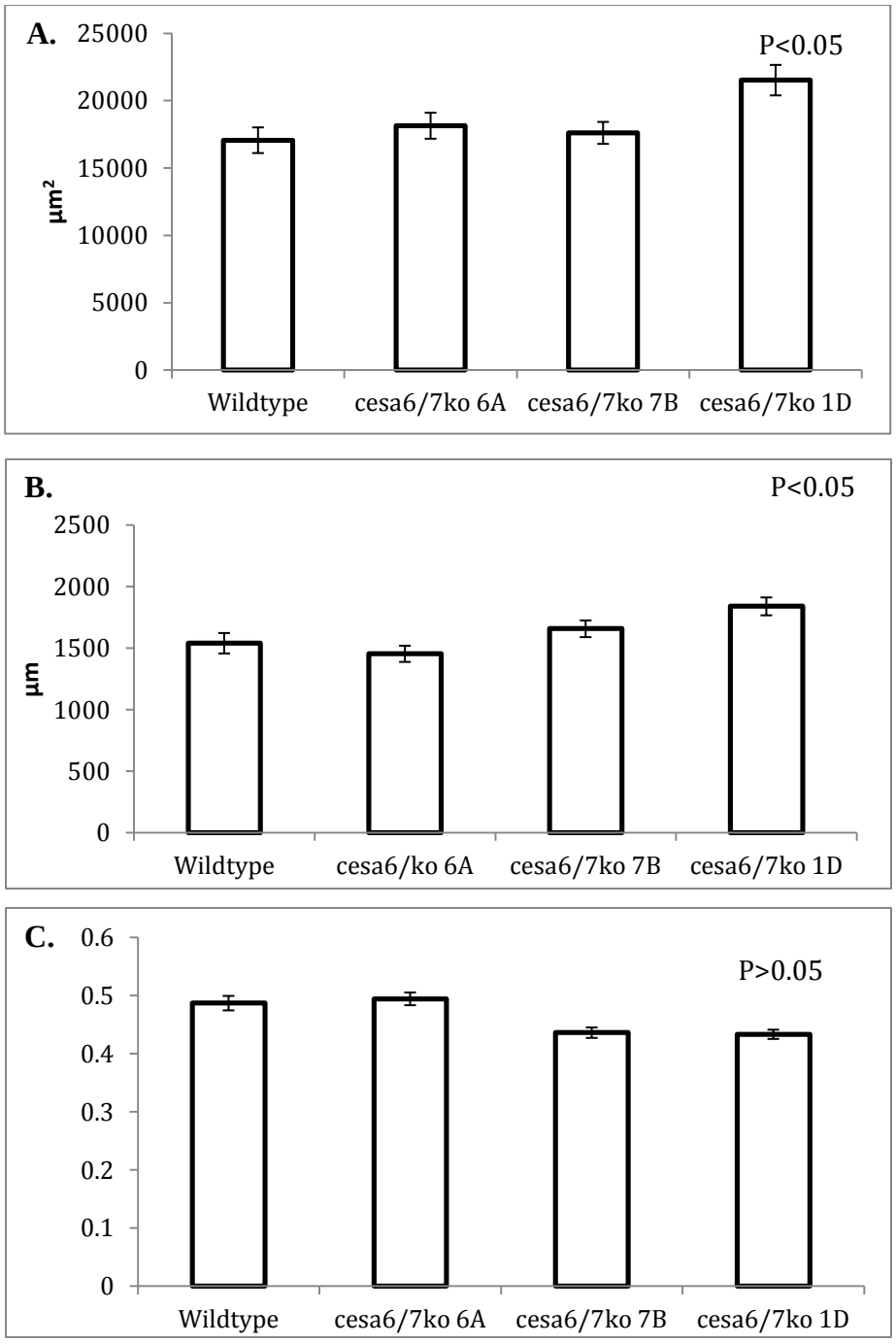

Figure 9. No morphology differences seen in *ppcesa6/7KO* compared to wildtype moss

ppcesa6/7KO mutant lines and wildtype moss were analyzed for (**A**) area, (**B**) perimeter growth, and (**C**) solidity, according to [31]. Solidity scale of 1 represents the highest solidity with 0 as the lowest solidity with the highest branching. Error bars display standard error of the mean between each data set. No significant differences were found (P>0.05).

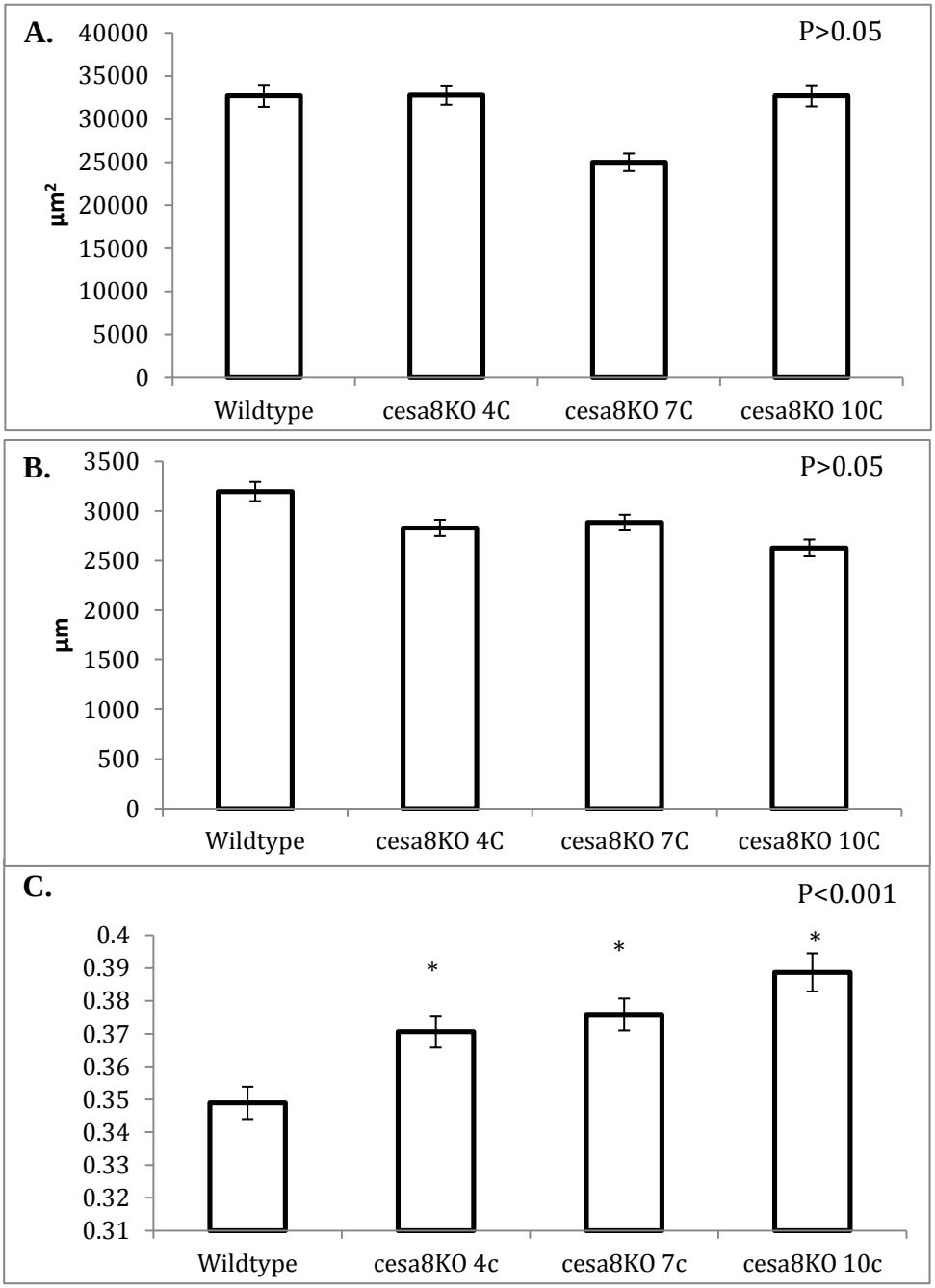

Figure 10. *ppcesa8KO* mutants have higher solidity than wildtype moss

ppcesa8KO mutant lines and wildtype were analyzed for (**A**) area, (**B**) perimeter growth, and (**C**) solidity, according to [31]. Solidity scale of 1 represents the highest solidity with 0 as the lowest solidity with the highest branching. Error bars display standard error of the mean between each data set. No significant differences were found in area and perimeter growth (P>0.05). *ppcesa8KO* lines: 4C, 7C, and 10C have significantly higher solidity compared to wildtype (Anova P value < 0.05).

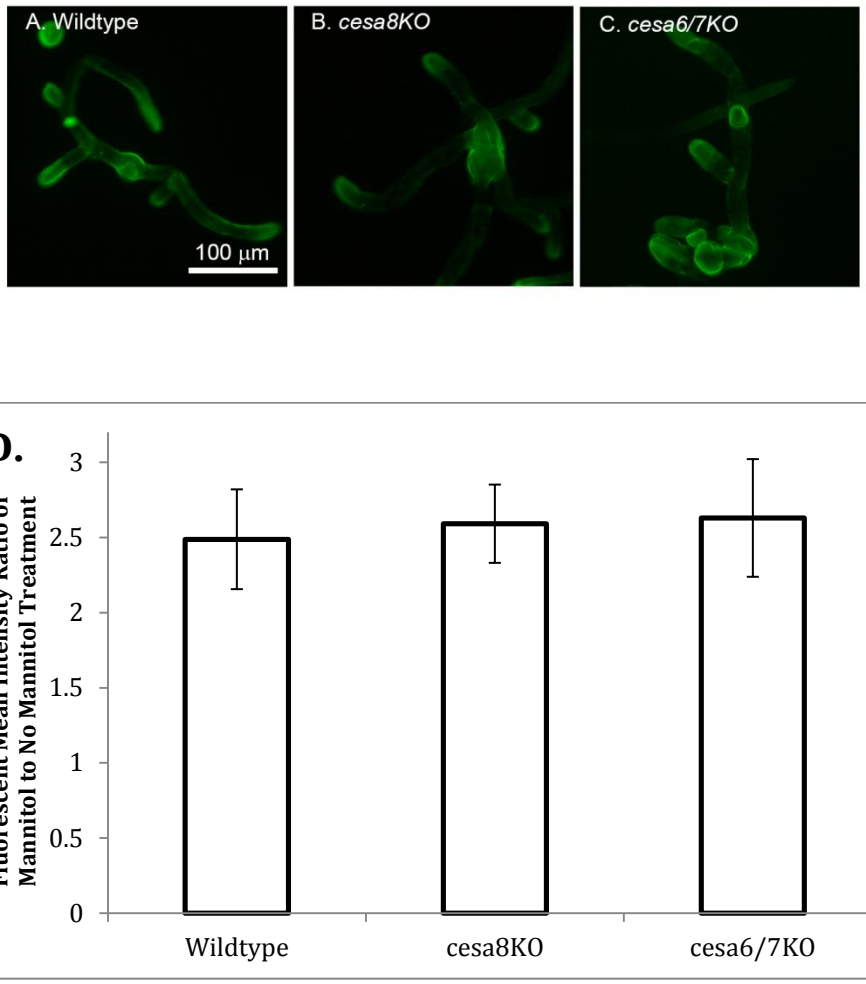

Figure 11. . CBM3a staining of *ppcesa8KO* and *ppcesa6/7KO* mutant lines

Three lines of (**A**) *ppcesa8KO* mutants, (**B**) *ppcesa6/7KO* mutants, and (**C**) wildtype protoplasts were grown on PRMB for 2 days and transferred to BCDAT for another 2 days. Regenerated filaments were collected and fix according toAW Roberts, CS Dimos, MJ Budziszek, Jr., CA Goss and V Lai [28]. Filaments were then stained with cellulose binding affinity antibody, CBM3A, and with AlexaFluor488 secondary. Images of filaments were captured and (**D**) ratios of fluorescences were measured where they show no significant differences between mutants and wildtype (Anova P value >0.05).

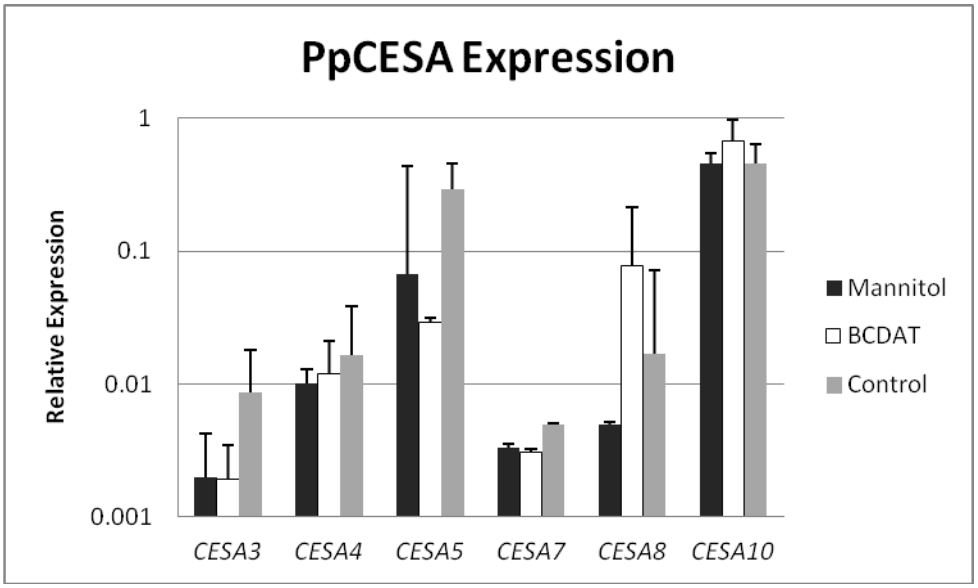

Figure 12. *PpCESA*s expression do not upregulation in mannitol

Expression levels were measured using qPCR and were normalized to PpVhpp and PpACT. Three independent samples were assayed in duplicate. No significant differences were seen in mannitol treated tissue compared BCDAT and no transfer control (Anova $P<0.05$).

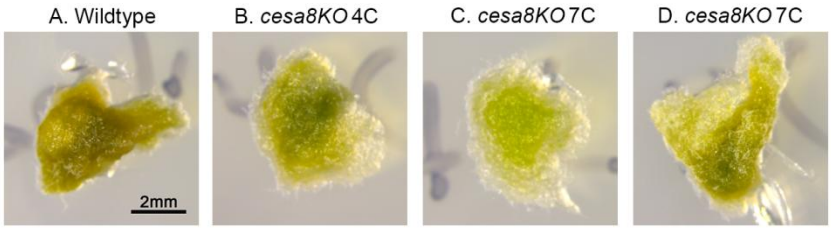

Figure 13. ***ppcesa8KO* is not sensitive to salinity treatments**

(**A**) Wildtype, (**B**) *ppcesa8KO* 4C, (**C**) *ppcesa8KO* 7C, and (**D**) *ppcesa8KO* 10C were grown in triplicates on BCDAT for 7 days and transferred to 7 mM NaCl BCD for 5 days. Assays were repeated twice.

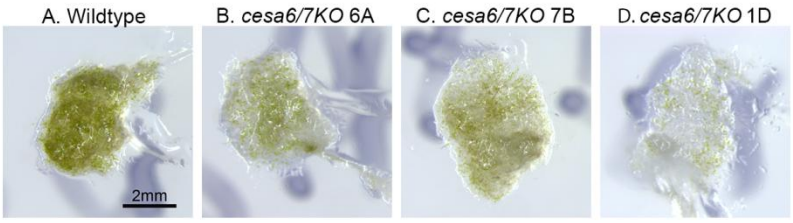

Figure 14. *ppcesa6/7KO* is sensitive to salinity treatment

(**A**) Wildtype, (**B**) *ppcesa6/7KO* 6A, (**C**) *ppcesa6/7KO* 7B, and D) *ppcesa6/7KO* 10C were grown in triplicates on BCDAT for 7 days and transferred to 7 mM NaCl BCD for 5 days. Assays were repeated twice.

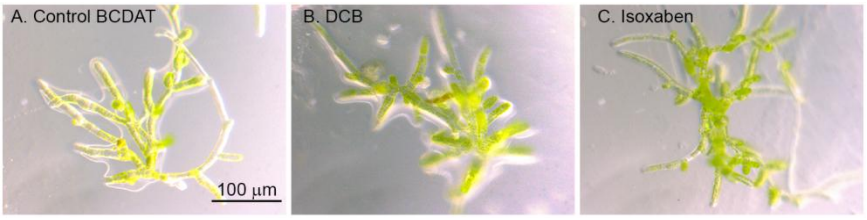

Figure 15. Cellulose synthesis inhibitor treatments

Protonemal tissue was grown BCDAT media for 7 d. Tip growth was monitored with (**A**) no treatment, (**B**) treatment with 20 μM DCB, and (**C**) treatment with 20 μM isoxaben for 15 min. No difference was seen in overall colony morphology.

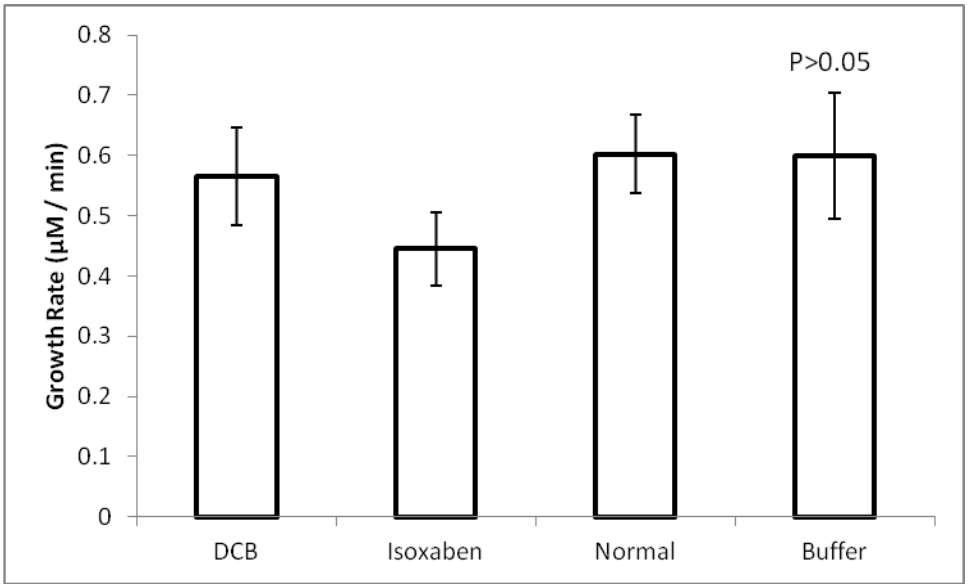

Figure 16. Growth rate of protonema with cellulose synthesis inhibitors
Tip growth rate of protonema tissue were measured on PNO3 media with no buffer, buffer, buffer with 20 µM DCB, and buffer with 20 µM isoxaben. Error bars display standard error of the mean between each data set. No significant differences were seen between treatments.

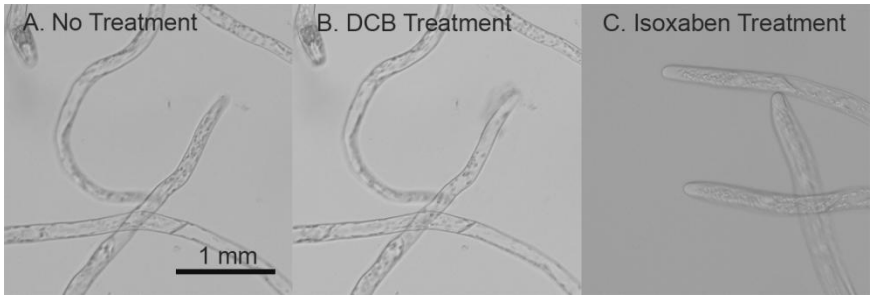

Figure 17. 20 µM DCB causes rupturing of tips

Wildtype protonemal tissue grown on PNO3 media for 7 days were treated with either (**A**) 20 µM DCB or (**B**) 20 µM isoxaben and were imaged from t=0 and t=15mins. DCB causes rupturing of tips after 15 mins of treatment. Isoxaben does not cause rupturing of tips.

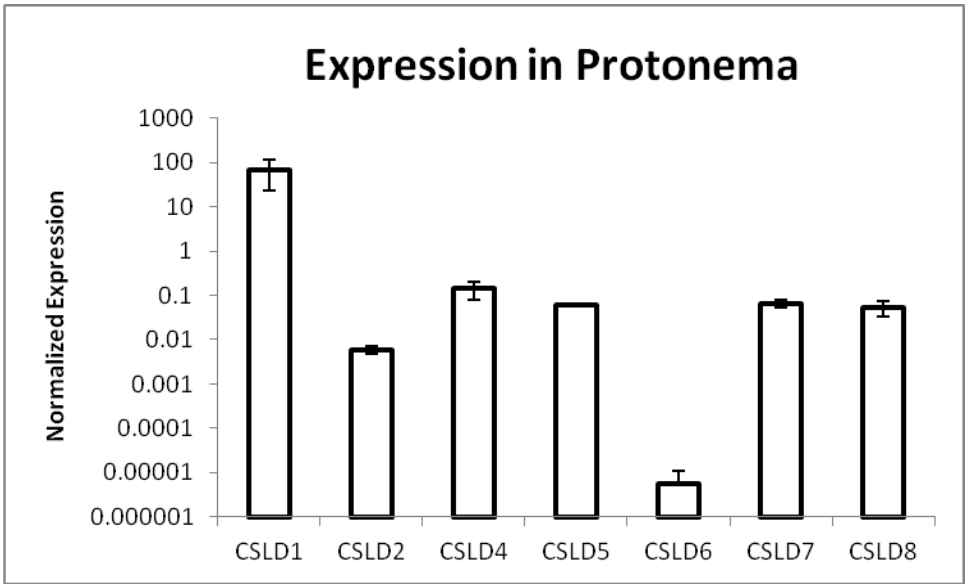

Figure 18. Expression of *CSLDs* in protonemal tissue

Expression levels of *CSLDs* in protonemal tissue were measured using qPCR and were normalized to PpC45 and PpUB1. Three independent samples were assayed in duplicate. Results show very high expression of *CSLD1* in the protonemal tissue and low to moderate expression of the other *CSLD*s.

References:

1. Cuming AC, Cho SH, Kamisugi Y, Graham H, Quatrano RS: **Microarray analysis of transcriptional responses to abscisic acid and osmotic, salt, and drought stress in the moss, *Physcomitrella patens***. *New Phytol* 2007, **176**:275-287.
2. Somerville C: **Cellulose synthesis in higher plants**. *Annu Rev Cell and Dev Biol* 2006, **22**:53-78.
3. Rensing SA, Lang D, Zimmer AD, Terry A, Salamov A, Shapiro H, Nishiyama T, Perroud PF, Lindquist EA, Kamisugi Y *et al*: **The *Physcomitrella* genome reveals evolutionary insights into the conquest of land by plants**. *Science* 2008, **319**:64-69.
4. Zimmer AD, Lang D, Buchta K, Rombauts S, Nishiyama T, Hasebe M, Van de Peer Y, Rensing SA, Reski R: **Reannotation and extended community resources for the genome of the non-seed plant Physcomitrella patens provide insights into the evolution of plant gene structures and functions**. *BMC genomics* 2013, **14**:498.
5. Schaefer D, Zryd J-P: **Efficient Gene Targeting in the moss *Physcomitrella patens***. *Plant J* 1997, **11**:1195-1206.
6. Reski R, Frank W: **Moss (*Physcomitrella patens*) functional genomics—Gene discovery and tool development, with implications for crop plants and human health**. *Briefings in Functional Genomics and Proteomics* 2005, **4**:48-57.
7. Cove D: **The Moss *Physcomitrella patens***. *Annu Rev Genet* 2005, **39**:339-358.
8. Roberts AW, Bushoven JT: **The cellulose synthase (CESA) gene superfamily of the moss *Physcomitrella patens***. *Plant Mol Biol* 2007, **63**:207-219.
9. Goss CA, Brockmann DJ, Bushoven JT, Roberts AW: **A CELLULOSE SYNTHASE (CESA) gene essential for gametophore morphogenesis in the moss *Physcomitrella patens***. *Planta* 2012, **235**:1355-1367.
10. Wise HZ, Saxena IM, Brown RM: **Isolation and characterization of the cellulose synthase genes PpCesA6 and PpCesA7 in *Physcomitrella patens***. *Cellulose* 2011, **18**:371-384.
11. Roberts AW. In.; 2015.
12. Moller I, Sorensen I, Bernal AJ, Blaukopf C, Lee K, Obro J, Pettolino F, Roberts A, Mikkelsen JD, Knox JP *et al*: **High-throughput mapping of cell-wall polymers within and between plants using novel microarrays**. *Plant J* 2007, **50**:1118-1128.
13. Dimos CS: **Functional Analysis of the Cellulose Synthase-Like D (CSLD) Gene Family in *Physcomitrella patens***. University of Rhode Island; 2010.
14. Reiss HD, Schnept E, Herth W: **The plasma membrane of the *Funaria* caulonema tip cell: morphology and distribution of particle rosettes, and the kinetics of cellulose synthase**. *Planta* 1984, **160**:428-435.
15. Roberts AW, Roberts EM, Haigler CH: **Moss cell walls: structure and biosynthesis**. *Front Plant Sci* 2012, **3**:166.
16. Hepler PK, Vidali L, Cheung AY: **Polarized cell growth in higher plants**. *Annu Rev Cell Dev Biol* 2001, **17**:159-187.

17. Geitmann A, Emons AM: **The cytoskeleton in plant and fungal cell tip growth**. *J Microsc* 2000, **198**:218-245.
18. Anderson JR, Barnes WS, Bedinger P: **2,6-Dichlorobenzonitrile, a cellulose biosynthesis inhibitor, affects morphology and structural integrity of petunia and lily pollen tubes**. *J Plant Physiol* 2002, **159**:61-67.
19. Hao H, Chen T, Fan L, Li R, Wang X: **2, 6-Dichlorobenzonitrile causes multiple effects on pollen tube growth beyond altering cellulose synthesis in Pinus bungeana Zucc**. *PLoS One* 2013, **8**:e76660.
20. Lazzaro MD, Donohue JM, Soodavar FM: **Disruption of cellulose synthesis by isoxaben causes tip swelling and disorganizes cortical microtubules in elongating conifer pollen tubes**. *Protoplasma* 2003, **220**:201-207.
21. DeBolt S, Gutierrez R, Ehrhardt DW, Somerville C: **Nonmotile cellulose synthase subunits repeatedly accumulate within localized regions at the plasma membrane in Arabidopsis hypocotyl cells following 2,6-dichlorobenzonitrile treatment**. *Plant Physiol* 2007, **145**:334-338.
22. Rudolph U, Gross H, Schepf E: **Investigations of the turnover of the putative cellulose-synthesizing particle "rosettes" within the plasma membrane of Funaria hygrometrica protonema cells**. *Protoplasma* 1989, **148**:57-69.
23. Pressel S, Duckett JG: **Cytological insights into the desiccation biology of a model system: moss protonemata**. *New Phytol* 2010, **185**:944-963.
24. Zhong R, Morrison WH, 3rd, Freshour GD, Hahn MG, Ye ZH: **Expression of a mutant form of cellulose synthase AtCesA7 causes dominant negative effect on cellulose biosynthesis**. *Plant Physiol* 2003, **132**:786-795.
25. Chen Z, Hong X, Zhang H, Wang Y, Li X, Zhu JK, Gong Z: **Disruption of the cellulose synthase gene, AtCesA8/IRX1, enhances drought and osmotic stress tolerance in Arabidopsis**. *Plant J* 2005, **43**:273-283.
26. Mishler BD, Oliver MJ: **Putting *Physcomitrella patens* on the tree of life: the evolution an ecology of mosses**. In: *The Moss Physcomitrella patens.* Edited by Knight C, Perroud PF, Cove D, vol. 36: John Wiley & Sons; 2009: 1-15.
27. Frank W, Ratnadewi D, Reski R: **Physcomitrella patens is highly tolerant against drought, salt and osmotic stress**. *Planta* 2005, **220**:384-394.
28. Roberts AW, Dimos CS, Budziszek MJ, Jr., Goss CA, Lai V: **Knocking out the wall: protocols for gene targeting in *Physcomitrella patens***. *Methods Mol Biol* 2011, **715**:273-290.
29. Goss CA, Roberts AW: **Functionaly Analysis of Two Cellulose Synthase Genes in *Physcomitrella patens*: *PpCESA5* and *PpCESA8***. University of Rhode Island; 2008.
30. Nishiyama T, Fujita T, Shin IT, Seki M, Nishide H, Uchiyama I, Kamiya A, Carninci P, Hayashizaki Y, Shinozaki K *et al*: **Comparative genomics of *Physcomitrella patens* gametophytic transcriptome and *Arabidopsis thaliana*: implication for land plant evolution**. *Proc Natl Acad Sci* 2003, **100**:8007-8012.
31. Bibeau J, Vidali L: **Morphological Analysis of Cell Growth Mutants in Physcomitrella**. In: *Plant Cell Morphogenesis.* Edited by Žárský V, Cvrčková F, vol. 1080: Humana Press; 2014: 201-213.

32. Vidali L, Augustine RC, Kleinman KP, Bezanilla M: **Profilin is essential for tip growth in the moss Physcomitrella patens**. *Plant Cell* 2007, **19**:3705-3722.
33. Furt F, Liu YC, Bibeau JP, Tuzel E, Vidali L: **Apical myosin XI anticipates F-actin during polarized growth of *Physcomitrella patens* cells**. *Plant J* 2013, **73**:417-428.
34. Galway ME, Eng RC, Schiefelbein JW, Wasteneys GO: **Root hair-specific disruption of cellulose and xyloglucan in AtCSLD3 mutants, and factors affecting the post-rupture resumption of mutant root hair growth**. *Planta* 2011, **233**:985-999.
35. Aouar L, Chebli Y, Geitmann A: **Morphogenesis of complex plant cell shapes: the mechanical role of crystalline cellulose in growing pollen tubes**. *Sex Plant Reprod* 2010, **23**:15-27.
36. Park S, Szumlanski AL, Gu F, Guo F, Nielsen E: **A role for CSLD3 during cell-wall synthesis in apical plasma membranes of tip-growing root-hair cells**. *Nat Cell Biol* 2011, **13**:973-980.
37. Wang W, Wang L, Chen C, Xiong G, Tan XY, Yang KZ, Wang ZC, Zhou Y, Ye D, Chen LQ: ***Arabidopsis* CSLD1 and CSLD4 are required for cellulose deposition and normal growth of pollen tubes**. *J Exp Bot* 2011, **62**:5161-5177.
38. Persson S, Paredez A, Carroll A, Palsdottir H, Doblin M, Poindexter P, Khitrov N, Auer M, Somerville CR: **Genetic evidence for three unique components in primary cell-wall cellulose synthase complexes in *Arabidopsis***. *Proc Natl Acad Sci* 2007, **104**:15566-15571.
39. Taylor NG, Scheible W-R, Cutler S, Somerville CR, Turner SR: **The irregular xylem3 Locus of Arabidopsis Encodes a Cellulose Synthase Required for Secondary Cell Wall Synthesis**. *Plant Cell* 1999, **11**:769-779.
40. Taylor NG, Howells RM, Huttly AK, Vickers K, Turner SR: **Interactions among three distinct CesA proteins essential for cellulose synthesis**. *Proc Natl Acad Sci* 2003, **100**:1450-1455.

BIBLIOGRAPHY:

1. Roberts AW, Roberts EM, Haigler CH: **Moss cell walls: structure and biosynthesis**. *Front Plant Sci* 2012, **3**:166.
2. Somerville C: **Cellulose synthesis in higher plants**. *Annu Rev Cell and Dev Biol* 2006, **22**:53-78.
3. Delmer DP: **CELLULOSE BIOSYNTHESIS: Exciting Times for A Difficult Field of Study**. *Annu Rev Plant Physiol Plant Mol Biol* 1999, **50**:245-276.
4. Roberts AW, Bushoven JT: **The cellulose synthase (CESA) gene superfamily of the moss *Physcomitrella patens***. *Plant Mol Biol* 2007, **63**:207-219.
5. Richmond TA, Somerville CR: **The cellulose synthase superfamily**. *Plant Physiol* 2000, **124**:495-498.
6. Kimura S, Laosinchai W, Itoh T, Cui X, Linder R, Brown RM: **Immunogold Labeling of Rosette Terminal Cellulose-Synthesizing Complexes in the Vascular Plant *Vigna angularis***. *Plant Cell* 1999, **11**:2075-2086.
7. Lerouxel O, Cavalier D, Liepman A, Keegstra K: **Biosynthesis of plant cell wall polysaccharides - a complex process**. *Curr Opin Plant Biol* 2006, **9**:621 - 630.
8. Taylor NG, Howells RM, Huttly AK, Vickers K, Turner SR: **Interactions among three distinct CesA proteins essential for cellulose synthesis**. *Proc Natl Acad Sci* 2003, **100**:1450-1455.
9. Persson S, Paredez A, Carroll A, Palsdottir H, Doblin M, Poindexter P, Khitrov N, Auer M, Somerville CR: **Genetic evidence for three unique components in primary cell-wall cellulose synthase complexes in *Arabidopsis***. *Proc Natl Acad Sci* 2007, **104**:15566-15571.
10. Schaefer DG: **A new moss genetics: targeted mutagenesis in Physcomitrella patens**. *Annual review of plant biology* 2002, **53**:477-501.
11. Goss CA, Brockmann DJ, Bushoven JT, Roberts AW: **A CELLULOSE SYNTHASE (CESA) gene essential for gametophore morphogenesis in the moss *Physcomitrella patens***. *Planta* 2012, **235**:1355-1367.
12. Wise HZ, Saxena IM, Brown RM: **Isolation and characterization of the cellulose synthase genes PpCesA6 and PpCesA7 in *Physcomitrella patens***. *Cellulose* 2011, **18**:371-384.
13. Dimos CS: **Functional Analysis of the Cellulose Synthase-Like D (CSLD) Gene Family in *Physcomitrella patens***. University of Rhode Island; 2010.
14. Cuming AC, Cho SH, Kamisugi Y, Graham H, Quatrano RS: **Microarray analysis of transcriptional responses to abscisic acid and osmotic, salt, and drought stress in the moss, *Physcomitrella patens***. *New Phytol* 2007, **176**:275-287.
15. Zhong R, Morrison WH, 3rd, Freshour GD, Hahn MG, Ye ZH: **Expression of a mutant form of cellulose synthase AtCesA7 causes dominant negative effect on cellulose biosynthesis**. *Plant Physiol* 2003, **132**:786-795.

16. Frank W, Ratnadewi D, Reski R: **Physcomitrella patens is highly tolerant against drought, salt and osmotic stress**. *Planta* 2005, **220**:384-394.
17. Chen Z, Hong X, Zhang H, Wang Y, Li X, Zhu JK, Gong Z: **Disruption of the cellulose synthase gene, AtCesA8/IRX1, enhances drought and osmotic stress tolerance in Arabidopsis**. *Plant J* 2005, **43**:273-283.
18. Mishler BD, Oliver MJ: **Putting *Physcomitrella patens* on the tree of life: the evolution an ecology of mosses**. In: *The Moss Physcomitrella patens.* Edited by Knight C, Perroud PF, Cove D, vol. 36: John Wiley & Sons; 2009: 1-15.
19. Wang XQ, Yang PF, Liu Z, Liu WZ, Hu Y, Chen H, Kuang TY, Pei ZM, Shen SH, He YK: **Exploring the Mechanism of Physcomitrella patens Desiccation Tolerance through a Proteomic Strategy**. *Plant Physiol* 2009, **149**:1739-1750.
20. Kang JS, Frank J, Kang CH, Kajiura H, Vikram M, Ueda A, Kim S, Bahk JD, Triplett B, Fujiyama K *et al*: **Salt tolerance of Arabidopsis thaliana requires maturation of N-glycosylated proteins in the Golgi apparatus**. *Proceedings of the National Academy of Sciences of the United States of America* 2008, **105**:5933-5938.
21. Zhu J, Lee BH, Dellinger M, Cui X, Zhang C, Wu S, Nothnagel EA, Zhu JK: **A cellulose synthase-like protein is required for osmotic stress tolerance in Arabidopsis**. *Plant J* 2010, **63**:128-140.
22. Roberts AW. In.; 2015.
23. Hao H, Chen T, Fan L, Li R, Wang X: **2, 6-Dichlorobenzonitrile causes multiple effects on pollen tube growth beyond altering cellulose synthesis in Pinus bungeana Zucc**. *PLoS One* 2013, **8**:e76660.
24. Moller I, Sorensen I, Bernal AJ, Blaukopf C, Lee K, Obro J, Pettolino F, Roberts A, Mikkelsen JD, Knox JP *et al*: **High-throughput mapping of cell-wall polymers within and between plants using novel microarrays**. *Plant J* 2007, **50**:1118-1128.
25. Lee KJ, Sakata Y, Mau SL, Pettolino F, Bacic A, Quatrano RS, Knight CD, Knox JP: **Arabinogalactan proteins are required for apical cell extension in the moss *Physcomitrella patens***. *Plant Cell* 2005, **17**:3051-3065.
26. Kulkarni AR, Pena MJ, Avci U, Mazumder K, Urbanowicz BR, Pattathil S, Yin Y, O'Neill MA, Roberts AW, Hahn MG *et al*: **The ability of land plants to synthesize glucuronoxylans predates the evolution of tracheophytes**. *Glycobiology* 2012, **22**:439-451.
27. Liepman AH, Nairn CJ, Willats WG, Sorensen I, Roberts AW, Keegstra K: **Functional genomic analysis supports conservation of function among cellulose synthase-like a gene family members and suggests diverse roles of mannans in plants**. *Plant Physiol* 2007, **143**:1881-1893.
28. Schuette S, Wood AJ, Geisler M, Geisler-Lee J, Ligrone R, Renzaglia KS: **Novel localization of callose in the spores of Physcomitrella patens and phylogenomics of the callose synthase gene family**. *Ann Bot* 2009, **103**:749-756.
29. Cosgrove D: **Growth of the plant cell wall**. *Nature Rev Mol Cell Biol* 2005, **6**:850 - 861.

30. Hepler PK, Vidali L, Cheung AY: **Polarized cell growth in higher plants**. *Annu Rev Cell Dev Biol* 2001, **17**:159-187.
31. Doonan JH, Cove DJ, Lloyd CW: **Microtubules and microfilaments in tip growth: evidence that microtubules impose polarity on protonemal growth in *Physcomitrella patens***. *Journal of cell science* 1988, **89**:533-540.
32. Anderson JR, Barnes WS, Bedinger P: **2,6-Dichlorobenzonitrile, a cellulose biosynthesis inhibitor, affects morphology and structural integrity of petunia and lily pollen tubes**. *J Plant Physiol* 2002, **159**:61-67.
33. Aouar L, Chebli Y, Geitmann A: **Morphogenesis of complex plant cell shapes: the mechanical role of crystalline cellulose in growing pollen tubes**. *Sex Plant Reprod* 2010, **23**:15-27.
34. DeBolt S, Gutierrez R, Ehrhardt DW, Somerville C: **Nonmotile cellulose synthase subunits repeatedly accumulate within localized regions at the plasma membrane in Arabidopsis hypocotyl cells following 2,6-dichlorobenzonitrile treatment**. *Plant Physiol* 2007, **145**:334-338.
35. Rudolph U, Gross H, Schepf E: **Investigations of the turnover of the putative cellulose-synthesizing particle "rosettes" within the plasma membrane of Funaria hygrometrica protonema cells**. *Protoplasma* 1989, **148**:57-69.
36. Park S, Szumlanski AL, Gu F, Guo F, Nielsen E: **A role for CSLD3 during cell-wall synthesis in apical plasma membranes of tip-growing root-hair cells**. *Nat Cell Biol* 2011, **13**:973-980.
37. Reiss HD, Schnept E, Herth W: **The plasma membrane of the *Funaria* caulonema tip cell: morphology and distribution of particle rosettes, and the kinetics of cellulose synthase**. *Planta* 1984, **160**:428-435.
38. Taylor NG: **Identification of cellulose synthase AtCesA7 (IRX3) in vivo phosphorylation sites--a potential role in regulating protein degradation**. *Plant Mol Biol* 2007, **64**:161-171.
39. Taylor NG, Laurie S, Turner SR: **Multiple Cellulose Synthase Catalytic Subunits Are Required for Cellulose Synthesis in *Arabidopsis***. *Plant Cell* 2000, **12**:2529–2539,.
40. Brown DM, Zeef LA, Ellis J, Goodacre R, Turner SR: **Identification of novel genes in *Arabidopsis* involved in secondary cell wall formation using expression profiling and reverse genetics**. *Plant Cell* 2005, **17**:2281-2295.
41. Desprez T, Juraniec M, Crowell EF, Jouy H, Pochylova Z, Parcy F, Hofte H, Gonneau M, Vernhettes S: **Organization of cellulose synthase complexes involved in primary cell wall synthesis in *Arabidopsis thaliana***. *Proc Natl Acad Sci* 2007, **104**:15572-15577.
42. Schaefer DG: **A new moss genetics: targeted mutagenesis in *Physcomitrella patens***. *Annu Rev Plant Biol* 2002, **53**:477-501.
43. Nishiyama T, Fujita T, Shin IT, Seki M, Nishide H, Uchiyama I, Kamiya A, Carninci P, Hayashizaki Y, Shinozaki K *et al*: **Comparative genomics of *Physcomitrella patens* gametophytic transcriptome and *Arabidopsis thaliana*: implication for land plant evolution**. *Proc Natl Acad Sci* 2003, **100**:8007-8012.

44. Roberts AW, Dimos CS, Budziszek MJ, Jr., Goss CA, Lai V: **Knocking out the wall: protocols for gene targeting in *Physcomitrella patens***. *Methods Mol Biol* 2011, **715**:273-290.
45. Rensing SA, Lang D, Zimmer AD, Terry A, Salamov A, Shapiro H, Nishiyama T, Perroud PF, Lindquist EA, Kamisugi Y *et al*: **The *Physcomitrella* genome reveals evolutionary insights into the conquest of land by plants**. *Science* 2008, **319**:64-69.
46. Wang Y, Secco D, Poirier Y: **Characterization of the PHO1 gene family and the responses to phosphate deficiency of *Physcomitrella patens***. *Plant Physiol* 2008, **146**:646-656.
47. Ye J, Coulouris G, Zaretskaya I, Cutcutache I, Rozen S, Madden TL: **Primer-BLAST: a tool to design target-specific primers for polymerase chain reaction**. *BMC Bioinforma* 2012, **13**:134.
48. Le Bail A, Scholz S, Kost B: **Evaluation of reference genes for RT qPCR analyses of structure-specific and hormone regulated gene expression in *Physcomitrella patens* gametophytes**. *PLoS One* 2013, **8**:e70998.
49. Hiss M, Laule O, Meskauskiene RM, Arif MA, Decker EL, Erxleben A, Frank W, Hanke ST, Lang D, Martin A *et al*: **Large-scale gene expression profiling data for the model moss *Physcomitrella patens* aid understanding of developmental progression, culture and stress conditions**. *Plant J* 2014, **79**:530-539.
50. Zimmermann P, Hirsch-Hoffmann M, Hennig L, Gruissem W: **GENEVESTIGATOR. *Arabidopsis* microarray database and analysis toolbox**. *Plant Physiol* 2004, **136**:2621-2632.
51. Sakakibara K, Nishiyama T, Sumikawa N, Kofuji R, Murata T, Hasebe M: **Involvement of auxin and a homeodomain-leucine zipper I gene in rhizoid development of the moss *Physcomitrella patens***. *Development* 2003, **130**:4835-4846.
52. Cove D, Quatrano RS: **The Use of Mosses for the Study of Cell Polarity**. In: *New Frontiers in Bryology*. Springer Netherlands; 2004: 189-203.
53. Xu B, Ohtani M, Yamaguchi M, Toyooka K, Wakazaki M, Sato M, Kubo M, Nakano Y, Sano R, Hiwatashi Y *et al*: **Contribution of NAC transcription factors to plant adaptation to land**. *Science* 2014, **343**:1505-1508.
54. Knox JP: **Revealing the structural and functional diversity of plant cell walls**. *Curr Opin Plant Biol* 2008, **11**:308-313.
55. Cosgrove DJ: **Growth of the plant cell wall**. *Nat Rev Mol Cell Biol* 2005, **6**:850-861.
56. Bergounioux C, Perennes C, Miege C, Gadal P: **The effect of male sterility on protoplast division inPetunia hybrida. Cell cycle comparison by flow cytometry**. *Protoplasma* 1986, **130**:138-144.
57. Chen XY, Kim JY: **Callose synthesis in higher plants**. *Plant Signal Behav* 2009, **4**:489-492.
58. Pattathil S, Avci U, Baldwin D, Swennes AG, McGill JA, Popper Z, Bootten T, Albert A, Davis RH, Chennareddy C *et al*: **A comprehensive toolkit of plant cell wall glycan-directed monoclonal antibodies**. *Plant Physiol* 2010, **153**:514-525.

59. Marcus S, Verhertbruggen Y, Herve C, Ordaz-Ortiz J, Farkas V, Pedersen H, Willats W, Knox JP: **Pectic homogalacturonan masks abundant sets of xyloglucan epitopes in plant cell walls**. *BMC Plant Biol* 2008, **8**:60.
60. Pena MJ, Darvill AG, Eberhard S, York WS, O'Neill MA: **Moss and liverwort xyloglucans contain galacturonic acid and are structurally distinct from the xyloglucans synthesized by hornworts and vascular plants**. *Glycobiology* 2008, **18**:891-904.
61. Knox JP, Linstead PJ, Cooper JPC, Roberts K: **Developmentally regulated epitopes of cell surface arabinogalactan proteins and their relation to root tissue pattern formation**. *The Plant Journal* 1991, **1**:317-326.
62. Yates EA, Valdor JF, Haslam SM, Morris HR, Dell A, Mackie W, Knox JP: **Characterization of carbohydrate structural features recognized by anti-arabinogalactan-protein monoclonal antibodies**. *Glycobiology* 1996, **6**:131-139.
63. Zimmer AD, Lang D, Buchta K, Rombauts S, Nishiyama T, Hasebe M, Van de Peer Y, Rensing SA, Reski R: **Reannotation and extended community resources for the genome of the non-seed plant Physcomitrella patens provide insights into the evolution of plant gene structures and functions**. *BMC genomics* 2013, **14**:498.
64. Schaefer D, Zryd J-P: **Efficient Gene Targeting in the moss *Physcomitrella patens***. *Plant J* 1997, **11**:1195-1206.
65. Reski R, Frank W: **Moss (*Physcomitrella patens*) functional genomics—Gene discovery and tool development, with implications for crop plants and human health**. *Briefings in Functional Genomics and Proteomics* 2005, **4**:48-57.
66. Cove D: **The Moss *Physcomitrella patens***. *Annu Rev Genet* 2005, **39**:339-358.
67. Geitmann A, Emons AM: **The cytoskeleton in plant and fungal cell tip growth**. *J Microsc* 2000, **198**:218-245.
68. Lazzaro MD, Donohue JM, Soodavar FM: **Disruption of cellulose synthesis by isoxaben causes tip swelling and disorganizes cortical microtubules in elongating conifer pollen tubes**. *Protoplasma* 2003, **220**:201-207.
69. Pressel S, Duckett JG: **Cytological insights into the desiccation biology of a model system: moss protonemata**. *New Phytol* 2010, **185**:944-963.
70. Goss CA, Roberts AW: **Functionaly Analysis of Two Cellulose Synthase Genes in *Physcomitrella patens*: *PpCESA5* and *PpCESA8***. University of Rhode Island; 2008.
71. Bibeau J, Vidali L: **Morphological Analysis of Cell Growth Mutants in Physcomitrella**. In: *Plant Cell Morphogenesis.* Edited by Žárský V, Cvrčková F, vol. 1080: Humana Press; 2014: 201-213.
72. Vidali L, Augustine RC, Kleinman KP, Bezanilla M: **Profilin is essential for tip growth in the moss Physcomitrella patens**. *Plant Cell* 2007, **19**:3705-3722.
73. Furt F, Liu YC, Bibeau JP, Tuzel E, Vidali L: **Apical myosin XI anticipates F-actin during polarized growth of *Physcomitrella patens* cells**. *Plant J* 2013, **73**:417-428.

74. Galway ME, Eng RC, Schiefelbein JW, Wasteneys GO: **Root hair-specific disruption of cellulose and xyloglucan in AtCSLD3 mutants, and factors affecting the post-rupture resumption of mutant root hair growth**. *Planta* 2011, **233**:985-999.
75. Wang W, Wang L, Chen C, Xiong G, Tan XY, Yang KZ, Wang ZC, Zhou Y, Ye D, Chen LQ: ***Arabidopsis*** **CSLD1 and CSLD4 are required for cellulose deposition and normal growth of pollen tubes**. *J Exp Bot* 2011, **62**:5161-5177.
76. Taylor NG, Scheible W-R, Cutler S, Somerville CR, Turner SR: **The irregular xylem3 Locus of Arabidopsis Encodes a Cellulose Synthase Required for Secondary Cell Wall Synthesis**. *Plant Cell* 1999, **11**:769-779.